Recovery of SiO_2 and Al_2O_3 from coal fly ash

Grant Sedres

A thesis submitted in fulfilment of the requirements for the degree of Magister Scientiae in the Department of Chemistry, University of Western Cape

Supervisor: Professor Leslie F. Petrik

Co-supervisor: Dr Olanrewaju O. Fatoba

May 2016

Abstract

Most of the world's energy production is still mainly achieved by the combustion of coal in power stations. Coal fly ash is the inevitable waste product that accumulates to metric ton volumes each year. These vast volumes pose a problem in the disposal of the coal fly ash which conventionally is loaded onto ash dumps located near the coal power stations. Alternatives need to be investigated for the use of the coal fly ash in applications that would make the coal fly ash useful and thereby help to mitigate the environmental strain imposed by conventional ash dump disposal.

This study focussed on investigating the extraction of Si and Al from CFA. The investigation into the removal of the magnetic iron oxide content and calcium content from coal fly ash was also carried out to enhance the extraction of the Si and Al from CFA e.g. the removal of calcium was attempted to promote the leaching of aluminium from the ash. The rationale for this process was that by removing and recovering these major constituent elements from the ash, it would be easier to concentrate and isolate the trace elements especially the rare earth elements that are present in the CFA.

Coal fly ash sourced from Matla coal power station was characterised using x-ray diffraction to determine the mineral phases present in the raw coal fly ash and elemental composition determined by x-ray fluorescence and laser ablation ICP-MS. The main mineral phases in coal fly ash were determined to be quartz, mullite, magnetite and lime (CaO).

Magnetic extraction was initially carried out on the coal fly ash to remove the iron rich magnetic material. Extraction tests were then performed on the coal fly ash using alkaline and acidic media namely; NaOH, HCl and H_2SO_4. The extraction tests were assessed and a sequential extraction experimental procedure developed to achieve the highest extraction yield for Si, Al, Fe, Ca, and Mg from the coal fly ash. Lastly the rare earth element content in

coal fly ash was tracked from the beginning till the end of the sequential extraction procedure to ascertain whether the rare earth elements partitioned to the leachates or the solid residues. The total element recoveries for Al, Si, Ca Fe, Mg were 53.36 %, 39.96 %, 93.8 %, 25.6 % and 67.3 % respectively using the sequential extraction procedure developed in this study. The rare earth elements contents were not affected by the sequential extraction procedure and on the whole remained in the solid residues at the completion of the sequential extraction, resulting in a residue with enriched levels of recoverable or extractable REE content after the removal of the major oxides from the CFA.The lowest enrichment being approximately 5 % for Thulium and the highest being approximately 76 % for Erbium

Keywords

coal fly ash

extraction

leaching

alkaline leaching

acidic leaching

magnetic extraction

sequential extraction treatment

aluminium

silicon

calcium

iron

rare earth elements

Declaration

I declare that *Recovery of SiO_2 and Al_2O_3 from coal fly ash* is my own work, that it has not been submitted before for any degree or examination in any other university, and that all the sources I have used or quoted have been indicated and acknowledged as complete references.

Grant Sedres May 2016

Signed: ……..

Acknowledgements

I want to thank my supervisor, Professor Leslie Petrik, for accepting me for into her Environmental and Nanosciences research group and allowing me to undertake my MSc study. I want to thank her for her guidance in compiling this study and also to my co-supervisor Dr Olanrewaju Fatoba for his guidance and advice on the initial planning of the study.

I want to also thank the ENS (Environmental and Nano-Sciences) group administration staff for their help in making this work reach completion. Averil Abbot, Vanessa Kellerman and Ilse Wells for handling the logistical administration aspects for the study and to Ilse Wells and Rallston Richards for their assistance with the analysis. I also want to thank Remy Bucher, Stuart Moir, Kelly Moir, Riana Rossouw and Mareli Grobbelaar for their assistance with analysis. Thank you to fellow ENS group colleagues for their troubleshooting advice and support.

Lastly, I would like to thank my wife for her continual encouragement and support to pursue this MSc study.

List of Abbreviations

ASTM	American Standard of Testing and Measurement
CCE	calcium carbonate equivalent
CFA	coal fly ash
cps	counts per second
DAL	direct acid leaching
ICDD	International Center for Diffraction Data
ICP-MS	Inductively coupled plasma- mass spectrometry
ICP-OES	Inductively coupled optical emission spectrometry
LOI	loss on ignition
MW	megawatt
NIST	National Institute of Standards and Technology
PDF	powder diffraction file
REEs	rare earth elements
RF	radio frequency
SET	sequential extraction treatment
USGS	United States Geological Survey
UV-Vis	ultraviolet-visible spectrometry
XRD	x-ray diffraction
XRF	x-ray fluorescence

Table of Contents

List of Figures

List of Tables

Chapter One

1. Introduction

This chapter provides details about the background of the work that is undertaken in this research. This chapter is divided into sub headings describing the rationale of the study, the problem statement and the aims and objectives. The research approach is given followed by the research questions addressed by the study. The scope and delimitations of the study are set so as to provide a guideline of what experimental results will be presented. Lastly, brief descriptions of the subsequent chapters to follow are outlined.

1.1 Background

Coal fly ash (CFA) is the inorganic remainder and end product of the coal burning process that is used to produce electricity at coal power stations worldwide. It is generally considered to be a waste product. CFA is actually an inorganic particulate matter of varying micron sizes ranging from 0.5 μm to 300 μm that becomes airborne due to the convection air currents created by the heat energy of coal burning. This is typically called the flue gas (Ahmaruzzaman, 2010). Due to the large volumes of coal that are burnt to produce electricity for our daily use, these particulates being released to the atmosphere contribute a great deal to air pollution levels and eventually ground pollution in our environment.

Electricity power stations are fitted with bag filters or electrostatic precipitators that are used to control the release of these CFA particulates into the atmosphere and prevent their release into the local environment. These bag filters or electrostatic precipitators trap the particulates before the flue gases are released through the smoke stacks of the power plant. The inorganic content of coal solidifies rapidly while suspended in the flue gases after being released from the burning coal. The result of this rapid cooling is that only a few minerals have time to

crystallise and mainly amorphous glassy material forms. Not all mineral phases in the coal will melt entirely and thus a portion of the inorganic content will remain in its original crystalline form. CFA is thus a heterogeneous material.

The appearance of CFA is a grey, fine, powdery material that is mainly spherical in shape and can be solid or hollow and mostly glassy (amorphous) in nature. The main chemical composition of CFA is SiO_2, Al_2O_3, Fe_2O_3, CaO and TiO_2. Moreover many trace elements are present in the ash.

1.2 Rationale of the Study

This study was undertaken to develop an effective method to extract the silicon, aluminium, iron and calcium components from CFA. Since CFA is a general waste product containing a range of elements, it can be seen as a potential raw material source for applications currently being researched. Reclaimed silicon has use in research applications such as the production of nano silica with one of its uses being in self-compacting concrete. It was seen to increase the mechanical and durability properties of the self- compacting concrete (Quercia et al., 2014). Reclaimed silicon has also been used as an anti-reflection coating for solar cells (Liu et al., 2013) and silicon in its amorphous form has use in photonic devices (Corte et al., 2013). Reclaimed aluminium in the form of Al_2O_3 can be used for production of adsorbents of toxic metals such as lead, zinc and cadmium (Asencios et al., 2012). Aluminium as metal has a high strength to weight ratio making it suitable to be used in the automotive as well as aviation industry (Simcoe, 2014). Reclaimed Al_2O_3 also has potential use in the manufacture of ceramic fibres that provide increased heat shielding capabilities as part of the manufacture of modern aircraft and gas turbines (Grashchenkov, 2012). In general iron is used to make alloys that are used in the construction industry and in the manufacture of machinery components and tools. Reclaimed iron has use in the production of iron based sorbent

materials used for toxic element removal from water (Ilavský, 2015). Reclaimed calcium compounds can potentially be used for wastewater treatment. $CaSO_4$ has been tested as an alternative for aluminium sulphate in the treatment of wastewater (Vázquez-Almazán et al., 2012).

A secondary rationale for this process is that by removing and recovering these major constituent elements from the ash, it would be easier to concentrate and isolate the trace elements that are present in the CFA. These trace elements, especially the rare earth elements, also have various industry applications. The rare earth elements (REEs) are used in the manufacture of high strength permanent magnets, catalysts in petroleum refining, in metal and glass additives and also in additives for phosphors used in electronic displays (Jordens et al., 2013).

1.3 Problem Statement

The disposal of the ash in itself is an environmental problem due to the large volumes generated. Since the volumes are so vast, it would be very useful if the CFA could be recycled for other purposes instead of being disposed of on landfill sites.

Currently CFA is being used in the building and civil engineering industry for concrete production as a substitute for portland cement and sand, structural fillers, road construction etc. (Manz, 1999; Sumner, 2000). It is also being used to manufacture geo-polymers (Nyale, 2013), the treatment of acid mine drainage (Madzivire, 2015) and as a raw material for zeolite production on a small scale (Musyoka, 2012).

If the useful components of CFA can be extracted, it could be used as an alternative resource and in effect conserve our natural resources.

1.4 Aims and Objectives

The aim is to recover the useful major constituents of CFA as an alternative to normal disposal. The secondary aim is to track the solubility behaviour of the rare earth elements so that they could be recovered as well.

The objectives would be,

- to find a way to selectively extract the silicon, aluminium, iron and calcium from the CFA
- To determine the best way to recover the elements of interest
- to up concentrate trace elements

1.5 Research Questions

As explained previously, the CFA is mainly an amorphous glassy phase where some of the crystalline structure of the coal is not entirely broken down and remains in its original crystalline form. Since the glassy phase is formed by rapid cooling, these crystalline structures containing the trace minerals would be trapped inside the glassy phase and its removal would allow access to these metals. The questions that would be considered in the study are as follows:

- What percentage of the major constituents of CFA can be recovered by removing the amorphous glassy phase of the CFA?
- Can major elements be selectively extracted from CFA?
- Do REEs and trace elements partition to the liquid extract or remain entrapped in the solid residues?

Since the main focus is the selective recovery of the major constituents of CFA and tracking the behaviour of the REEs and trace elements, these questions will be reviewed at the end of the study.

1.6 Hypothesis

Selective extraction of the major constituents from CFA would allow their recovery for reuse and would make it possible to up concentrate REEs or the trace elements present in CFA.

1.7 Research Approach

The selective extraction of the major constituents in CFA is the main focus of this study. The trace elements would only be tracked during the process to see whether these elements could be concentrated for their possible recovery. The research approach was to adopt the processes that have previously been used for extraction of major elements from other types of CFA but also track how trace elements behave in the extraction systems. Not many studies have actually looked at the mineral association of the trace elements since they constitute a very small percentage of the CFA composition and most studies investigated removing a single major element at a time. Elements such as Al, Si, Fe, Ca, and Mg were targeted by process of leaching and sequential extraction directly from the raw CFA.

The first method was a physical extraction of the magnetic fraction in CFA using de-ionised water as a solvent. The ash residue from this step was used as the starting material for the experimental methods that were applied for extraction of Si and Al using strong acid and alkaline solutions.

This study also explored a sequential extraction route in which Ca was removed with HCl, whereafter H_2SO_4 was used to recover Al, Mg and residual Fe. Lastly NaOH was used to selectively recover Si.

The problem is not an easy task because any liquid to solid contact with the CFA would leach some elements however small its effect is (Akinyemi et al., 2011; Eze et al., 2013b; Nyale, 2014). Therefore this study employs a step by step analysis procedure to track how the elements partition between the liquid and solid phases. Analysis of solids was done using XRD, XRF and laser ablation ICP-MS and extracts were analysed using ICP-OES, ICP-MS or UV-Vis. At the end of the study it could also be determined at what step the highest amount of each element could be recovered. At the end of this study, an optimum extraction procedure where the highest amount of each element could be recovered will be developed.

1.8 Scope and Delimitations of the Study

Many studies have been carried out on Si and Al removal as their main focus but such studies were not concerned about the selective recovery of each element in sequence. The tracking of the trace elements were also not of concern and the oversight could be attributed to low concentrations needing expensive equipment for accurate determination. Therefore this study will focus on selective recovery of silicon, aluminium, iron and calcium. It will also entail a comparative study between different methods of extraction of the respective elements. The extracted Si and Al were not converted to solid compounds for the study. The percentage element extractions from the CFA were the main determinations with regard to the leaching of the CFA.

Although the study also has a focus on quantifying the movement of REEs and trace elements during extraction, their recovery is beyond the scope of this study.

1.9 Outline of thesis chapters

The chapters to follow in the study are:

Chapter 2: The literature review on the methods that have been performed related to the subject matter

Chapter 3: The description of the experimental procedure that was selected for the study. The analytical methods are included as well.

Chapter 4: The presentation of the results obtained from the experiments.

Chapter 5: The conclusions that can be drawn from the study. Finally, the study is evaluated for how effectively the goals were achieved and recommendations are made.

Chapter Two

2. Literature Review

This chapter provides information on the origin of coal fly ash (CFA) and the uses thereof. The extractive removal behaviour of the various elements in CFA is discussed as well as the methods that are used for their recovery. Techniques used for characterisation and analysis are reviewed and the chapter ends with a critical assessment of the relevant gaps that made this study necessary.

2.1 Origin of coal fly ash

Coal fly ash (CFA) originates from the combustion of coal to generate electricity. Coal is a fossil fuel source that is excavated on a large scale from coal deposits in beds or seams. These coal seams can reach up to hundreds of metres in thickness. Coal is in effect a solid carbonaceous rock that is brittle and combustible. It was formed from the decomposition and alteration of vegetation by compaction, temperature and pressure over geological time. Coal varies in colour from brown to black and is usually stratified (Speight, 2005).

In coal combustion power stations, coal is firstly pulverised before it enters a boiler where the flame temperatures reach up to 1500 °C. After combustion of the coal, during the cooling down process, the residual inorganic matter changes from the vapour state to the liquid and solid state. This is a rapid process and it is here that individual, spherical particles, commonly called coal fly ash (CFA) are formed. CFA is a fine particulate material, less than 0.05 mm in diameter, composed largely of silicious material which is trapped by electrostatic precipitators or bag filters prior to the release of flue gases from the coal power station's smoke stacks (Sumner, 2000). The CFA particles are therefore collected by the electrostatic precipitators or bag filters and stored in ash dumps. The CFA is tested for physical properties

such as fineness, loss on ignition and moisture. In U.S.A., 25 % of CFA is reused as a cement additive, in structural fills, roadbases and other engineering applications. The remainder is stored onsite in lagoons or landfills (Sumner, 2000).

CFA forms as a result of chemical changes that take place in the mineral matter of coal during the ashing process, i.e. combustion. Loss of water from silicate materials, loss of carbon dioxide from carbonate materials, oxidation of pyrite (iron sulphide, FeS) to iron oxide and formation of oxides from Ca, Mg etc. are some of the chemical changes that occur during combustion (Speight, 2005).

The composition of CFA differs significantly from wood ash solely due to the nature of the fuel. Coal has greater ash content as a result of mineral inclusion in the coal as it was deposited and modified over geological time. Clay minerals deposited in the bearing strata result in high Si and Al content of the coal. Iron deposited as pyrite (FeS, iron sulphide) within the coal also adds Fe and a range of trace metals as well. The two types of minerals in coal are called extraneous mineral matter and inherent mineral matter. Extraneous mineral matter is calcium, magnesium, ferrous carbonate, pyrites, marcasite, clay, shale, sand and gypsum. Inherent mineral matter is the combination of inorganic elements and organic components of coal that originated from the plant material from which the coal was formed (Sumner, 2000).

CFA can be divided into two classes as per the American Standard of Testing and Measurement (ASTM). CFA is classified according to ASTM C618, (2008) as either being a Class F or Class C type. The differentiation is made by the amount of calcium, silica, alumina (Al_2O_3) and iron present in the ash. CFA having a total silica, alumina and iron content of 70 % with lime content (CaO) less than 15 % is defined as Class F CFA. Class F CFA is also described as being pozzolanic in nature. A pozzolan is defined by Mehta, (1987) as a

siliceous or a siliceous and aluminous material that on its own has no cementitious value but when mixed in its finely divided form with water and CaOH at room temperature, forms compounds that exhibit cementitious properties according to ASTM C618.

Bituminous coals have high sulphur content and produce acidic to neutral pH ash. Bituminous ash also has higher Fe content with lower Ca and Mg content. Sub-bituminous coal fly ash has low sulphur content, lower Fe and associated metals and is classified as Class C CFA. Class C CFA has higher lime content in the range of 15 % to 30 %. This factor gives Class C CFA a more pozzolanic nature with a unique irreversible, self-hardening characteristic that gains strength over time. This characteristic is similar to portland cement and therefore makes it very suitable as a cement additive (Sumner, 2000).

Originally CFA was seen as a waste product from electricity production and was dumped on land nearby the power stations. Eventually it was realised to be a problem due to the sheer volumes that were being generated over time and a means had to be found to deal with this ever growing problem.

2.1.1 Matla Power Station

The CFA utilised in this study was obtained from Matla power station, which is situated approximately 30 km from Secunda in the Mpumalanga province in the Republic of South Africa. It has six 600 megawatt (MW) units giving it an installed generating capacity of 3600 MW.

Figure 2.1 Matla Power Station

(http://www.construction.murrob.com/projects/MatlaPowerStation.htm)

Matla power station was the first of the giant 3600 MW coal fired power stations started in the late 1980s. Its construction was started late in 1974 and by July 1983 it was fully operational. It is one of the few power stations in the world with a concrete boiler house superstructure. Its outward appearance is therefore very different from other power stations in South Africa. The use of concrete reduced the construction time as well as capital costs at the time when there was a steel shortage (Eskom, 2016a)

2.2 General overview of CFA utilisation

2.2.1 Global generation of CFA

In 2011, coal power generation made up 29.9 % of the world's electricity supply and is estimated to increase to 46 % by 2030. CFA makes up 5 – 20 wt % of feed coal and typically is found in the form of coarse bottom ash and fine fly ash that represents 5 – 15 % and 85 – 95 % respectively (Yao, 2013).

The high prices for oil and natural gas make coal power generation more economically favourable especially in coal resource rich nations such as China, US and India (Lior, 2010). China with 50.2 % of coal consumption makes it the world's largest consumer of coal followed by the US (11.7 %), India (8 %), Japan (3.3 %), Russian Federation (2.5 %), South Africa (2.4 %), South Korea (2.2 %), Germany (2.1 %), Poland and Indonesia (1.4 %) (Yao et al., 2015). An estimate of the annual worldwide generation of CFA for 2012 was approximately 750 million tonnes (Blisset et al., 2012; Izquierdo et al., 2012). As per the Eskom Generation Communication CO 0007 Revision 14 report, updated February 2016, (Eskom, 2016b) coal combustion covers approximately 72.1 % of the annual electricity demand in South Africa. Approximately 224 million tons of coal is produced annually in South Africa of which 25 % is exported internationally. As per the Eskom Generation Communication CO 0004 Revision 12 report, updated February 2016, (Eskom, 2016c), approximately 109 million tons of coal per annum is used to produce the country's annual electricity demand. This coal combustion results in an annual production of 25 million tons of coal fly ash with only approximately 1.2 million tons being sold and used mainly by the cement and construction industry

2.2.2 Global use of CFA

Approximately 20 % of CFA produced is used in concrete production. Other uses include road construction, soil amendment, zeolite synthesis, fillers in polymers etc. (Cho et al., 2005). These applications are not sufficient to utilise all the CFA produced globally. The unused CFA is treated as waste and stored in ash ponds, lagoons or landfills. This creates an exponentially growing problem where the availability of disposal areas will eventually decrease and this is coupled with an increase in disposal costs. The only viable way to alleviate this problem is to develop additional recycling processes of CFA (Yao et al., 2015).

The following sub-headings will provide some insight on a few of these applications mentioned above.

i) Agriculture

Lime and dolomite is commonly used to ameliorate soil. However it is not always economic and environmentally friendly. The amelioration time is also considerably longer using lime and dolomite as opposed to CFA to improve the physical properties of the soil structure (Ram et al., 2006). The physiochemical properties of CFA makes it a suitable soil ameliorant due to it having silt and clay particle sizes, low bulk density, higher water holding capacity, favourable pH and also trace elements present in CFA can serve as a source of plant nutrients (Ram et al.,2007; Pandey et al., 2010).

The addition of CFA as a soil amendment has proved to increase crop yields. CFA was shown to increase porosity, water holding capacity, pH, and conductivity due to dissolved SO_4^{2-}, CO_3^{2-}, Cl^- and basic cations such as Ca^{2+}, Mg^{2+}, Na^+, H^+, NH_4^+ and K^+ in high clay soils. Field and lab trials have also showed that after adding CFA to the soil, the vegetative yield had been maintained for several years well above those of other treatments. The various crops treated were corn, beans, legumes, grasses etc., (Palumbo, 2007).

However, Class F ashes have low soil nutrient value. Major nutrient concentrations are low and availability studies indicated that potassium, in particular, is not readily soluble in water. It also has a low CCE (calcium carbonate equivalent) content, 1 – 10% making it overall a limited quality fertiliser with limited potential as lime substitute (Sumner, 2000).

CFA has also been used to pasteurise sewage sludge with the sludge product shown to be an excellent soil ameliorant (Reynolds et al., 1999). Although it has not been commercialised in South Africa similar technologies have been successfully applied elsewhere in the world where CFA was blended with a variety of organic and inorganic materials such as lime, gypsum, farmyard manure, sewage sludge and composts. This serves to enhance the soil ameliorant properties of the CFA (Adriano et al., 1980; Haynes, 2009; Belyaeva et al., 2012).

Additionally, preliminary results from field and laboratory experiments indicate CFA to aid in CO_2 sequestration in soil (Amonette et al., 2003; Palumbo, 2004, Muriithi, 2011). This could serve to be of great help in minimising and mitigating CO_2 emissions.

The growing concern with the use of CFA as a soil amendment agent is the potential leaching of hazardous metals which, although not significant in small amounts, is raised exponentially when higher volumes of ash are used (Adriano et al., 2002; Adamson, 2010). This cumulative effect of using large amounts of ash has caused an increase in the toxic element levels in crops. Investigations conducted by Sharma et al., (2006) have confirmed that there were increased uptake levels of boron, molybdenum, aluminium and selenium in maize crops.

ii) Construction

CFA has mainly been used as a substitute in the construction industry either in the form of a raw material or additive in the cement industry. CFA is either called cementitious or pozzolanic depending on its CaO content. Class C CFA having high CaO content has both

cementitious and pozzolanic properties according to ASTM, (2008). Class F CFA is mainly pozzolanic due to its lower CaO content (Yao et al., 2013). The silica in CFA reacts with calcium hydroxide to produce calcium silicate hydrate (Nonavinakere et al., 1995). The pozzolanic properties make it suitable for cement replacement and other building applications (González et al., 2009). Partial addition of class F CFA as a binder in concrete reduces the heat of hydration and minimises crack development in the concrete's early curing stage (Sarker et al., 2009). CFA also adds value by improving the long term durability properties of concrete by reducing the ingress of aggressive agents such as chloride ions (Nath et al., 2011). CFA containing concrete also exhibits increased strength with low permeability (Taylor, 1997; Maroto-Valer et al., 2001). The partial replacement of cement with fly ash reduces production costs. Generally, 15 to 35 wt. % CFA is used for concrete mixing. It can increase up to 70 wt. % for concrete constructs such as pavements, walls and parking lots (Dilmore et al., 2001). CFA based geopolymer has emerged as a promising new cement alternative in the field of building and construction materials (Yao et al., 2015). Research is still ongoing with regard to the use of geopolymers and there are various types that are being produced each having varying physical properties. Geopolymers can be used for various applications in the construction industry (Temuujin et al., 2010; Sarker, 2011; Sarker et al., 2012; Nyale, 2014; Böke et al., 2015).

iii) Raw material source

The use of CFA as a raw material source for developmental research is ongoing. CFA research includes small scale synthesis of zeolites from CFA. Zeolite X, Zeolite P and Zeolite A has been synthesised and tested (Musyoka et al., 2012). Hydrotalcites and zeolite NaX, NaY has been synthesised from CFA for use in CO_2 sequestration (Muriithi, 2013b). Zeolite NaX prepared from CFA has also been used as a solid base catalyst to produce biodiesel (Babajide et al., 2012). CFA has also been utilised to counteract acid mine drainage

(Madzivire et al., 2015). CFA also contains valuable metals such as germanium (Ge), gallium (Ga), vanadium (V), titanium (Ti) and aluminum (Al). All these elements are potentially extractable provided an acceptable and economically viable process can be obtained. Ge is a valuable element used in the manufacture of light-emitting diodes, infrared optics, fibre optics, photovoltaic cells and as a polymerization catalyst for polyethylene terephthalate (Font et al., 2005).

2.3 Chemical Composition of CFA

CFA contains three different types of macro constituents: crystalline minerals (quartz, mullite, spinel, etc.), unburnt carbon particles and non-crystalline alumina-silicate glass. Most of the ash is typically made up of glassy material (Ward et al., 2005). Due to its poorly ordered atomic structure, porous nature and overall abundance, the glassy phase is usually the main constituent involved in chemical reactions associated with ash utilisation in the cement industry. The same applies to geopolymer and zeolite production. The glass also appears to be a major host within the ash for adsorbed trace elements. These trace elements may be loosely bound on the glassy surface thus increasing the potential for their release into the surrounding environment.

Silicon in CFA exists in forms of amorphous SiO_2, quartz crystals and mullite, also known as the aluminosilicate component. The mullite phase is produced from the combination of Al_2O_3 and SiO_2 that is formed under the high temperatures to which the coal is subjected during the coal burning process (Bai et al., 2010).

From studies conducted it was determined that the micron surface layer of CFA particles contains a significant amount of leachable material that is deposited during the rapid cooling phase after combustion (Wibberley et al., 1982). The leaching of elements from CFA has been extensively reviewed (Mattigod et al., 1990) and studies conducted around the

behaviour of CFA with water, as a simulation of how CFA is exposed in the environment, have shown that the main cations present in water extracts are calcium, sodium, potassium, magnesium and barium (Fatoba, 2007). The anions are sulphates, hydroxides and carbonates (Fatoba, 2007; . Lecuyer et al., 1996; Elseewi, et al., 1980))

The mineral and glass phases of CFA are formed over a large temperature range in the furnace environment and are unstable (Iyer, 2002). These phases dissolve and precipitate as stable and less soluble secondary phases. The dissolution and hydrolysis of the CaO and MgO oxide components of CFA causes the pH of CFA to increase. This is represented by:

$$CaO + H_2O \rightleftharpoons Ca(OH)_2 \rightleftharpoons Ca^{2+} + 2\ OH^- \quad (1)$$

$$MgO + H_2O \rightleftharpoons Mg(OH)_2 \rightleftharpoons Mg^{2+} + 2\ OH^- \quad (2)$$

This increase in pH is offset by the dissolution of soluble acid anhydrides such as B_2O_3 (boron trioxide) and salts that contain hydrolysable entities such as $Fe_2(SO_4)_3$ and $Al_2(SO_4)_3$ (Iyer, 2002).

2.4 Elements of interest

The following sub-sections will discuss the elements of interest that could be extracted from CFA. It discusses the background of the elements and the knowledge base gained from research conducted over a span of many years.

2.4.1 Silicon

More than half the chemical composition of CFA consists of SiO_2 depending on its coal source. SiO_2 itself consists of approximately 47 % elemental silicon. The mineral forms containing silica in CFA are quartz, amorphous silica and aluminosilicate minerals (mullite) (Blisset et al., 2012). Amorphous silica is the more reactive form while quartz is an extremely hard mineral that is very difficult to dissolve (Iler, 1979). Even though silicon has rather low

solubility, it tends to have quite a bit of interaction with H_2O molecules when dissolved in water. The soluble form of silica is monomeric, meaning it only contains 1 Si atom and is generally formulated as $Si(OH)_4$. It is called monosilicic acid or orthosilicic acid. Its state of hydration is not known but at high pressure there is some indication that one water molecule is probably linked to each OH group by hydrogen bonding. The hydrated molecule was represented as $Si(OH{:}OH_2)_4$ (Willey, 1974).

Reactive silica is achieved by the hydrolysis of SiO_2 in excess H_2O to create the compound monosilicic acid, H_4SiO_4, represented as follows;

$$SiO_2 + 2\ H_2O \rightleftharpoons H_4SiO_4 \qquad (3)$$

It can be re-arranged as follows;

$$SiO_2 + 2\ H_2O \rightleftharpoons Si(OH)_4 \qquad (4)$$

and is represented graphically as;

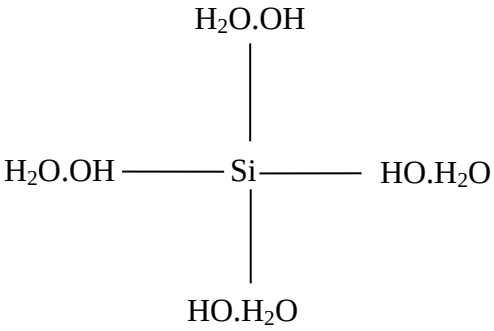

Monosilicic acid

where $Si(OH)_4$ is termed monomer to represent soluble silica. The structure of monosilicic acid is assumed to have Si co-ordinated with 4 oxygen atoms as in amorphous vitreous silica (clear, gel like silica) and in crystalline quartz (Ilyer, 1979). The stishovite (Lyon, 1962) and thaumasite (Mitsyuk et al., 1966) forms have 6 co-ordinated oxygen atoms but the common majority is 4 oxygen atoms. All these forms are essentially non-ionic in neutral and weakly acidic solutions and not transported by electrical current unless ionised in alkaline solution.

These species cannot be salted out of water nor can they be extracted by neutral organic solvents. Soluble silica can remain in the monomeric state for long periods of time in H_2O at 25°C as long as the concentration is < $2x10^{-3}$ M whereas polymerisation occurs rapidly at higher concentrations to firstly form low molecular weight polysilicic acids and then larger polymeric species recognisable as colloidal particles (Ilyer, 1979). In pure H_2O, pure amorphous silica dissolves to give monosilicic acid of 100 – 110 ppm. However if polyvalent ions such as Fe, Al etc. are present, then colloidal silicates are formed with much lower solubility than that of monosilicic acid. Iler, (1973) showed that soluble aluminium decreases the solubility of amorphous silica from about 110 ppm to 10 ppm.

Quartz (SiO_2) is the anhydride form of monosilicic acid (H_4SiO_4). For this reason, in general, quartz will not react or be attacked by acids since it can be seen to be an acid itself. Hydrofluoric acid (HF) is the only acid exception that decomposes quartz to initially form silicone fluoride (SiF_4) that converts to hydrofluorosilicic acid;

$$SiO_2 + 6\ HF \rightarrow H_2SiF_6 + 2\ H_2O \quad (6)$$

HF volatises silicon but it can be overcome by having the reaction vessel environment contained or have the volatile gas trapped in a scrubber type system set-up.

Silica is relatively un-ionised at most natural pH levels. At pH of 8.5 approximately 10% of monosilicic acid is ionised and at pH 9-10, only about 50 % is ionised.

$$pKa = \frac{[H_3SiO_4][H^+]}{[H_4SiO_4]} = 9\text{-}10 \text{ (being concentration dependent)} \quad (7)$$

2.4.1.2 Amorphous Silica

Frondel, (1962) stated that amorphous silica is not truly amorphous but consists of regions of local atomic order or crystals of extremely small size that was shown to have a cristobalite

(polymorph of quartz) structure by careful XRD studies. Under ordinary diffraction procedures the material gives a broad band without multiple peaks such as those obtained with macroscopic crystals and is thus termed amorphous. Precipitated amorphous silica is an important chemical made from the chemical reaction between a solvable silicate and an acid under certain conditions. It is widely used in plastics or as filler in rubber and paper products, coating materials, anti-sticking agents, printing ink, electronic materials etc. (Gaoxiang et al., 2009). It is also an important catalyst in the chemical industry and used as the raw material for the production of silicone (Mittal, 1997). Soluble silicates produced from silica are widely used in glass or ceramics as a major component in cement, pharmaceuticals, in cosmetics, in the detergent industry and as a bonding agent in the adhesives industry (Laxamana, 1982). Silica is also used as a precursor for a variety of inorganic and organo-metallic materials having application as catalysts in synthetic chemistry and in thin films/coatings for electronic and optic materials (Lender et al., 1990; Brinker et al.; 1990).

The silicate used in various applications is obtained via chemical means. Firstly SiO_2 in a primarily amorphous state is obtained from an acid leached residue. This amorphous silica is then reacted with NaOH to form sodium silicate. The reaction is represented as;

$$nSiO_2 + 2\ NaOH \rightarrow Na_2O.nSiO_2 + H_2O \quad (8)$$

where n represents the modulus ratio between SiO_2 and Na_2O. The modulus needs to be controlled between 3.0 and 3.4 to prepare SiO_2 of a superfine size with high specific area (Gaoxiang et al., 2009).

The solubility of amorphous silica is very low at a pH <10 and increases sharply at pH >10. This unique solubility behaviour enables reclamation of silica from rice hull ash in pure form by solubilising under alkaline conditions and subsequently precipitating at a lower pH (Iler, 1979; Kamath et al.,1998). This solubility behaviour also has relevance to CFA. Studies

conducted showed that there was increased solubility of amorphous silica at 40 °C using various strengths of 0.1N – 2N NaOH, KOH, Na_2CO_3 and K_2CO_3 (Dmitrevski et al., 1969). There is an increase in the solubility of amorphous silica from pH 9 to 10.7. This is attributed to the formation of silicate ions together with the monomer, $Si(OH)_4$, that is in equilibrium with the solid phase. Since the silicate ion is almost instantly converted to monomer in acid, both the monomer and silicate ion are therefore included in the determination of soluble silica by the molybdate reagent (an acid in itself). In this pH range amorphous silica is in solubility equilibrium with neutral monomer as well as silicate ions,

$$(SiO_2)_x + 2\ H_2O \Leftrightarrow Si(OH)_4 + (SiO_2)_{x-1} \quad (9)$$

$$Si(OH)_4 + OH^- \Leftrightarrow Si(OH)_5^- \text{ (or } HSiO_3^-) \quad (10)$$

Above pH 10.7 all of the amorphous silica present in its solid phase dissolves to form soluble silicates. This occurs due to the decrease in the concentration of $Si(OH)_4$. At this higher pH range, the $Si(OH)_4$ is converted to ionic species thereby upsetting the equilibrium so that no amorphous solid can remain in equilibrium (Iler, 1979).

2.4.1.3 Colloidal Silica and Silica Gel

Colloidal silica comprises suspensions of silica in a liquid and it forms a charged species. They are dense, amorphous silica units that have polymerised with one another. The colloidal particle diameters size range from 10 Å to 50 Å. If the particle sizes increase then the silica will precipitate out of the colloidal solution. Studies carried out by Goto et al., (1953) proved the negative charge carrying capability of colloidal silica. Electrophoresis and transport studies were carried out in a mixture of monosilicic acid, $Si(OH)_4$, in equilibrium with colloidal silica particles at pH 7-8. It was determined that the colloidal particles carry the negative charge and not the molecularly soluble monosilicic acid.

Silica gel is a rigid 3-d network of colloidal silica and is classified as an aquagel having its pores filled with water. If the aqueous phase is removed via evaporation it is termed a xerogel and an aerogel if the solvent is removed via supercritical extraction. Xerogel gels are used to prepare dense ceramics. Its high porosity and surface area leads to applications such as catalytic substrates, ultra filters and chromatography column packing materials (Brinker et al., 1990). Relatively purer forms of silica are however needed for these applications.

2.4.1.4 Silicate chemistry

(i) Dissolution of silica

The dissolution of silica is influenced by various factors but the overall requirement for dissolution is a catalyst. The dissolution can therefore be described as a depolymerisation through hydrolysis with the solubility being the concentration of $Si(OH)_4$ reached in the depolymerisation-polymerisation equilibrium (Iler, 1979). The catalyst is described as the material that is chemosorbed onto the silicon atom. It therefore increases the co-ordination number of the silicon atom on the surface to more than four thereby weakening the oxygen bonds between the silicon and oxygen (Iler, 1979).

The hydroxyl ion (OH^-) is a unique catalyst in alkaline solutions. The structure of amorphous silica has a more open arrangement than that of cristobalite (to which it is closely related) and on the surface there are large enough spaces between oxygen atoms to accommodate hydroxyl ions (Ilyer, 1979). The surface then acquires a negative ionic charge and silica is constantly being exchanged in equilibrium between solution and surface according to the following steps:

Step 1: Absorbtion of OH^-

Step 2: Si goes into solution as silicate ion. If the pH is below 11, the silicate ion hydrolyses to soluble silica $Si(OH)_4$ and OH^- ions and the process repeats

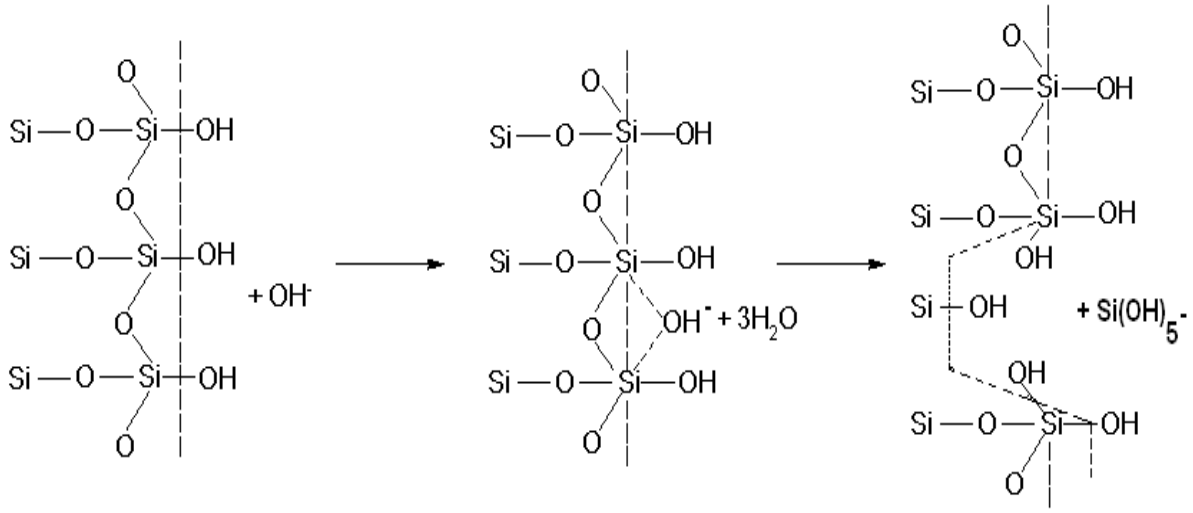

Figure 2.2: Hydrolysis of silicate ion (Ilyer, 1979)

Above pH 11, OH^- converts $Si(OH)_4$ to silicate ions and if the solution is kept unsaturated the silica continues to dissolve. Below pH 11 to pH 3, OH^- is the only rate controlling catalyst for the silica dissolution till the solution reaches saturation (Ilyer, 1979).

HF acts in the same way as depicted in Figure 2.2. There is initially chemisorption of the F^- ion, which is approximately the same size as the OH^- ion. The catalytic effect of F^- is not identical to OH^- as proven by silica dissolving in NaOH but not NaF. It requires the presence of H^+ and F^- for the catalytic effect to occur. Stöber (1963) made this important observation with stishovite, the only form of silica where Si is surrounded by 6 instead of 4 oxygen atoms, being insoluble in HF but dissolves in even weak alkali. In his observation of stishovite he saw that HF firstly converts the SiOH surface to a SiF group. The SiOH surface is hydrophilic and since the SiF group has no H atoms to bond with H_2O it renders the surface hydrophobic. Stishovite, that is much denser than quartz, has its surface converted to a close packed monolayer of hydrophobic fluorine atoms making it similar to a fluorocarbon surface. The exclusion of H_2O from the surface does not allow for dissolution to take place. Quartz on

the other hand, has a more open structured surface where the fluorine atoms are not as closely packed and water is not excluded from its surface. There is therefore still room for F^- to penetrate the surface thereby raising the co-ordination number and allowing dissolution to occur.

Certain impurities such as Al in minute amounts reduce the dissolution rate of silica. Chemisorption of Al onto the surface of silica, even if it is a monolayer reduces the solubility of silica at equilibrium. Jephcott and Johnston, (1950) showed that the apparent solubility of amorphous finely divided silica in water decreased from 0.017% at 37 °C to 0.003-0.0097 % when Al_2O_3 was added to the system. It decreased to less than 0.0001 % if powdered Al was used instead.

(ii) Silicate formation

Above pH 11, all silica will dissolve as soluble silicate. Active silica is defined by Rule, (1951) as silica that depolymerises completely to soluble silicate in 100 min at 30 °C in an excess of pH 12, 0.01M NaOH solution. Silica particles are negatively charged in alkaline, neutral or weakly acidic solutions and therefore electrostatically repel each other. When the levels of monomeric silica are too high, it polymerises with itself forming larger silica particles or nuclei onto which the silica will deposit (Iyer, 1979). This process is called a condensation process and eventually a uniform, 3-dimensional gel network of these agglomerated silicate particles are formed (Hamouda et al., 2014). Self-condensation of the monomer catalysed by OH^- ions is commonly written as

$$2\,Si(OH)_4 \xrightarrow{OH^-} (HO)_3SiOSi(OH)_3 + H_2O \qquad (11)$$

The silanol (Si-OH) group contained in the polymers condense and build up larger particles. At first the newly formed sodium silicate solution is transparent but over time the solution

becomes cloudy and thickens as the silica gel develops The polymerisation rate of the silica gel depends on pH, silica concentration, temperature and concentration of divalent cations (Hamouda et al., 2014).

The formation of a gel in the silicic acid system is brought about by the condensation of $Si(OH)_4$ into siloxane chains. These then branch out by cross-linking to form a 3-d molecular network. This siloxane gel network might be obtained under conditions where depolymerisation is least likely to occur thereby ensuring that condensation is irreversible and the siloxane bonds cannot be hydrolysed once formed. Another way of saying that the siloxane bonds are not readily broken is that the condensation polymer of siloxane chains cannot undergo re-arrangement into particles. The reaction steps for the condensation reaction to form the siloxane bond chains of the silica gel are presented in Figure 2.3 below. The mechanism requires a transition state to form oxo bridges between the Si atoms via an oxolation process.

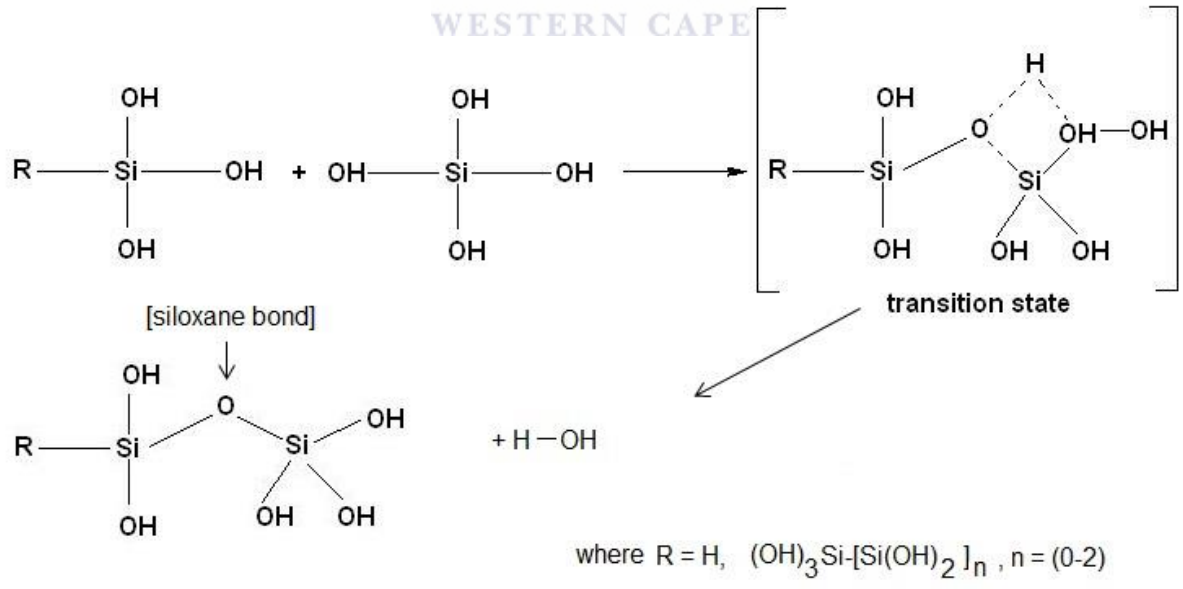

Figure 2.3: Condensation reaction for silica gel polymerisation (Trinh et al., 2006)

At low pH silica polymerises in stages to nuclei of silica that increase in size to 2 – 3 nm. These nuclei of silica then aggregate into chains to form higher molecular weight polymers.

Above pH 6-7 the behaviour is entirely different. The ionisation of polymeric species is much higher so that the monomer polymerises and decreases in concentration very rapidly. Simultaneously the particles grow rapidly to a size that is temperature dependent. Only above pH 7 can silica particles of suitable size be prepared and concentrated for industrial use. In the pH 8 - 10 range monomer polymerises to colloidal silica particles that form quickly and grow spontaneously to recognisable size (Ilyer, 1979).

As stated previously, colloidal silica consist of stable dispersions or sols of discrete particles of amorphous silica. This term excludes solutions of polysilicic acid in which the polymer molecules or particles are so small that they are not stable. These colloidal solutions can be obtained by acidifying sodium silicate solutions till neutral pH range. The colloidal solutions are used as precursors for the formation of colloidal particles (Ilyer, 1979).

Colloidal silica particles dry irreversibly to insoluble silica. Once the siloxane bond Si-O-Si is formed it cannot be broken by acid. Primary particles of colloidal silica are generally non-porous if formed or grown in alkaline solution and especially if formed at temperatures above 60 °C. Silica can be modified by the attachment of different atoms or groups to modify the physical and chemical behaviour. If the silica surface is completely covered with a layer of alumina, even as thin as 1 to 2 molecules thick, it acts as though it were a solid aluminium particle that bears a positive charge and is stable at low pH (Ilyer, 1979). Si and Al can both assume a co-ordination number of 4 or 6 toward oxygen with both having approximately the same diameter. Since the aluminate ion, $Al(OH)_4^-$, is geometrically similar to $Si(OH)_4$, an ion can be inserted or exchanged into the SiO_2 surface and thus create an aluminosilicate site having a fixed negative charge. Destabilisation of the sol can be achieved by leaching Al^{3+} from the surface at very low pH (Ilyer, 1979). Traces of aluminium are present in all commercial silicates and may still be present as $SiAlO_4^-H^+$ sites on the silica surface in sufficient amounts to contribute to the stability at pH 3.

2.4.1.5 Uses of colloidal silica

One of the earliest proposed uses of colloidal silica produced from Na silicate by ion exchange was to improve the strength of ceramic cement (Carter, 1943). Colloidal silica is used to make silica gels having surface area, pore size and mechanical strength determined by the particle size of the colloidal silica e.g. catalyst bases and adsorbents. As mentioned earlier colloidal silica particles dry irreversibly to insoluble silica. This property makes it suitable for stiffening and binding inorganic fibres and granular powders. It is used to increase the friction of surfaces ("invisible sand") for e.g. railway racks, waxed floors and textile fibres. It provides anti-sticking, anti-blocking and anti-static effect on organic films. These anti-soiling treatments also provide an ultrasmooth, oleophobic surface on porous materials by filling micopores to exclude dirt particles e.g. textiles, paper and painted surfaces. Colloidal silica forms a component of thin refractory electrically insulating films on conducting surfaces e.g. laminations in transformer cores, conducting films on insulating materials e.g. graphite coatings on paper. It is used as a polishing agent for silicon wafers used in the electronics industry. It has application in biological research where it is used in culture media and as a centrifuging medium. It is also best suited as a source of chemically reactive silica (Ilyer, 1979).

2.4.1.6 Approaches to silica removal

From the review of most of the previous work done on CFA pertaining to silicon removal, alkaline leaching seems to be the best method to extract the largest amounts of Si from CFA. Panagiotopoulou et al., (2007) determined that Si dissolution was higher when NaOH in used as the leaching reagent. For this study it was thus decided to use NaOH as the test alkaline reagent.

Extraction of Si from CFA in the form of sodium silicates is also advantageous since sodium silicate itself has a myriad of uses. SiO_2 and Al_2O_3 are soluble in NaOH and in the studies

done by Bai et al., (2010) their experimental results showed that only SiO_2 is soluble in NaOH when the temperature is below 160 °C. This information will also be applied in the extraction tests of CFA as done by Bai et al., (2010), to try and extract Al and Si separately from CFA.

Al_2O_3 and SiO_2 are both soluble in NaOH under certain conditions as represented by;

$$SiO_2 + 2\ NaOH \rightarrow Na_2SiO_2 + H_2O \quad (12)$$

$$Al_2O_3 + 2\ NaOH \rightarrow 2\ NaAlO_2 + H_2O \quad (13)$$

Their solubilities depend upon NaOH concentration, temperature, phase composition and the dissolution competition between the two ions. Various experiments conducted yielded results that indicated Al_2O_3 is insoluble in NaOH when the temperature was below 160 °C under standard atmospheric pressure (Bai et al., 2010). Bai and co-workers achieved a maximum SiO_2 extraction yield of 62.5 % leaching with a 30 % NaOH solution at 100°C for 30-60 minutes. Increasing the time to 120 min slightly decreased the SiO_2 extraction efficiency which was deduced to be an effect of the formation of insoluble aluminosilicate compounds. The time limit for silicon extraction for this study was therefore limited to two hours only and time was not considered as a variable in the leaching experiments.

Since alkaline leaching will be used to dissolve the silicon present in CFA and thereby extracting it, the sodium silicates formed in solution could be separated from the CFA solid residue and then precipitated with an acid medium. The reaction would be stopped when the pH range is around 7. The solution could then be slowly filtered off from the silica gel formed and the gel allowed to air dry.

2.4.2 Iron

Iron is present in CFA in its oxide form that originates from the oxidation of iron sulphides such as pyrite and marcasite present in coal during coal combustion for electrical power generation. The crystalline phases of the CFA iron oxide are magnetite, hematite and maghemite. Iron oxide is present in CFA in the range of 2 % - 12 % depending on where the coal was sourced from. Iron is also introduced from the degradation of the iron grinding balls used in the coal milling process.

2.4.2.1 Approaches to iron recovery

Iron can be extracted from CFA via the conventional acid leaching treatments. However since the ash contains a multitude of components, it is actually possible to remove the magnetic component of CFA via magnetic extraction techniques without chemically altering the CFA to a great degree (Gilbert, 2013). This method is a physical separation process that does not require costly corrosive acid lixiviants but instead the magnetic component is removed by magnetic stirring. This method also proves to be non-destructive in that the CFA residue after magnetic treatment could be re-used for another waste recycling process such as Si or Al extraction.

Magnetic extraction could be undertaken under dry conditions that require special apparatus specifically tailored for the process. Electromagnets are usually used to provide the strong magnetic fields necessary to execute the dry extraction (Shumkov, 2002; Shumkov 2004). The CFA is normally passed around a magnetic drum where the particulate magnetic material is removed and suspended onto the drum. The non-magnetic CFA ash residue is re-collected for possible secondary waste recycling. An alternate method of magnetic extraction would be a wet technique. The CFA is mixed with water and stirred at high rpm to agitate the CFA particles to form a slurry. The slurry is then stirred while subjected to a strong magnetic field that retains the magnetic material and allows for the non-magnetic CFA residue to be

decanted (Gilbert, 2013). On a large scale it is stirred in a magnetic drum. Non-magnetic crystalline phases such as quartz, aluminium and calcium silicates are also removed along with the magnetic components. This is due to the micro sized CFA particles that remain in the magnetic extract. Shoumkova, (2006) extracted magnetic material from Bulgarian CFA and the main iron containing crystalline phases were determined to be impure maghemite, hematite and Ca – Fe oxide. The different iron crystalline phases differ in magnetic strength from each other. Maghemite and magnetite are strongly magnetic while hematite and goethite are weakly magnetic. There are non-magnetic fractions such as FeS (pyrite), iron containing aluminosilicate crystals and glassy phase iron compounds also present in the CFA which would make it difficult to achieve 100 % extraction of Fe containing species in the CFA using magnetic extraction. The biggest advantage of using the magnetic extraction step, for the greater effect of isolating Fe containing compounds in the CFA, is that it minimises chemical and to an extent physical degradation of the CFA. This makes it possible for the CFA to be recycled again for extraction of components of value; which otherwise would have been damaged/ degraded or altered by chemical extractions. Trivalent iron oxides are sparingly soluble in 4 M – 5 M alkaline solutions having approximate solubility of 100 ppm at temperatures between 120 °C and 220 °C. The solubility is much lower, approximately 1 ppm if the alkaline leaching takes place at 60 °C (Basu, 1983; Hudson et al., 2000). This very low solubility results in the trivalent iron oxides being highly non-leachable under atmospheric pressure and elevated temperatures in highly alkaline solutions of sodium hydroxide (Mazzocchitti et al., 2009). This additional knowledge will help minimise iron contamination when the alkaline leaching for silicon extraction from CFA is performed.

2.4.2.1.1 Potential uses of reclaimed iron oxide from CFA

Another interesting point that was noted was that silica or waste reclaimed silica modified with FeO can be used as a low cost absorbent for metal removal (Unob et al., 2007). Due to

iron oxides having high surface area and surface charge, it has been previously used in water treatment as flocculant for organic compounds and for metal removal in its hydroxide form (Eckenfelder, 2000).

Silica gel is commonly used in the purification and separation of organic mixtures because of its absorption properties, high surface area and its porosity (Unob et al., 2007). Zeng, (2003), proposed a method for preparing silica containing iron (III) oxide adsorbent to remove arsenic from water. Unob and co-workers, (2007) determined that Fe_2O_3 coated silica had higher absorption efficiencies for metal ions Pb^{2+}, Cu^{2+}, Cd^{2+}, Ni^{2+} than uncoated silica. The optimal pH for recovery was between 6 and 7 and the presence of salt decreased removal efficiency. Potentially the magnetically removed iron oxides from CFA could be re-introduced into the extracted silica from CFA and be used as a metal absorbent.

2.4.3 Aluminium

Al_2O_3 occurs naturally in its mineral ore bauxite and is the main source of aluminium in the world. CFA generally contains 26 – 31 % Al_2O_3 with bauxite containing 30 – 60 % Al_2O_3 (Authier-Martin et al., 2001). This makes CFA suitable as bauxite substitute. However the higher silica content of CFA and the aluminium occurring mainly in the chemically stable mullite form leads to lower aluminium yields and high operating costs if the commercial Bayer process is used (Yao et al., 2014).

An important property of aluminium is that it is amphoteric, meaning that it is soluble in an acidic or alkaline medium and is recoverable by chemical as well as hydrometallurgical means (Shemi et al., 2012). Aluminium recovery from bauxite makes use of the hydrometallurgical method since the ore has less silica content and impurities compared to CFA. This just means that the aluminium extracted from CFA is more susceptible to contamination from other elements e.g. iron, calcium etc. due to co-dissolution and co-

precipitation. The mineralogical composition of CFA also determines the ease of metal content leaching from its matrix (Soroczak et al., 1987).

Earlier investigations into the possibility of recovering aluminium from CFA were conducted by Grzymek in Poland during the 1950s (Hosterman et al., 1990), mainly driven by the economic sanctions imposed on bauxite trading during the cold war. The developed process initially comprised of forming a CFA sinter containing calcium aluminates and dicalcium silicate. The sinter was then mixed with sodium carbonate and after a series of chemical reactions, that included carbonisation and water scrubbing, produced alumina (Al_2O_3) and portland cement (Grzymek, 1976). The USA also began to realise the concept of CFA as an aluminium resource during the late 70s and early 80s since the stockpile of CFA was growing steadily and could serve as a good substitute for the shortage of aluminium from domestic sources (Kelmers et al., 1981; Felker et al., 1982). Their recovery process used direct acid leaching (DAL) in relatively strong acid conditions of 6 – 8 N (Kelmers et al., 1981; Kelmers et al., 1982).

CFA has two aluminium containing phases, the amorphous phase and the mullite crystal phase (Nayak et al., 2009; Matjie et al., 2005). The crystalline mullite phase is not directly soluble in acidic media but the non-crystalline amorphous phase is, making its recovery relatively easier. Indirect acid leaching involves a pre-conditioning step where the CFA is sintered with an alkaline or carbonate compound at high temperatures in the region of 1000 °C. The sintered end product is then leached with acid media to extract the aluminium content of both the amorphous and crystal mullite phases (Shemi et al., 2014). Direct acid leaching has the advantages of having low running costs, milder processing conditions and lower energy demand. Indirect acid leaching has the disadvantage of higher energy consumption but the advantage of higher aluminium recovery efficiencies (Shemi et al., 2014).

2.4.3.1 Approaches to Aluminium recovery

Research has been conducted since the 1980s using CFA as an alternative source to bauxite and to development new ways for aluminium recovery (Yao et al., 2014). There are three main methods of recovering aluminium from CFA. A brief overview of these three methods will be discussed and provides an account of the research that contributed to the development of these methods.

Aluminium can be extracted via

i) Indirect acid leaching, more accurately known as lime sinter processing that may be further upgraded to lime - soda sintering
ii) direct acid leaching and
iii) the Hichlor process

(i) Lime - Sinter Processing/ Indirect acid leaching

Lime sinter processing is a modification of the Pederson process, (Pederson, 1924; Pederson 1927), that is used to manufacture pig iron and calcium aluminate slags from a mixture of bauxite, iron ore, coke and limestone (Yao et al., 2014). The Pederson process for aluminium recovery can be described briefly as leaching the metal oxide slag with a sodium carbonate solution. In the lime - sinter process, limestone (a sedimentary rock form of calcium carbonate) is added to CFA and reacted in the temperature range of approximately 1100 °C to form a sintered end product containing calcium aluminate and dicalcium silicate. The sintered end product is mixed with a liquid extractant of either H_2O or a dilute alkaline solution of Na_2CO_3 or NaOH (Padilla et al., 1985a; Padilla et al., 1985b). The effectiveness of the separation is based on the advantage of calcium aluminate being soluble in the liquid extractant while the insoluble calcium silicate remains in the solid residue. After the extraction, CO_2 is bubbled through the leachate to precipitate the aluminium as $Al(OH)_3$ and

thereafter calcining the precipitate to produce α-Al_2O_3 and γ-Al_2O_3. The solid residue obtained after the leaching step, rich in calcium silicates, is sintered again and then mixed with gypsum ($CaSO_4$) during a grinding process to manufacture cement (Yao et al., 2014).

The chemical process of the sinter step serves to activate the CFA. The limestone is decomposed to CaO at high temperature and reacts with the inactive mullite and quartz of the CFA to form 12 $CaO.7Al_2O_3$ (calcium aluminate) and 2 $CaSiO_2$ (calcium silicate). The formation of 12 $CaO.7Al_2O_3$ is an essential requirement in the recovery process because it dissolves very readily in a liquid extractant to form $NaAlO_2$ (sodium aluminate) while 2 $CaSiO_2$ is insoluble. This makes the isolation of the aluminium species of CFA possible. The chemical reactions for the sinter step are as follows, (Yao et al., 2014) ;

$$CaCO_3 \xrightarrow{\Delta} CaO + CO_2 \quad (14)$$

$$7\,(3Al_2O_3.2SiO_2) + 64\,CaO \xrightarrow{\Delta} 3\,(12CaO.7Al_2O_3) + 14\,(2CaO.SiO_2) \quad (15)$$

$$3\,Al_2O_3.2SiO_2 + 5\,CaO \xrightarrow{\Delta} 3\,(CaO.Al_2O_3) + 2\,(CaO.SiO_2) \quad (16)$$

$$2\,CaO + SiO_2 \xrightarrow{\Delta} 2\,CaO.SiO_2 \quad (17)$$

A phenomenon termed auto-disintegration occurs when the sintered product cools to < 500 °C. The sintered matrix literally shatters to form a fine powder thereby mitigating the need to grind the sinters. The auto-disintegration phenomenon has been ascribed to occur from the transformation of the metastable monoclinic β – polymorph of 2 $CaO.SiO_2$ to its orthorhombic γ - polymorph form. The transformation entails an 11 % volume increase which results in the matrix self-shattering (Eriksson et al., 2004; Guzzon et al., 2007).

The cooled sinter leaching reactions, using Na_2CO_3 solution as the extracting medium, are represented as follows;

$$12CaO.7Al_2O_3 + 12\ Na_2CO_3 + 5\ H_2O \rightarrow 14\ NaAlO_2 + 12\ CaCO_3 + 10\ NaOH \quad (18)$$

$$3CaO.Al_2O_3 + 3\ Na_2CO_3 + 2\ H_2O \rightarrow 2\ NaAlO_2 + 3\ CaCO_3 + 4\ NaOH \quad (19)$$

$$CaO.Al_2O_3 + Na_2CO_3 \rightarrow 2\ NaAlO_2 + CaCO_3 \quad (20)$$

$$2CaO.SiO_2 + 3\ Na_2CO_3 + H_2O \rightarrow 2\ CaCO_3 + 2\ Na_2SiO_3 + 2\ NaOH \quad (21)$$

$$2CaO.SiO_2 + 2\ NaOH + H_2O \rightarrow 2\ Ca(OH)_2 + Na_2SiO_3 \quad (22)$$

As can be seen some from chemical equations (21) and (22) above, the dissolution of small amounts of silicon during leaching is unavoidable. The lime sinter process therefore includes an aluminium purification step before it is precipitated as $Al(OH)_3$ (aluminium hydroxide) (Yao et al., 2014). De-silication is achieved by adding $Ca(OH)_2$ (calcium hydroxide) and precipitating calcium aluminosilicates of relatively low solubility. The chemical reactions are represented as follows;

$$2\ Na_2SiO_3 + 2\ NaAlO_2 + Ca(OH)_2 + 2\ H_2O \rightarrow CaO.Al_2O_3.2SiO_2 + 6\ NaOH \quad (23)$$

$$Na_2CO_3 + Ca(OH)_2 \rightarrow CaCO_3 + 2\ NaOH \quad (24)$$

Carbonisation of the desilicated $NaAlO_2$ solution is carried out by blowing CO_2 gas from the bottom of the solution while stirring vigorously. The $NaAlO_2$ is hydrolysed to precipitate $Al(OH)_3$ as the solution pH changes. The chemical reactions are represented as follows;

$$2\ NaAlO_2 + CO_2 + 3\ H_2O \rightarrow Na_2CO_{3(l)} + 2\ Al(OH)_{3\ (ppt)} \quad (25)$$

$$2\ NaOH + CO_2 \rightarrow Na_2CO_3 + H_2O \quad (26)$$

The precipitated $Al(OH)_3$ is then calcined to form alumina;

$$2\ Al(OH)_3 \xrightarrow{\Delta} Al_2O_3 + 3\ H_2O \quad (27)$$

(Yao et al., 2014)

The lime - soda sintering process was first patented by Kayser in 1902 to separate Si from Al (Yao et al., 2014). It differs from the lime sinter process by the inclusion of sodium carbonate soda (Na_2CO_3) in the lime sintering step to form the same soluble sodium aluminate and insoluble calcium silicates. The sintered end product is then also leached with either H_2O, dilute NaOH or sodium carbonate solution. A similar de-silication step to refine the sodium aluminate solution is included before precipitation of $Al(OH)_3$ and lastly calcining it to form alumina. The inclusion of the soda helps to increase the aluminium extraction efficiency.

The US Oak Ridge National laboratory developed the calsinter process (Yao et al., 2014). In the calsinter process CFA is mixed with gypsum ($CaSO_4$) and limestone prior to sintering at 1000 °C – 1200 °C. The sinter end product is then leached with dilute acid and the metals of value recovered from the filtrate. Goodboy, (1976) reported a study of alumina extraction from coal waste products and clays mixed with limestone and $CaSO_4$. 90 % Al extraction was achieved after sintering at 1200 °C for 5 minutes.

The sinter process has been modified and tested for various mixtures and conditions. Salt-soda sinter, ammonium sulphate sinter and fluoride sinter have been tested. In the salt-soda sinter process, a NaCl - Na_2CO_3 - CFA mixture was sintered and thereafter the sinter quenched in water before being leached with a dilute acid solution. Decarlo et al., (1978) studied the effect of individual component sintering of the salt- soda sinter process for aluminium recovery. In their study CFA was sintered with NaCl at 1050 °C for 2 hours and leached with Na_2CO_3 and nitric acid solutions. An aluminium recovery of 27 % was reported. When the CFA was sintered with Na_2CO_3 at 1050 °C for 2 hours an aluminium recovery of 66 % was reported. Decarlo and co-workers also reported a sinter mixture of CFA - $CaCl_2$ - Na_2CO_3 and another sinter mixture of CFA - NaCl - $CaCO_3$. Both mixtures were sintered at 1050 °C for 2 hours and thereafter leached with H_2O and HNO_3. The aluminium recovery yields were 78 % and 74 % respectively. Another study conducted by Decarlo and co-

workers tested a $CaCl_2$ - $CaSO_4$- NaCl - CFA sinter mixture at 700 °C and thereafter leached with 2N H_2SO_4. An aluminium recovery yield of 30 % was reported.

In US patent 4254088, McDowell et al., (1981), sintered a NaCl - Na_2CO_3 - CFA mixture at 700 °C - 900 °C. The sintered product was then leached with either nitric or sulphuric acid and a 90 % - 99 % aluminium recovery was achieved. Nehari et al., (1996) did a study using hydrated $CaCl_2$ for the CFA sinter mix. The sintering temperature was 1000 – 1100 °C and the sintered end product was leached with HCl to recover the aluminium in the form of crystallised $AlCl_3$. Tong et al., (2008) sintered a CFA-KF mixture at 800 °C. The sintered end product was then leached with HCl to attain a 96 % aluminium recovery.

(ii) Direct acid leaching

Direct acid leaching avoids the sintering step and uses H_2SO_4, HCl and HNO_3 in the leaching of CFA. However, direct acid leaching is not recommended at ambient temperature using low acid concentrations since the Al yields are very low (Kelmers et al, 1982; Seidel et al., 1998). Acid leaching is primarily the method of choice for aluminium recovery since it helps to alleviate the high silica content problem of CFA. It uses the advantage of silica being relatively insoluble in acidic media as opposed to alkaline media that is capable of dissolving both silica and aluminium material (Nayak et al., 2009; Shcherban et al., 1995).

Direct acid leaching uses the chemical mechanism of proton attack to achieve the aluminium recovery. However, it is unfortunately not specific since it also leaches other components present in the CFA as well viz. iron, titanium, calcium, magnesium etc. Seidel et al., (1998) stated that the dissolution of Al and Fe from CFA with a H_2SO_4 lixiviant is assumed to be an irreversible, heterogenous non- catalytic reaction. The hydronium ion, H_3O^+, displaces the cation from the ash particle matrix to induce dissolution of the metals. The hydronium ions react with the solid aluminium, iron and other metal compounds that are progressively

exposed on the surface and within the pores of the CFA particles as the leaching proceeds. The chemical reactions describing the dissolving of the major element compounds in CFA that include Al and Fe are represented as follows;

$$3\ H_2SO_4 + 2\ H_2O \rightleftharpoons 2\ H_3O^+ + SO_4^{2-} \quad (28)$$

$$MO + 2\ H^+ \rightleftharpoons M^{2+} + H_2O \text{ where (M = Ca, Mg, Fe, etc.)} \quad (29)$$

$$J_2O + 2\ H^+ \rightleftharpoons 2\ J^+ + H_2O \text{ where (J = Na, K, etc.)} \quad (30)$$

$$Al_2O_3 + 6\ H^+ \rightleftharpoons 2\ Al^{3+} + 3\ H_2O \quad (31)$$

$$Al^{3+} + 3\ H_2O \rightleftharpoons Al(OH)_3\downarrow + 3\ H^+ \quad (32)$$

$$Fe_2O_3 + 6\ H^+ \rightleftharpoons 2\ Fe^{3+} + 3H_2O \quad (33)$$

$$Fe^{3+} + 3H_2O \rightleftharpoons Fe(OH)_3\downarrow + 3\ H^+ \quad (34)$$

$$Ca^{2+} + SO_4^{2-} \rightleftharpoons CaSO_4 \quad (35)$$

Seidel et al., (1998), obtained lower aluminium extraction yields when higher amounts of CFA were present in the sulphuric acid leaching medium. This was due to $CaSO_4$ deposition originating from the reaction between leached calcium ions from the CFA and sulphate ions from the H_2SO_4. The $CaSO_4$ deposits within and around the active leaching sites of the CFA particle matrix. This lowers the reaction mass transfer between the CFA particles and acid media (Seidel et al 1998). It was coined as the self-inhibiting effect of CFA.

To alleviate this problem, Seidel et al., (1998) used a pre-conditioning step before sulphuric acid leaching. The CFA was pre-leached with a hydrochloric acid solution maintained at pH 4 for 24 hours to partially remove calcium ions from the ash matrix. The kinetics of the aluminium leaching increased when it was leached with sulphuric acid thereafter. However the calcium extraction step was also not specific since iron, calcium, as well as aluminium were present in that HCl pre - leach matrix. It has been proposed that the glassy phase of CFA easily dissolves while the more stable quartz and mullite phases remain or dissolve

extremely slowly. Attempts have thus been made to enhance and increase the efficacy of the aluminium recovery process by acid leaching of CFA. Wu et al., (2012) conducted acid leaching under high pressure. Their optimum experimental conditions were determined to be a 50 % H_2SO_4 solution maintained at a temperature of 180 °C and a four hour leaching time. The aluminium recovery yield was 82 %.

Industrial applications of the acid leach processes have not been readily pursued due to the excessive use of acid and fluoride. A method to overcome this limitation was to calcine the CFA and then leach with sulphuric acid under heated conditions. Matjie et al., (2005) calcined a CFA – CaO mixture at 1000 °C – 1200 °C. The optimal parameters for their aluminium leaching study were determined to be a 6.12 M H_2SO_4 solution maintained at a temperature of 80 °C for 4 hours to achieve an aluminium recovery yield of 85 %.

Ji et al., (2007) carried out a study where a CFA – soda mixture was calcined at 900 °C to form soluble aluminates to be leached with sulphuric acid. The aluminium extraction yield reached approximately 90 %. Bai et al., (2011) and Liu et al., (2012) omitted the addition of lime and soda to the CFA in the sinter step. Instead they used an acid sinter leaching process where a CFA - concentrated H_2SO_4 sinter mixture was calcined in order to convert most of the aluminium in the CFA into $Al_2(SO_4)_3$. This aluminium sulphate was then extracted with hot water and thereafter calcined to form alumina. An aluminium recovery of 70 % - 90 % was achieved with lower processing temperatures and less solid residue.

(iii) Hichlor process

The third recovery method, the hichlor process, provides an alternative to extract aluminium as well as other metals from CFA and was first investigated by Burnet et al., (1977). The first step was to subject the CFA to a magnetic separation. In that study, approximately a third of the iron remained with the non-magnetic fraction and about 10 % of the total aluminium

content in the CFA was removed along with the magnetic fraction. The non-magnetic fraction was then mixed with carbon and chlorinated in a fixed bed to convert the aluminium in the CFA to $AlCl_3$. This aluminium chloride was then electrolytically decomposed to aluminium. Compared to the electrolysis step in the bauxite process, the hichlor process used approximately 30 % less energy. However, the aluminium extraction efficiency of the hichlor process was only maximised at 25 %.

Another extraction method was carried out by Shemi et al., (2012). They tested the recovery of aluminium from CFA via a gas phase extraction technique using acetylacetone, a metal chelating beta diketone ligand, as the extractant. The acetylacetone was vaporised and passed through a 50 g bed of CFA. The extraction efficiency was 17.9 % after 6 hours at 250° C using an acetyl acetone flowrate of 6 ml/min. Shemi et al., (2012) also conducted a direct acid leaching test of aluminium using sulphuric acid. Their optimium experimental parameters gave 23.5 % aluminium extraction after 8 hours 45 min at 75° C using 50 g CFA samples.

The leaching process of CFA described by Cussler, (1984) was considered to be a shrinking core model framework of heterogenous, non-catalytic reactions. The shrinking core model assumes that the reaction products and/or the inert matter remaining in the solid phase form an ash coating that encapsulates the unreacted core (Cussler, 1984). In the Perry's chemical engineers handbook, Kuang-Hui Lin, (1984) made the assumption that the continual formation of a solid reaction product as well as inert material coinciding with the reduction of the unreacted core material size would leave the particle size unchanged. The degree of aluminium recovery was found to decrease when more CFA was used in the leaching medium. The result could not be explained by mass action laws of dissolution reactions but instead by mass transfer concerns. It was shown by Seidel et al., (1999) that the leaching process exhibited a self- inhibiting mechanism where the precipitation of $CaSO_4$ on the

surface and within the pores of the CFA particles blocks the reaction between the H_2SO_4 lixiviant and the unreacted core of the CFA particle.

2.5 Characterisation methods

XRF and XRD analytical techniques are useful in characterising the solid samples in respect of determining the major and minor elements levels as well as the mineral phases present in CFA. Laser ablation ICP-MS is used to characterise the trace metals present and ICP-OES and UV-Visible spectroscopy is used to measure elements leached elements from CFA.

2.5.1 X-Ray Fluorescence Spectrometry

X-Ray Fluorescence (XRF) spectrometry is a useful rapid analytical technique which is relatively inexpensive for the determination of the major and minor element composition in soils, rocks and other materials. (Sumner, 2000). The basis of the XRF analytical technique is to measure the secondary characteristic x-rays emitted by the elements present in the sample after being irradiated with white x-rays (x-rays of continuous energy distribution) generated from a primary x-ray producing source commonly an x-ray tube but it could also be a synchrotron (a type of particle accelerating device that uses bending magnets to accelerate charge particles in a circular path to produce x-ray radiation) or a radioactive source. The secondary fluorescent x-rays are diffracted by a rotating analysing crystal that separates the fluoresced x-rays into the various x-ray wavelengths present. The x-ray wavelengths detected are characteristic (specific) to each element and are used to determine what element is present as well as quantifying the amount of element present in the sample (Sumner 2000, Brouwer, 2010).

2.5.2 Inductively Coupled Plasma Optical Emission Spectrometry

Inductively coupled plasma optical emission spectrometry (ICP-OES) is a popular analytical tool for elemental analysis. The ICP-OES technique involves the uptake of a liquid sample that has been aspirated via a sample delivery system called a nebuliser. The aspirated sample mist is injected by the nebuliser into argon gas plasma that is maintained by a radio frequency (RF) source. The core of the plasma maintains a temperature of approximately 10 000 K (9727 °C) and allows quick vaporisation and drying of the sample mist particles. This process releases free atoms of the analyte elements in the gaseous state which are excited to higher energy states by the collisions between these particles due to the high plasma temperature. There is ample energy available to also convert the atoms to ions that are in turn promoted to higher energy states. These atoms and ions then release photons upon return to the ground state characteristic to that specific element. These characteristic photons have wavelengths that can be measured to identify the elements and the total number of photons is directly proportional to the concentration of the element present in the sample (Hou et al., 2000). The concentrations of the analyte elements are then determined from known calibration standards.

2.5.2.1 Laser ablation Inductively Coupled Plasma (ICP) Mass Spectrometry

Laser ablation ICP-MS spectrometry uses a solid sampling technique of laser ablation to introduce the sample into the inductively coupled plasma mass spectrometer.

2.5.2.1.1 Laser Ablation

LASER is an acronym that stands for light amplification by stimulation of emitted radiation. Due to its light amplifying property, a laser is able to produce spatially narrow and very intense beams of radiation all having identical frequency, phase, direction and polarisation properties These lasers are focussed onto a sample and the photons are converted to thermal energy due to the irradiation of the spot where the laser is focussed. This thermal energy

causes vaporisation of the sample and this entire process is called laser ablation, the removal of sample material from a sample's surface by means of laser vaporisation. The ablated material is then carried away by an argon gas stream into the ICP-MS instrument. The laser ablation thus acts as the nebuliser described in Section 2.5.2. The actual interaction between the laser and the sample material is a complex process. It consists of;

(1) ablation (vaporisation)

(2) ejection of atoms, ions, molecular species and particulates

(3) shock waves

When the laser strikes the sample's solid surface, electronic excitation occurs inside the solid sample material. Electrons are ejected from the sample surface through photoelectric and thermionic emission (heat energy induced electron emission from the sample material). At the same time the energetic electrons in the bulk of the solid material transfer energy to the sample's lattice through a variety of scattering mechanisms to cause the sample target spot melt and vaporise. Ionisation takes place and an expanding plasma plume consisting of the sample constituents interacts with the surrounding gas to form a shock wave. This shock wave further ionises the surrounding air and exerts a force back onto the sample target spot that flushes out the melted volume to be swept away to the ICP-MS (Borisov et al., 2000).

2.5.2.1.2 Inductively Coupled Plasma (ICP) Mass Spectrometer

ICP-MS was commercially introduced in 1983 and it combines an ICP source with a mass spectrometer. The plasma of the ICP is used to make positively charged ions that are sent to the mass spectrometer via an interface region that is maintained under vacuum at 1 – 2 Torr by a mechanical pump. The interface region is comprises of two metallic cones usually made of nickel, named a sampler and skimmer cone that are spaced a small distance apart parallel to each other. The first sampler cone has an orifice 0.8 - 1.2 mm wide and the second

skimmer cone has an orifice size of 0.4 – 0.6 mm wide. These interface cones act as a filter to limit the amount of total dissolved solids that can be introduced into the mass spectrometer. A grounded metal disk called a shadow stop is placed inline. Its purpose is to block particulate matter, neutral species and photons emitted from the intense energy plasma source from reaching the detector (Thomas, 2004). The commonly used mass spectrometer is the quadrupole mass filter and its function is to separate the ions by their mass to charge ratio. It consists of 4 rods, 10 mm in diameter and 150-200 mm long, in a 2 x 2 parallel arrangement. The rods are conductive and are made from either gold coated ceramic or molybdenum. AC and DC voltages are applied to each set of opposing rod pairs. These voltages are rapidly switched with an RF field to form an electrostatic field that acts as a filter allowing only the passage of ions with a single mass to charge (m/e) ratio through the rods to the detector at any given time. The settings on the quadrupole are changed for each specific m/e ratio at a time. The quadrupole therefore acts as a sequential filter working at a very rapid rate due to the switching voltages (Thomas, 2004).

2.5.3 X-Ray Diffraction Spectroscopy

In 1912, Maz von Lue found that crystals could diffract x-rays (Malainey, 2011). X-ray diffraction technique can be described using the analogy of a light microscope. In light microscopy, light is either reflected from or transmitted through an object. The overall effect in both instances is that the scattered light is focused by a series of lenses to form an image of the object. The image can be magnified infinitely but the maximum resolution is tapered to 0.2 microns, the wavelength of visible light (van Holde, 1998).

Diffraction is the scattering of x-rays by the ordered crystal structure of the material. As the x-rays strike the surface of a sample, one part of it is scattered and the other part of it

transmitted to the next layer of atoms present in the sample. The process repeats again where part of the x-ray is scattered and the other part transmitted to the next layer of atoms.

In XRD instrumentation the angle of incidence, theta (θ), of the incoming x-ray beam is changed by moving the x-ray source in a clockwise arc direction and the detector in an ant-clockwise arc direction while the sample remains stationary. The arc rotational movement of the x-ray source and detector are done by the goniometer which is the central part of the XRD diffractometer. 155° 2θ is the maximum angle that the detector can read without the detector and x-ray source knocking into each other (Birkholz, 2006). When the x-ray beams that are diffracted between the layers are in phase, constructive interference takes place and a diffraction peak is obtained. If it is out of phase then destructive interference takes place and no diffraction peak is obtained. Since the x-rays cannot be focused by lenses as in light microscopy to form an image of the object, mathematical calculation is used as the lens to transform the diffraction pattern back into the original structure (van Holde, 1998). The x-rays scattered from the repeating array of molecules from the ordered crystal structure give a pattern representing the macromolecular order and structure of the crystal. Since a crystal structure is needed to scatter the x-rays, non-crystalline amorphous materials will not exhibit prominent diffraction peaks for amorphous material. The XRD technique is therefore limited to materials that have crystal forms. XRD also has size limitations in that it is more accurate for measuring large crystalline structures where often nanosized structures present in trace amounts will go undetected by XRD analysis (Malainey, 2011).

2.5.4 Ultraviolet – Visible Spectroscopy

Ultraviolet – visible spectroscopy, commonly abbreviated as UV-Vis spectroscopy, is used to measure and provide information about the transition of the external electrons of atoms. It has application in physical and analytical chemistry to identify substances through the amount of

the spectrum absorbed by the particular substance of interest. The ultraviolet (UV) region is situated from 100 nm to 350 nm wavelengths on the electromagnetic spectrum. The visible (Vis) region is situated form 350 nm to 800 nm on the electromagnetic spectrum. Light in the UV-Vis region is able to excite electrons in low energy molecular orbitals to high energy anti-bonding molecular orbitals. Routine UV-Vis spectroscopy use wavelengths greater than 200 nm since it is useful for measuring molecules containing conjugated bonds, carbonyl compounds, metal complexes and aromatic groups that absorb energy with longer wavelengths. The substance of interest can therefore be quantified by this method using the Beer – Lambert law that relates the absorption of radiation to the properties of the material through which it is passing. The Beer – Lambert law states that there is a logarithmic dependence between the transmission, T, of light through a substance and the product of the absorption co-efficient of the substance, α; and the distance the beam travels through the material (i.e. the path length, *l).* The absorption co-efficient can then be written as the product of molar absorptivity (ε) and concentration (c) of absorbing species in the material. For liquids the relation is written as:

$$\log T = \log \frac{I}{I_0} = \varepsilon l \qquad (36)$$

where I and I_0 are the intensity of incident and transmitted light respectively. Transmission can also be expressed in terms of absorbance (A), as A = -log T. This translates into the Beer – Lambert equation being written as A= ε*l*c (Malainey, 2011).

UV-Vis spectroscopy was used to measure Si in this study since the method is specific to Si and does not suffer potential interference from aluminium present in the sample when analysed by ICP-OES. The silicomolybdic spectrophotometric method makes use of silicic acid forming silico-12-molybdic acid, a heteropolyacid, in an acidified ammonium heptamolybdate medium. It is represented as;

$$7\ Si(OH)_4 + 12\ H_6\,Mo_7\,O_{24}{\cdot}4H_2O + 17\ H_2O \Leftrightarrow 7\ H_4SiMo_{12}O_{40}{\cdot}29H_2O \qquad (37)$$

The resulting molybdic silicic acid is a yellow compound that can be measured spectrophotometrically in the visible region of the electromagnetic spectrum at 400 ± 10 nm. There are two isomeric forms of molybdate silicic acid, the alpha (α) and beta (β) isomers, which differ only by their degree of hydration and their formation is pH dependent. The α-form is present between pH 3.8 and 4.8 and very stable once formed while the less stable β-silicomolybdate form is present between pH 1.0 and 1.8 (Truesdale, 1975).

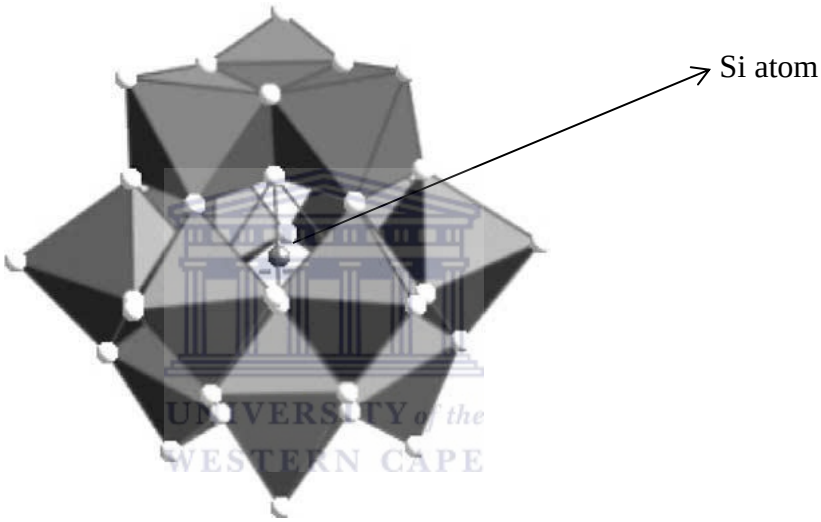

Figure 2.4: Silicomolybdic acid cluster (Coradin et al., 2004)

The silicomolybdic acid is a cage-like structure as illustrated in Figure 2.4 above. The silicon atom is located in a tetrahedral cavity of oxygen atoms belonging to four of the twelve MoO_6 octahedra of the heteropolyacid (Feist et al., 1980). Since only one Si atom is able to be incorporated into the silicomolybdic cluster only monomeric silicic acid $Si(OH)_4$ can form the yellow compound.

The disadvantage of the yellow molybdic silicic acid compound is that if phosphate ions are present in the analyte solution, yellow phosphomolybdic polyacid will also be formed that measures at the same wavelength as silicomolybdic acid. The intensity of the yellow colour of the silicomolybdic acid is also too low. It was shown by Schwartz, 1942 that oxalic acid

can be used to break the phosphomolybdic complex. This was therefore adopted into the method and it also prevents any excess molybdate from reacting further (Coradin et al., 2004). The yellow silicomolybdic acid complex is then reduced with a suitable reducing agent that yields an intense blue coloured complex commonly named the molybdenum blue complex. Ascorbic acid is used but other reagents such as p-methylaminophenol sulphate and sulphite could be used as well (Mullin et al., 1955; Truesdale, 1975). Care has to be taken to add the reductant reagent directly after adding the oxalic acid since the silico complex has very limited stability in oxalic acid. The blue complex stabilises 30 minutes after the oxalic and reducing agent are added to the heteropoly acid and remains stable for a few hours (Grasshoff et al., 1999). The absorption maximum of molybdenum blue complex reads at 810 nm and has an extinction co-efficient, ε, of 44700 ± 150 L mol^{-1} cm^{-1}. This allows concentrations as low as 5×10^{-6} mol L^{-1} to be accurately measured (Isaacs, 1924; Coradin et al., 2004).

Since the silicomolybdate complex is only formed from one $Si(OH)_4$, it is important to dilute the sample to an acceptable level where Si remains in the monomer state and does not start co-agulating together to form dimers, trimers, oligomers and the gel network of silica that forms when the solution is allowed to stand. The monomer would be stable till about 200 ppm, therefore dilution of the leach solution would need to be diluted immediately to this range and stored till the analysis can be undertaken. The samples should be stored in plasticware (polycarbonate, polyethylene or polypropylene) to prevent interference from silica glass.

2.6 Literature review assessment for this study

From the background information and review of aluminium extraction it was seen that the sinter methods use extremely high temperatures and require labware that can withstand these

test conditions. Specialised equipment would also need to be designed for the pressure leaching tests which would increase the costs if up scaling of the process would be considered. The sinter projects, although having very good extraction yields, also pose the question of energy consumption which ultimately may add to the costs of production of CFA by increasing the need for increased electricity supply. However, due to improvements in industrial and electronics applications, induction principle based furnaces using less energy to provide high temperatures should become cheaper over time. The main advantage of the sinter method is that the solid residue remaining after aluminium extraction can be used in the cement industry thereby making 100 % reuse of the CFA. The calcium content of Matla CFA is in the range of 5 % - 7 % total composition. The other major metals such as magnesium and titanium are present at less than 2 % total composition of CFA. Since these metals are susceptible to leaching, they need to be monitored along with the extraction of the major silicon and aluminium components as well. Pre-leaching of CFA to remove calcium has been done in order to enhance the leaching of the major aluminium component (Seidel et al., 1998). This information has been applied in this study as well especially with regard to acidic leaching of CFA with sulphuric acid.

For the silicon extraction the literature has made use of alkaline reagents, mainly NaOH, to remove and reclaim silica from CFA as well as other materials such as rice hull ash and siliceous rocks. It is therefore best suited to make use of these methods to extract silicon from CFA since NaOH as a reagent is not too expensive. There are advantages in the use of NaOH because many of the metals will not be dissolved at high pH besides aluminium and iron in the Fe^{2+} state. This can be used in this study for the attempts at removing the components in CFA separately.

This study was necessary because it not only addresses a method to remove elements of value such as Si, Al, Fe, Ca from CFA but also adds to the collective studies by tracking the rare

earth element behaviour during these extractions. Tracking of the rare earth elements is not looked at when Si and Al extractions are normally undertaken on CFA nor has a sequential extraction been carried out to try and isolate single elements in solution from CFA.

In the following chapter 3, the approach to the removal of the iron, calcium, aluminium and silicon from CFA is presented and the approach taken to design an experimental protocol that will allow the highest possible extraction from the CFA.

Chapter Three

3. Experimental and Analytical Methods

This chapter serves to detail the experimental conditions and procedures selected for the extraction of the elements of interest including Si, Al, Fe, trace elements and monitoring of REEs from CFA. It also provides information with regards to the analytical methods used to measure the elements of interest in the study as well as the sampling procedure.

3.1 Sampling

Coal fly ash (CFA) was sampled from Matla power station in the Mpumalanga province in the Republic of South Africa. This fly ash was sealed in plastic bags and was placed in sealable 100 litre plastic drums. These sealed drums were stored in a designated storeroom that had no exposure to direct sunlight and chemicals. The CFA was lifted from bottom to top and stirred circularly with a wooden stick while in the drum. After this the coal fly ash for this study was transferred to a new plastic bag where it was stored for the duration of this study.

3.2 Analytical Methods

3.2.1 X-Ray Fluorescence Spectrometry

The CFA and the resulting solid residues after leaching were analysed via X-ray fluorescence (XRF) spectrometry to measure the concentration of the major and minor elements present in the samples. XRF analysis reports the major and minor elements in their oxide forms as weight percentage (%). The major elements reported in the oxide forms are SiO_2, Al_2O_3, Fe_2O_3, CaO, MgO, K_2O, TiO, Cr_2O_3, MnO, P_2O_5 and Na_2O. The reported weight percentage (%) values were converted to elemental concentrations using the online software calculator located at http://www.marscigrp.org/oxtoel.html

The samples were crushed to a fine powder of particle size < 70 µm with a jaw crusher and thereafter milled in a tungsten-carbide Zibb mill. The jaw crusher and mill were cleaned with uncontaminated quartz between samples to prevent cross contamination of the samples. Fused glass disks were then prepared for XRF analysis. It comprised of: 0.65 g of sample + 5.60 g high purity trace element and rare earth element-free flux, where the flux consists of: 66.67 % $Li_2B_4O_7$, 32.83 % $LiBO_2$ and 0.50 % LiBr. The final reported values are corrected for these dilutions.

LOI (loss on ignition) was determined by weighing and recording ± 2 g of sample in a pre-weighed crucible and heating in a muffle furnace for 4 hours at 900 °C. The LOI was provided in the final reported values but all reported elemental values were calculated on a dry weight basis for the experimental work carried out in this study since the LOI can vary due to volatile carbon content as well as residual moisture, both of which are not part of the CFA inorganic matrix.

A Pananalytical PW2400 WD (wavelength dispersive) XRF spectrometer type fitted with a 3 kW end-window rhodium x-ray tube was used for the solid sample analysis. It was fitted with various analysing crystals comprising of LiF (200,220), Ge, PE & PX using appropriate kV and mA tube power settings to determine the common major elements.

Table 3.1: Analysing crystals used for the major elements

Analysing crystal	Target element
LiF 200	Mn and Fe
LiF 220	Ca, Ti and K
Ge	P
PE	Al and Si
PX	Na and Mg

The instrument was fitted with a gas-flow proportional counter using a 90% Argon-10% methane gas mixture and a scintillation detector.

Matrix effects in the samples were corrected by applying theoretical alpha factors and measured line overlap factors to the raw intensities using the SuperQ PANalytical software. Suitable certified reference materials were used to calibrate each element. Amongst these standards are NIM-G (Granite from the Council for Mineral Technology, South Africa) and BE-N (Basalt from the International Working Group).

3.2.2 Inductively Coupled Plasma Optical Emission Spectrometry

Inductively coupled optical emission spectrometry (ICP-OES) was used to measure the selected elements of interest present in the supernatants acquired from the extraction experiments. A Spectro Arcos ICP-OES was used for the analysis of liquid samples. The instrument was equipped with CCD detectors and a radial view plasma orientation to limit the matrix effects. The operating conditions are tabulated below;

Table 3.2: ICP operating conditions

Parameter	Condition/ Type
Plasma power (w)	1400
Pump speed (rpm)	30
Coolant flow (L/min)	14.00
Auxiliary flow (L/min)	2.10
Nebuliser flow (L/min)	0.80
Nebuliser	Crossflow

In addition, the sample injection mode was by continuous nebulisation and the signal processing or line measurement was based on the peak height. Polynomial plotting was used to correct for the background.

The aqueous standards were prepared by dilution of 1000 ppm stock of individual standards. All standards contained 10 % (v/v) HNO_3 for acidification. The samples were matrix matched with the standards by diluting in 10 % (v/v) HNO_3. Plots of emission intensity, counts per second (cps), versus concentration were constructed via ICP-OES spectroscopy. A 7 point calibration on all elements was plotted to determine the unknown values. The ICP values were reported as ppm and the values were corrected to mg/g to represent the quantification of the element extraction content in relation to CFA mass.

3.2.3 Laser Ablation/Inductively Coupled Plasma- Mass Spectrometry

Inductively coupled plasma- mass spectrometry (ICP-MS) was used to analyse for trace element concentration present in CFA as well as in the CFA solid residues after the extraction tests. The elements analysed were scandium, vanadium; chromium, cobalt; nickel, copper; zinc, rubidium; strontium, yttrium; zirconium, niobium; molybdenum, caesium; barium, lanthanum; cerium, praseodymium; neodymium, samarium; europium, gadolinium; terbium, dysprosium; holmium, erbium; thulium, ytterbium; lutetium, hafnium; tantalum, lead; thorium and uranium.

Laser ablation was used to introduce the sample into the plasma of the ICP-MS instrument. Laser ablation is the process of focussing a laser on a sample's surface. This process removes the material from the sample area where the laser was focussed and allows it to be introduced into the plasma of the ICP-MS instrument.

The sample preparation for laser ablation required fused glass disks to be made. The fused glass disks were prepared in the same manner as described in Section 3.2.1 for XRF analysis.

The fused glass disks were then coarsely crushed and a chip of sample mounted along with up to 12 other samples in a 2.4 cm round resin disk. The mount was mapped and then polished for analysis.

A Resonetics 193 nm Excimer laser connected to an Agilent 7500ce ICP-MS instrument was used in the analysis of trace elements. Laser ablation was performed in helium gas at a flow rate of 0.35 L/min, mixed with argon (flow rate of 0.9 L/min) and nitrogen (flow rate of 0.004 L/min) just before introduction into the ICP plasma. Two 173 µm diameter spots were ablated on each fused glass sample disk using a frequency of 10 Hz and 100 mJ energy. The trace elements were quantified by using standard – sample bracketing. The internal standard used for the standard – sample bracketing was the % SiO_2 content of the sample's XRF reported value. The standard NIST (National Institute of Standards and Technology) 612 was then used for the calibration. Two replicate measurements were made on each sample and the calibration standard was run after every 12 samples. A quality control standard was run in the beginning of the sequence as well as with the calibration standards throughout. BCR-2 or BHVO 2G, both basaltic glass certified reference standards produced by United States Geological Survey (USGS) (Dr Steve Wilson, Denver, CO 80225), were used for this purpose. A fusion control standard from certified basaltic reference material (BCR-2, also from USGS) was also analysed in the beginning of a sequence to verify the effective ablation of fused material.

Data was processed using Glitter software, distributed by Access Macquarie Ltd., Macquarie University NSW 2109.

3.2.4 X-Ray Diffraction

X-Ray Diffraction (XRD) was used to check any changes in the mineral phase or removal of the mineral phases present in the CFA during the extraction experiments. The main phases of

interest would be the quartz (SiO_2) and mullite phases of CFA. Mullite is an aluminosilicate compound containing both the elements Si and Al.

Samples should generally be finely ground or in powdered form because x-rays can only penetrate the uppermost atomic layers of the sample particles. The powdered sample residues were placed on a sample holder that had been previously cleaned with acetone to ensure that no contamination of sample readings occurred between different samples. Qualitative XRD analysis was done using a Bruker AXS (Germany) D8 Advance diffractometer coupled with a (position sensitive detector) PSD Vantec-1 detector. The radiation source tube provided Cu-Kα radiation for the XRD analysis.

Table 3.3: XRD instrument settings for qualitative analysis of CFA and solid residues

Radiation source	Cu-Kα
Radiation wavelength	$\alpha K\alpha_1$=1.5406Å
Voltage	40 kV
Tube current	40 mA
2θ	$6° \leq \theta \geq 90°$
Step increment	0.02
Variable Slit	V20 variable slit

The XRD data were analysed and corrected for background using EVA software from Bruker. The mineral phases were identified using ICDD: PDF database 1998 (ICDD = International Center for Diffraction Data, PDF = powder diffraction file)

3.2.5 Ultraviolet – Visible Spectroscopy

The UV-Vis method used to measure Si was developed by Grasshoff in 1964 and modified by Koroleff in 1971 where he used ascorbic acid as the reducing agent in the method (Grasshoff et al., 1999). The necessary precaution to be adhered to is that only plasticware be used for all calibration standards and sample dilutions. De-ionised water conductivity readings should measure ≤ 0.5 μS/cm. This provides a positive indication of low silicate content in the de-ionised water. The analyte samples were sequentially diluted X1000 times prior to storage with de-ionised water.

The reagents required were made up as follows:

4.5 M Sulphuric acid:	250 mL concentrated H_2SO_4 was added to 750 mL of de-ionised water in a plastic beaker. It was allowed to cool and made up to 1 litre in a 1000 mL volumetric plastic flask
Acid molybdate reagent: (0.0512 M)	38 g $(NH_4)_6Mo_7O_{24}.4H_2O$ (ammonium heptamolybdate tetrahydrate) was dissolved in 300 mL de-ionised water. This acid molybdate solution was added to 300 mL of the made up 4.5 M H_2SO_4 solution. [Note: Do not add in reverse order, i.e. do not add acid to the molybdate solution]. The total volume was therefore 600 mL and it was stored away from direct sunlight. It remains stable for several months.
Oxalic acid solution: (0.7937 M)	10 g oxalic acid dihydrate, $(COOH)_2.2H_2O$ was quantitatively transferred to an approximate 50 mL volume of de-ionised water in a 100 mL volumetric flask. It was dissolved and made up to the 100 mL mark with de-ionised water. This saturated solution was stored in a plastic container at room temperature. It is stable

indefinitely.

Ascorbic acid: (0.1637 M) — 2.8 g ascorbic acid, $C_6H_3O_6$, was quantitatively transferred to approximate 50 mL volume de-ionised water in a 100 mL volumetric flask. It was dissolved and thereafter made up to the 100 mL mark with de-ionised water. The solution was kept in a dark container at a temperature under 8 °C. The solution remains suitable for use as long as it remains colourless.

Standard stock solution: (0.0361 M) — 1000 ppm Si solution was prepared by quantitatively transferring 4.3459 g Na_2SiO_3, (sodium metasilicate), to an approximate 500 mL volume of de-ionised water in a 1000 mL plastic volumetric flask. It was dissolved and thereafter made up to the 1000 mL mark with de-ionised water. The stock solution is stable for at least a year.

Working standards: Freshly prepared calibration standards were prepared for each analysis run from the standard stock solution. Serial dilutions were done till the desired working standards were obtained. Dilutions were done with de-ionised water as well.

The calibration standards and samples were prepared for measurement as follows:

The 1000 ppm Si stock solution was sequentially diluted to 10 ppm. Firstly a 100 ppm Si standard was made by adding 5 mL of the 1000 ppm stock solution to a 50 mL plastic volumetric flask and made up to volume with de-ionised water. 5 mL of the 100 ppm Si standard was then added to another 50 mL plastic volumetric flask and made up to volume with de-ionised water. Working standards of 0.1, 0.3, 0.5, 0.7 and 1 ppm Si was then made by adding 0.5, 1.5, 2.5, 3.5 and 5 mL respectively of the 10 ppm Si standard to 50 mL plastic

volumetric flasks. The working standards were then made up to volume with de-ionised water.

8 mL of the X1000 times diluted analyte samples were added to plastic 50 mL volumetric flasks to bring the dilution factor up to X6250 times. 50 mL of blank sample solution (de-ionised water used to prepare working standards), analyte sample solution and working standards were then each transferred to its own plastic container. 2 mL of the prepared 0.0512 M molybdate acid solution was added to each solution container. The solutions were swirled and allowed to stand for 10 - 20 min. 2 mL of the prepared 0.7937 M oxalic acid followed directly by 1 mL of the prepared 0.1637 M ascorbic acid was then added to each solution container. The solution was swirled again and left to stand for 20-30 minutes. This was to allow the blue colour of the silicomolybdate complex to fully develop. If the blue colour of the analyte samples were darker than the calibration standards, then it could be suitably diluted with acidified zero water (ZW). ZW is made by adding 1 mL of the 4.5 M H_2SO_4 to each 100 mL of de-ionised water used. It will not disturb the complexed Si since oxalic acid is already present in the sample preparation. The blank solution, standards and samples were measured at 810 nm wavelength or 660 nm for higher concentrations. In this study 660 nm wavelength was used. A calibration line was plotted to determine the concentration of the measured samples. The measured concentration was corrected for dilution by multiplying the measured concentration by the factor $\frac{(6250)(50)}{55}$

3.3 Experimental Methods for Extraction

Table 3.4: Table of Chemicals and Lab Equipment used for experiments:

Reagent	**Manufacturer**
HCl 32 %	Merck
HNO_3 55%	Merck
H_2SO_4 min. 95%	Merck
NaOH (CP)	Kimix chemical & lab suppliers
Labware	**Manufacturer**
Hotplate magnetic stirrer 34532	Snijders Scientific, Tillburg Holland
Glassware	Schott Duran
Hot air oven	Memmert
Magnetic stirrer bars	Kimix chemical & lab suppliers
Buchner Funnel	Kimix chemical & lab suppliers

3.3.1 Magnetic Extraction

The first step in the extraction process utilises magnetic extraction. This step provides the removal of the magnetic component from CFA which is predominantly iron oxide (hematite) content from the coal combustion process.

The sampled coal fly ash was mixed with de-ionised water in a 1000 mL plastic beaker and stirred with a magnetic stirrer at 750 rpm for 1 hour. A strong bar magnet was placed at the base of the plastic beaker after stirring and the coal fly ash residue was poured off. The

magnetic extract remained adhered to the magnetic stirrer in the beaker and was washed with de-ionised water to remove as many fly ash particles as possible. The fly ash residue was stirred again with the magnetic stirrer and the process repeated. This was done until no visible amount of magnetic extract was retained on the magnetic stirrer in the plastic beaker after pouring off the fly ash residue. Thereafter the fly ash residue was filtered using a Buchner funnel and the filtrate containing readily soluble species was analysed by ICP-OES. The solid residue was dried in a hot air oven at 100 °C overnight. The dried CFA residue was analysed via XRF and laser ablation - ICP - MS. This dried CFA residue with low magnetic material and fewer soluble salts (due to water contact dissolution) was used as the starting CFA resource for all subsequent extractions.

The insoluble magnetic extract was analysed by XRF for major and minor elements. The insoluble magnetic extract was also analysed for trace elements content by laser ablation - ICP – MS. Both the XRF and laser ablation - ICP – MS results for the insoluble magnetic extract are presented in Chapter 4, Section 4.2, Table 4.3 and Table 4.4. The CFA residue after magnetic extraction was also analysed by XRF and laser Ablation - ICP – MS and the results are presented in Chapter 4, Section 4.2, Table 4.5 and Table 4.6. The insoluble magnetic extract and CFA residue after magnetic extraction were analysed for mineral phases using XRD analysis. The results are presented in Chapter 4, Section 4.2, Figure 4.4 and Figure 4.7 respectively.

3.3.2 Alkaline leaching tests

Indirect leaching and direct leaching was carried out using sodium hydroxide (NaOH) as the alkali of choice. This test was targeted at removing silicon from the CFA matrix.

3.3.2.1 Alkaline leach method 1: NaOH sintering

An indirect alkaline leaching method targeting Si extraction was done using NaOH as the alkaline reagent. The NaOH indirect leaching utilised a modification of the fusion method employed by Musyoka, (2012). A melt of the alkali and CFA was firstly formed and thereafter the sintered product was leached using de-ionised water as the leaching solvent while stirring. The sintered product was formed by heating a heterogeneous mixture of CFA and alkali at high temperature to form a homogenous fused melt mixture. 20 g CFA was mixed with 20 g NaOH pearls and heated in a furnace at 550°C for 2 hours. Once cooled, the fused sintered product was crushed and ground to a fine powder with a mortar and pestle. It was then mixed with 600 mL water and stirred rapidly for 2 hours at room temperature. Thereafter the mixture was filtered and the supernatant retained for ICP-OES analysis. The solid residue were not analysed at this test stage since the leached content in the filtrate were the main interest for these preliminary tests. The results are presented in Chapter 4, Section 4.3., Figure 4.9 and Figure 4.10.

3.3.2.2 Alkaline leach method 2: low temperature NaOH leaching

The NaOH direct leaching method targeting Si extraction entailed mixing 20 g CFA with 20 g NaOH dissolved in 600 mL de-ionised water. The mixture was then rapidly stirred for 2 hours while temperature was maintained at 95 °C. Thereafter the mixture was filtered and the supernatant retained for ICP-OES analysis. The solid residues were not analysed at this test stage since the leached content in the filtrate were the main interest for these preliminary tests. All the supernatants were sequentially diluted to X10, X100 and X1000 dilution. X10 dilution was done by adding 10 mL of the original supernatant sample into a 100 mL plastic flask and making up to volume with 2 % HNO_3. Subsequently, X100 dilution was done by adding 10 mL of the X10 dilution into a 100 mL plastic flask and making up to volume with 2 % HNO_3. X1000 dilution was made in the exact manner by adding 10 mL of the X100

dilution into a 100 mL plastic flask and making up to volume with 2 % HNO_3. The results are presented in Chapter 4, Section 4.3., Figure 4.9 and Figure 4.10.

3.3.3 Acid leaching tests

3.3.3.1 Acid leaching method 1: HCl leaching

HCl leaching tests were adapted from a method used by Muriithi, (2013a) in which 10 g CFA was reacted with 200 mL HCl. In this study the leaching test was carried out using 20 g CFA and 400 mL of varying HCl molarities from 0 M – 10 M HCl. The mixture was stirred rapidly at a temperature of 100 °C for 2 hours. Thereafter the mixture was filtered and X10, X100 and X1000 sequential dilutions as described above in Section 3.3.2.2 were prepared using 2 % HNO_3 prepared in de-ionised water as the diluent. The solid residues were not analysed at this test stage since the leached content in the filtrate was the main interest for these preliminary tests. The sequential dilutions were analysed by ICP-OES. The results are presented in Chapter 4, Section 4.4.1., Figures 4.16 - 4.21.

3.3.3.2 Acid leaching method 2: H_2SO_4 indirect leaching

A 2-step acidic leaching test was performed using sulphuric acid. The H_2SO_4 indirect leaching test was adapted from Lui et al., (2012). Varying concentrations of H_2SO_4 (5 M, 10 M, 15 M and 18.2 M) were mixed with 20 g CFA in a liquid: solid ratio of 1:2. The mixture was then stirred at 450 rpm while heating on a hotplate at 220 °C. The reaction was allowed to proceed until all the liquid evaporated. The reaction vessel then remained on the hotplate at that temperature for a further 30 minutes. This was to allow time for the CFA residue to calcine. Once cooled, de-ionised water was added to the CFA residue in a solid: liquid ratio of 1:6. The mixture was stirred rapidly at a temperature range of 85 - 90 °C for 30 minutes. The purpose of this secondary step was to separate the leached Al, in the form of Al_2SO_4, from the CFA matrix. Thereafter the mixture was filtered and the supernatant retained for

ICP-OES analysis. The solid residues were not analysed at this test stage since the leached content in the filtrate was the main interest for these preliminary tests. The results are presented in Chapter 4, Section 4.4.2., Figure 4.23 and Figure 4.24.

3.3.3.3 Acid leaching method 3: H_2SO_4 direct leaching

Direct H_2SO_4 leaching was performed where 200 mL of varying concentrations of H_2SO_4 (5 M, 10 M, 15 M and 18.2 M) were directly mixed with CFA. The mixture was then refluxed for 2 hours. The reaction vessel was removed and allowed to cool. De-ionised water was added to the experimental leach tests that were performed with H_2SO_4 concentrations higher than 5 M to bring down the concentration to approximately 5 M H_2SO_4. This was needed to facilitate filtration of the leached solutions without dissolving the filter media. All the supernatants were sequentially diluted to X10, X100 and X1000 dilution. X10 dilution was done by adding 10 mL of the original supernatant sample into a 100 mL plastic flask and making up to volume with 2 % HNO_3 prepared in de-ionised water. Subsequently, X100 dilution was done by adding 10 mL of the X10 dilution a 100 mL plastic flask and made up to volume with 2 % HNO_3 prepared in de-ionised water. X1000 dilution was made in the exact manner by adding 10 mL of the X100 dilution to 100 mL plastic flask and made up to volume with 2 % HNO_3 prepared in de-ionised water. The solid residues were not analysed at this test stage since the leached content in the filtrate was the main interest for these preliminary tests. The supernatants were retained for ICP-OES analysis. The results are presented in Chapter 4, Section 4.4.2., Figure 4.25 and Figure 4.26.

3.3.4 Optimisation Experiments

Optimisation experiments were undertaken to find the optimum conditions that resulted in the greatest yield during extraction of each element from CFA. The optimisations would have

one variable in its experimental plan changed at a time while keeping all the other experimental parameters constant.

3.3.4.1 Alkaline leaching optimisation

The method that yielded the best extraction for Si was optimised. Direct alkaline leaching was determined to be the best method and it was optimised by firstly setting the concentration of NaOH as the variable in the experimental procedure while the amount of CFA, solution volume and leaching temperature and leaching time remained constant. The NaOH was therefore varied from 0.83 M to 12.5 M while the solution volume was set at 600 mL, leaching time 2 hours and leaching temperature 100 °C. Once the optimal concentration of NaOH was determined (6.25 M NaOH), the amount of CFA was varied while the experimental parameters of time and temperature remained unaltered. The second optimisation step therefore used varied CFA ash amounts ranging from 5 g – 40 g while the 600 mL of 6.25 M NaOH, 2 hour leaching time and 100 °C leaching temperature remained constant. The solid residues were not analysed at this test stage since the leached content in the filtrate was the main interest for these optimisation tests. The results are presented in Chapter 4, Section 4.3., Figures 4.11 – 4.14. The mineral phases present in the CFA residue after extraction with the 6.25 M NaOH was analysed using XRD analysis. The result is presented in Chapter 4, Section 4.3., Figure 4.15.

3.3.4.2 Acidic leaching optimisation

It was seen that calcium was more effectively removed with HCl but Al was extracted during the process as well. The HCl concentration was firstly optimised for the maximum removal of Ca by varying the concentration of the HCl from 0 M – 0.25 M. for the leaching process. The solution volume of 400 mL, leaching temperature of 100 °C and leaching time of 2 hours were kept constant. Once that was determined, then the amount of CFA reacting with the

optimal HCl concentration was varied. The CFA amounts were varied from 5 g – 40 g and reacted with the optimal determined concentration of 0.1 M HCl. The solution volume of 400 mL, leaching temperature of 100 °C and leaching time of 2 hours were kept constant. Only the supernatants and not the solid residues analysed at this test stage since the leached content in the filtrate was the main interest for these optimisation tests. The results are presented in Chapter 4, Section 4.4.1, Figures 4.18 – 4.21. The mineral phases present in the CFA residue after extraction with the 0.1 M HCl was analysed using XRD analysis. The result is presented in Chapter 4, Section 4.4.1., Figure 4.22.

Direct H_2SO_4 leaching gave a higher yield of Al and it was further investigated to find the optimal conditions for the extraction. The molarity of the acid was varied from 1 M - 15 M. The leaching time of 2 hours under reflux, the amount of CFA (20 g) and 200mL solution volume was kept constant as per the experimental method described in Section 3.3.3.3. After the optimum H_2SO_4 acid molarity of 15 M was determined, the amount of CFA was varied from 5 g – 50 g while solution volume of 200 mL and leaching time of 2 hours under reflux remained constant. Only the supernatants and not the solid residues were analysed at this test stage since the leached content in the filtrate was the main interest for these optimisation tests. The results are presented in Chapter 4, Section 4.4.2, Figures 4.27 - 4.31. The mineral phases present in the CFA residue after extraction with 15 M H_2SO_4 was analysed using XRD analysis. The result is presented in Chapter 4, Section 4.4.2., Figure 4.32.

3.3.5 Sequential Extraction

After all the optimisation tests were completed, an experiment was designed and performed to determine the amount of the desired elements that could be sequentially extracted from the CFA. The optimal reagent amounts were used to extract the Ca, Al and then the Si in sequence. The sequence was thus acidic leaching followed by alkaline leaching.

The first step of magnetic extraction targeted the iron content present in CFA as described in Section 3.3.1. Since it was seen that calcium could be targeted for removal with HCl, calcium was to be the second element extracted from CFA as detailed in Section 3.3.4.2. The third target element for extraction from CFA was aluminium. This was leached using direct H_2SO_4 leaching as detailed in Section 3.3.4.2. The sequential extraction was designed with the initial removal of calcium so as to make aluminium extraction more amenable to H_2SO_4 leaching. The H_2SO_4 consumption would also be more available for aluminium extraction than when having to compete with calcium sulphate formation. Calcium sulphate (gypsum) precipitation serves to hinder the aluminium extraction process as explained in Section 2.4.3.1(ii). After calcium and aluminium extraction, silicon was removed using direct alkaline leaching as detailed in Section 3.3.2.2. At this stage of the experiment more Si should be able to be recovered since the simultaneous effect of Al co- leaching would be greatly minimised.

The entire extraction sequence was therefore magnetic extraction of CFA followed by direct acidic leaching of the magnetically extracted residue and thereafter direct alkaline leaching of the acid leached residue.

The process is outlined as follows;

3.3.5.1 Sequential Experiment flow diagram:

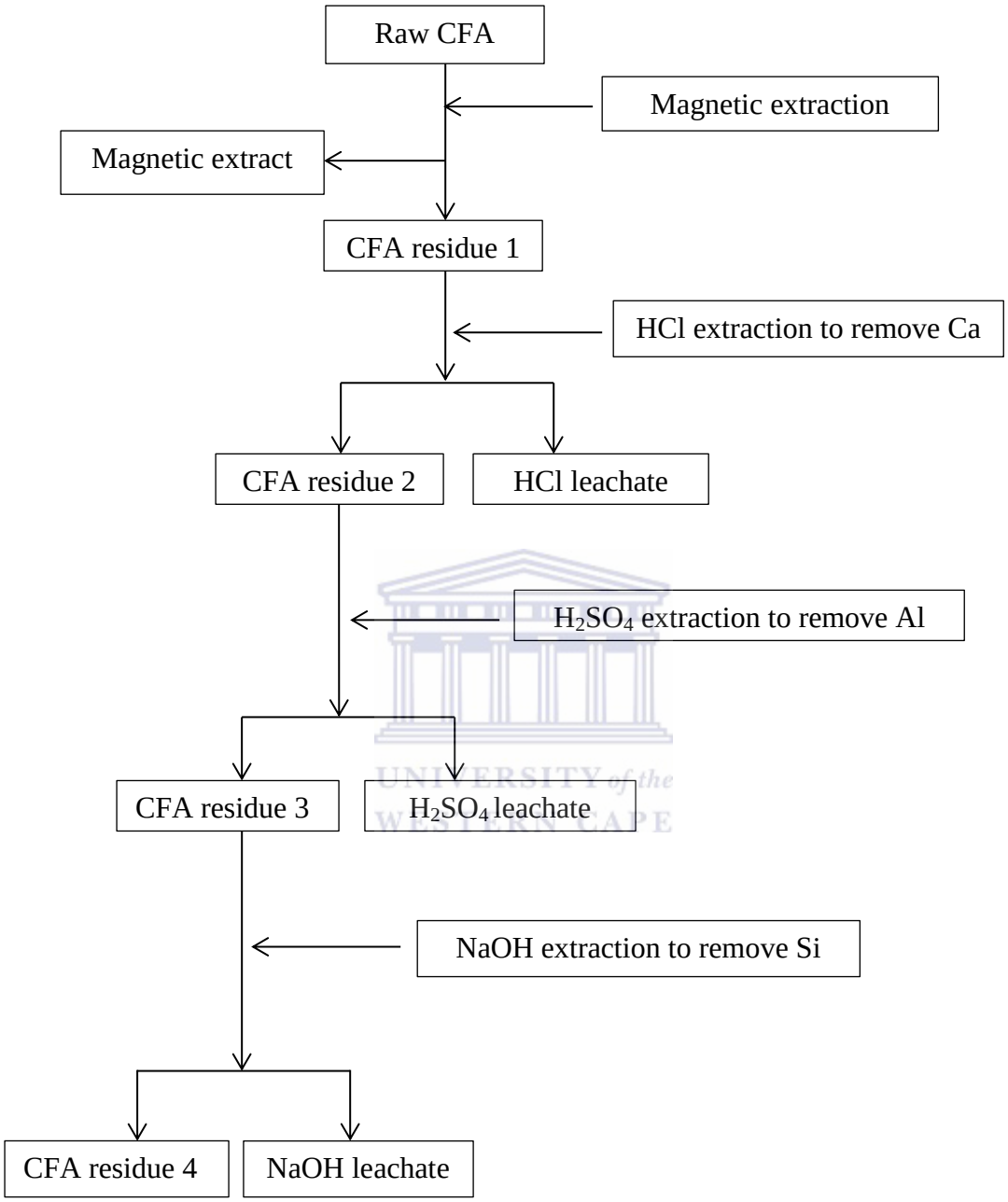

Figure 3.1: Sequential extraction experiment design

All the supernatants were retained for analysis of Al, Ca, Fe and Mg using ICP – OES analysis and UV-Vis spectroscopy for Si analysis. The results are presented in Chapter 4, Section 4.5, Figures 4.34 and Figure 4.35. The CFA residues were analysed for major and minor elements using XRF analysis and for trace elements using laser ablation - -ICP – MS

analysis. The results are presented in Chapter 4, Section 4.5, Tables 4.7 and Table 4.8. The final CFA residue was analysed with XRD analysis after the entire sequential leaching test was done to check the effect of the sequential leach test on the mineral phases of the CFA. The result is presented in Chapter 4, Section 4.5, Figure 4.36.

3.3.5.2 Solubility Behaviour of Rare earth elements

The solubility behaviour of the rare earth elements was tracked all the way from the start till the end of the sequential extraction process. It was measured using XRF and laser ablation ICP-MS spectroscopy analysis of the CFA solid residues and liquid leachates. The results are presented in Chapter 4, Section 4.5, Table 4.9, Table 4.10 and Figure 4.40.

In the following chapter 4 the results of all the experiments done are presented and the details on how the sequential experimental sequence was decided upon are given.

Chapter Four

4. Results and Discussion

This chapter documents the results from the experimental tests outlined in Chapter 3.3. The results will be discussed in a sequential manner so as to motivate the reasoning for choosing certain parameters during the progression of the study. XRD and XRF analytical techniques were used to characterise the solid samples which included the raw CFA, magnetic extract and CFA residues after extraction. ICP-OES, ICP-MS, and UV-Vis spectroscopy were the analytical techniques used to measure the elements of interest for all the liquid leachates.

4.1 Matla raw coal fly ash

The major and minor elemental composition present in raw CFA was analysed by XRF as described in Section 3.2.1. The trace elemental composition results obtained were analysed by laser ablation-ICP-MS as described in Section 3.2.3. The XRF % weight oxide results were converted to ppm using an online software conversion program located at [http://www.marscigrp.org/oxtoel.html]. The entire major, minor and trace element content is presented in Table 4.1 below.

Table 4.1: Major and Minor Elements in Raw Matla CFA

Raw Matla CFA (as is wet basis)		**Raw Matla CFA (dry basis: corrected and normalised for Loss on Ignition)**			
Elemental Compound	**Weight %**	**Elemental Compound**	**Weight %**	**Major & minor Elements**	**mg/kg**
SiO_2	51.07	SiO_2	50.24	Si	234872
Al_2O_3	31.08	Al_2O_3	30.57	Al	161776
Fe_2O_3	3.23	Fe_2O_3	3.18	Fe	22241
CaO	6.74	CaO	6.63	Ca	47385
MgO	2.54	MgO	2.50	Mg	15080
K_2O	0.81	K_2O	0.80	K	6641
P_2O_5	1.08	P_2O_5	1.06	P	4626
MnO	0.05	MnO	0.05	Mn	387
Na_2O	0.77	Na_2O	0.76	Na	5638
TiO_2	1.77	TiO_2	1.74	Ti	10431
LOI	1.64	Total	99.13		
Total	100.77				

Table 4.2: Trace Elements in Raw Matla CFA

Trace element	**mg/kg**	**Trace element**	**mg/kg**	**Trace element**	**mg/kg**	**Trace element**	**mg/kg**
Sc	30.84	Y	65.69	Nd	76.15	Yb	7.00
V	193.86	Zr	404.35	Sm	14.87	Lu	1.04
Cr	208.5	Nb	41.71	Eu	2.64	Hf	11.77
Co	30.16	Mo	13.76	Gd	12.29	Ta	3.25
Ni	89.31	Cs	12.32	Tb	2.06	Pb	79.22
Cu	87.52	Ba	2535	Dy	11.74	Th	44.01
Zn	78.89	La	99.29	Ho	2.59	U	13.80
Rb	53.68	Ce	207.86	Er	6.99		
Sr	2477	Pr	21.4	Tm	1.05		

Looking at the XRF results in Table 4.1 above, the sum total of SiO_2, Al_2O_3 and Fe_2O_3 is greater than 70 % with the CaO content being less than 15 %. This confirms the Matla CFA used in his study as a Class F CFA according to the American Standard of Testing and Measurement, ASTM C618 (Mehta, 1987). The loss on ignition is relatively low at 1.64 % showing that the volatile content remaining in the CFA after the coal combustion process is not very high and the CFA was sufficiently dried before its use. The trace elements present in CFA confirm the presence of rare earth elements (REEs). The toxic elements, Ba and Sr are present at levels greater than 1000 mg/kg (refer to Table 4.2). The presence of radioactive elements U and Th in the CFA is in accordance with reported work carried out by Eze et al., (2013a). The reported values for Ba, Sr, U, Th and Pb were similar to the values Eze and co-workers, (2013a) obtained for Matla CFA using the laser ablation ICP-MS analysing technique.

The raw CFA was analysed for its mineral composition by XRD as described in Section 3.2.4. The data scan was plotted and the mineral phases identified using ICDD: PDF database 1998. The XRD spectrum of raw CFA is presented in Figure 4.1 below.

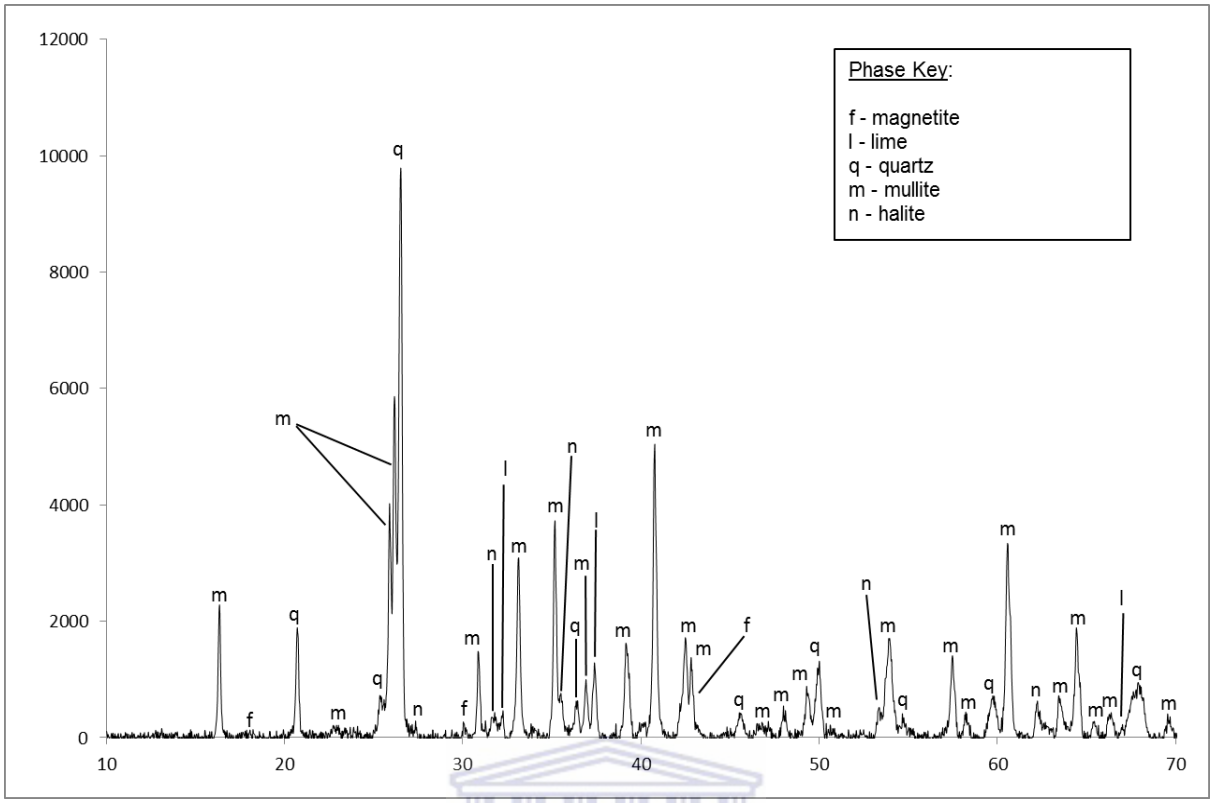

Figure 4.1: XRD spectrum of Matla raw coal fly ash

Looking at Figure 4.1 above, the XRD spectrum showed the mineralogical phases present in CFA are magnetite (iron oxide), lime (calcium oxide), quartz (silicon dioxide), mullite (aluminosilicate) and halite (sodium chloride). These mineral phases are typically found in CFA but the presence of halite (sodium chloride) peaks is not usually seen and could be due to conditioning of the ash with process brine for dust suppression at the Matla ash site.

4.2 Magnetic extraction

The procedure for magnetic extraction of Fe was carried out as outlined in Chapter 3.3.2. The raw CFA was mixed with de-ionised water and stirred with a magnetic stirrer in a plastic beaker. A strong bar magnet was used to retain the magnetic fraction and the residues were decanted into another plastic beaker. The magnetic extract remained in the original beaker. The decanted solution consisting of CFA and de-ionised water was stirred again and the process repeated. This process was carried out until no visible magnetic extract could be seen.

The decanted solution was then filtered and the CFA residue was dried and stored. The magnetic extract was rinsed with de-ionised water to free it of any CFA particles and dried prior to analysis being carried out.

The magnetic extract was analysed with XRF to measure the major and minor elemental composition as described in Section 3.2.1 and the trace elements by laser ablation-ICP as described in Section 3.2.3. The XRF % weight oxide results were converted to ppm using an online software conversion program located at [http://www.marscigrp.org/oxtoel.html]. The anion content was not measured to ascertain the presence of chlorides, sulphates etc. in the de-ionised water filtrate from the magnetic extraction procedure. The results obtained are presented in Table 4.3 and Table 4.4 below,

Table 4.3: Major and Minor Elements in Magnetic Extract from Raw CFA

Magnetic extract (as is wet basis)		**Magnetic extract (dry basis: corrected and normalised for Loss on Ignition)**			
Elemental Compound	**Weight %**	**Elemental Compound**	**Weight %**	**Major & minor Elements**	**mg/kg**
SiO_2	11.88	SiO_2	11.98	Si	56007
Al_2O_3	7.79	Al_2O_3	7.85	Al	41542
Fe_2O_3	75.38	Fe_2O_3	75.98	Fe	531
CaO	2.54	CaO	2.56	Ca	18296
MgO	1.56	MgO	1.57	Mg	9470
K_2O	0.13	K_2O	0.13	K	1079
P_2O_5	0.45	P_2O_5	0.45	P	1964
MnO	0.04	MnO	0.04	Mn	310
Na_2O	0.49	Na_2O	0.49	Na	3635
TiO_2	0.46	TiO_2	0.46	Ti	2758
LOI	-0.8	Total	100.72		
Total	99.92				

Table 4.4: Trace Elements in Magnetic Extract from CFA

Trace element	mg/kg	Trace element	mg/kg	Trace element	mg/kg	Trace element	mg/kg
Sc	7.76	Y	15.05	Nd	15.86	Yb	1.38
V	149.06	Zr	87.16	Sm	3.06	Lu	0.21
Cr	255.73	Nb	9.55	Eu	0.59	Hf	2.5
Co	33.04	Mo	6.65	Gd	2.77	Ta	0.57
Ni	114.86	Cs	1.08	Tb	0.45	Pb	12.74
Cu	88.80	Ba	738.07	Dy	2.73	Th	8.96
Zn	83.55	La	20.11	Ho	0.51	U	10.58
Rb	4.69	Ce	43.63	Er	1.63		
Sr	581.46	Pr	4.28	Tm	0.22		

As can be seen from the major element content results in Table 4.3, Fe was the major bulk element present as expected. The formula below was used to calculate the percentage elemental content from its reported oxide value obtained from the XRF analysis of the magnetic extract:

$$\%\ \text{Element} = \frac{\text{molecular weight element x n}}{\text{molecular weight element oxide}} \times \text{reported oxide value}$$

where n = stoichiometric number of element in element oxide (Nyale, 2011)

A negative loss on ignition (LOI) is reported for the magnetic extract (refer to Table 4.3). This is to be expected from iron containing samples since a gain in sample weight is obtained during the high temperature drying stage of XRF sample preparation. This is due to the oxidation of ferrous iron, as indicated in the half reaction below,

$$2\ FeO + \frac{1}{2}\ O_2 \rightarrow Fe_2O_3$$ (Potts, 2013)

The iron oxide content made up 74.84 % of the total magnetic extract composition on a dry weight basis. This value equated to 52.33 % elemental iron. The magnetic extract showed a decrease in concentration for all the trace elements, including the REEs except for Cr, Co, Ni and Zn which showed an enrichment in concentration when compared to raw Matla CFA (refer to Table 4.1). It can therefore be seen that the bulk of the trace elements, including all of the REEs were partitioned into the CFA residue after magnetic extraction. The following graphical representations depict the enrichment trends and the decrease in radioactive and toxic element concentration between the raw CFA and magnetic extract from CFA.

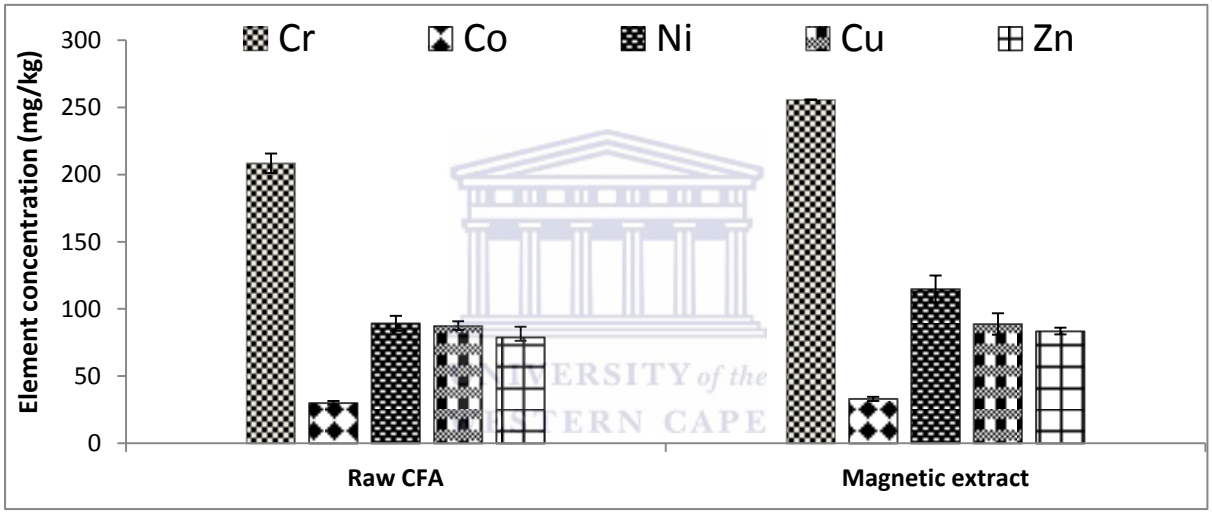

Figure 4.2: Cr, Co, Ni, Cu and Zn enrichment in magnetic extract from CFA

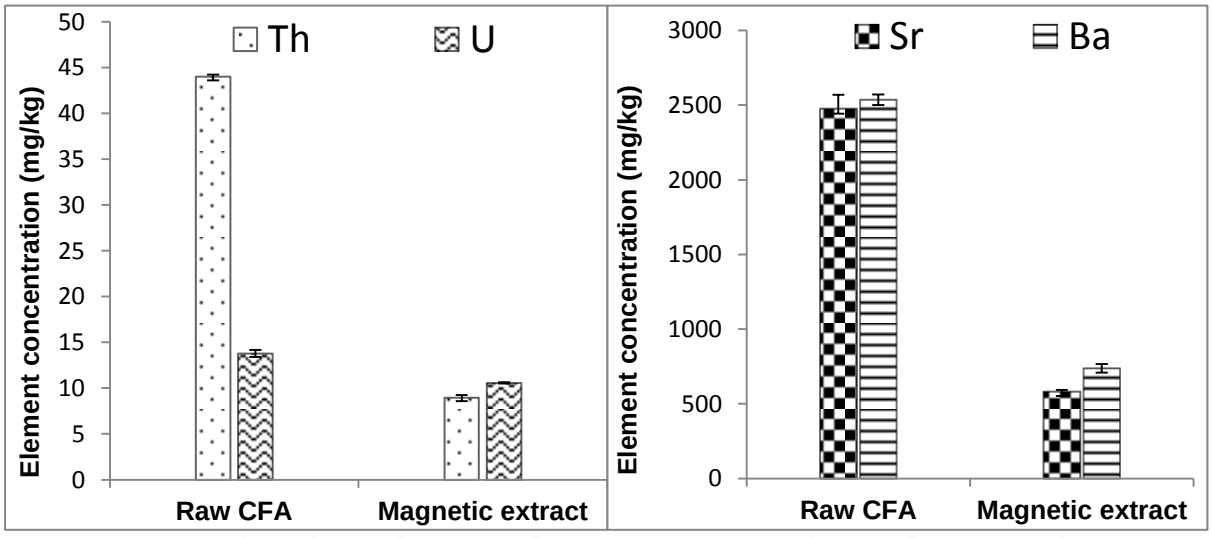

Figure 4.3: Th and U radioactive element grouping and Sr and Ba toxic element grouping representation trend in magnetic extract from CFA

As can be seen in Figure 4.2, the Cr content is more enriched in the magnetic extract compared to Co, Ni, Cu and Zn which show slight enrichment. This is probably attributed to the interaction of these elements with the iron oxide content of the magnetic extract. Studies have been conducted by Bliem et al., (2015) where Ti, Mn, Co, Ni and Zn were deposited onto the surface of laboratory synthesised magnetite (Fe_3O_4). Bliem and co-workers came to the conclusion that when a non-noble metal is deposited onto the iron oxide surface it becomes oxidised and if it is heated it diffuses into the bulk of the iron oxide. They also concluded that this occurrence is not specific to only Ti, Mn, Co, Ni and Zn but also other metals that form a solid solution with iron oxide (Bliem et al., 2015). Fe is present as the mineral phase pyrite (FeS_2) and marcasite (white pyrite) in coal. The combustion of coal allows for the conversion of these pyrite mineral phases into magnetite, hematite as well as maghemite (Akinyemi et al., 2012 and Demir et al., 2001). This conclusion stated by Bliem and co-workers provides a good explanation for what is seen in the magnetic extract since magnetite is one of the iron mineral phases, as well as maghemite and hematite, found in the magnetic extract as shown in the XRD spectrum (refer to Figure 4.4). As depicted in Figure 4.3 the toxic elements Sr and Ba as well as the radioactive U and Th were decreased in the magnetic extract. This shows that these elements are not readily associated with the magnetic extract.

The magnetic extract was analysed for its mineral composition by XRD as described in Section 3.2.4. The data scan was plotted and the mineral phases identified using ICDD: PDF database 1998. The XRD spectrum of the magnetic extract is presented in Figure 4.4 below.

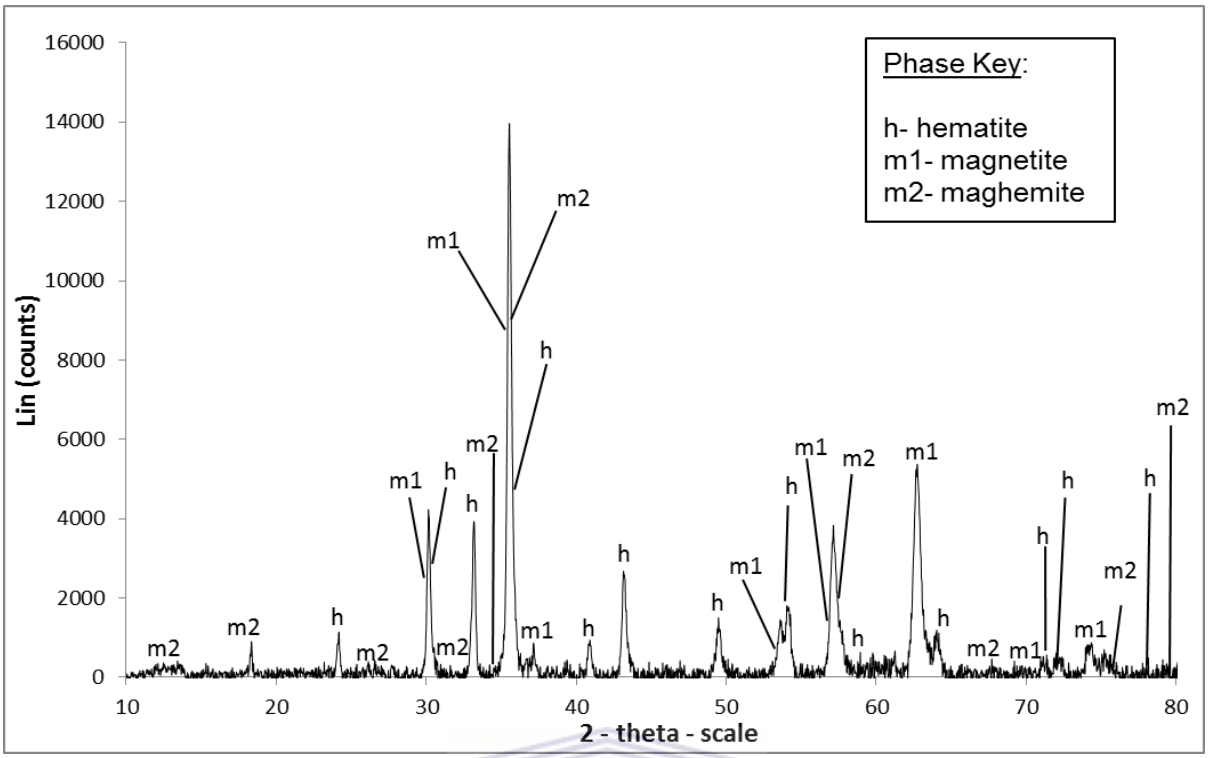

Figure 4.4: XRD spectrum of magnetic extract from raw CFA

The XRD spectrum, Figure 4.4 above, confirmed that hematite (α-Fe_2O_3), magnetite (Fe_3O_4) and maghemite (γ- Fe_2O_3) are the predominant Fe mineral phases present in the magnetic extract from CFA. However the XRF major analysis (refer to Table 4.3) showed that Si and Al were also present in the magnetic extract even though no mineral phases were detected from the XRD analysis (refer to Figure 4.4). The SiO_2 content in the magnetic extract was 11.80 % (that equated to 5.52 % Si) and Al_2O_3 content was reported as 7.73 % (that equated to 4.09 % Al). This is due to contamination of the magnetic extract by entrained finer CFA particles that are harder to remove using physical separation methods. Purification of the iron oxide could be achieved by dissolution with HCl and precipitating the Fe^{3+} as $Fe(OH)_3$. However, depending on the aluminium mineral phase of the CFA particles present in the magnetic extract, there is a possibility of aluminium dissolution in HCl. The magnetic extract also needs to be exposed to oxygen in the dissolution process in order to oxidise the part of the magnetic extract comprised of zero valent iron. This was not part of the study and was therefore excluded. CaO and MgO were the other two oxides that were higher than 1 %

abundance. CaO was reported at 2.52 % (that equated to 1.80 % Ca) and MgO was reported at 1.55 % (that equated to 0.93 % Mg).

The CFA residue remaining after magnetic extraction was also analysed with XRF to measure the major and minor elemental composition after soluble and magnetic phases were removed, as described in Section 3.2.1, and the trace elements by laser ablation- ICP- MS as described in Section 3.2.3. The XRF % weight oxide results were converted to ppm using an online software conversion program that is found at [http://www.marscigrp.org/oxtoel.html]. The results obtained are presented in Table 4.5 and Table 4.6 below.

Table 4.5: Major and Minor Elements in Matla CFA Residue after Magnetic Extraction

Matla CFA residue (as is wet basis)		**Matla CFA residue (dry basis: corrected and normalised for Loss on Ignition)**			
Elemental Compound	**Weight %**	**Elemental Compound**	**Weight %**	**Major & minor Elements**	**mg/kg**
SiO_2	51.97	SiO_2	50.76	Si	237303
Al_2O_3	31.55	Al_2O_3	30.81	Al	163047
Fe_2O_3	2.34	Fe_2O_3	2.29	Fe	16016
CaO	6.51	CaO	6.36	Ca	46527
MgO	2.56	MgO	2.50	Mg	15080
K_2O	0.81	K_2O	0.79	K	6558
P_2O_5	1.12	P_2O_5	1.09	P	4757
MnO	0.04	MnO	0.04	Mn	310
Na_2O	0.80	Na_2O	0.78	Na	5787
TiO_2	1.81	TiO_2	1.77	Ti	10611
LOI	2.38	Total	99.51		
Total	101.89				

Table 4.6: Trace Elements in Matla CFA Residue after Magnetic Extraction

Trace element	mg/kg	Trace element	mg/kg	Trace element	mg/kg	Trace element	mg/kg
Sc	29.66	Y	64.155	Nd	76.14	Yb	6.61
V	184.59	Zr	395.09	Sm	14.46	Lu	1.03
Cr	184.65	Nb	39.98	Eu	2.49	Hf	11.03
Co	20.38	Mo	12.48	Gd	11.73	Ta	3.22
Ni	84.09	Cs	11.64	Tb	2.07	Pb	68.90
Cu	75.04	Ba	2392	Dy	12.06	Th	41.64
Zn	70.47	La	96.07	Ho	2.46	U	13.01
Rb	51.50	Ce	198.55	Er	6.75		
Sr	2362	Pr	20.36	Tm	1.07		

The following graphical representations depict the trends of particular elements of interest as well as the radioactive and toxic element concentrations between the raw CFA, magnetic extract and the CFA residue after magnetic extraction. These trace elements were analysed using laser ablation ICP-MS. The error bars represent duplicate experimental results.

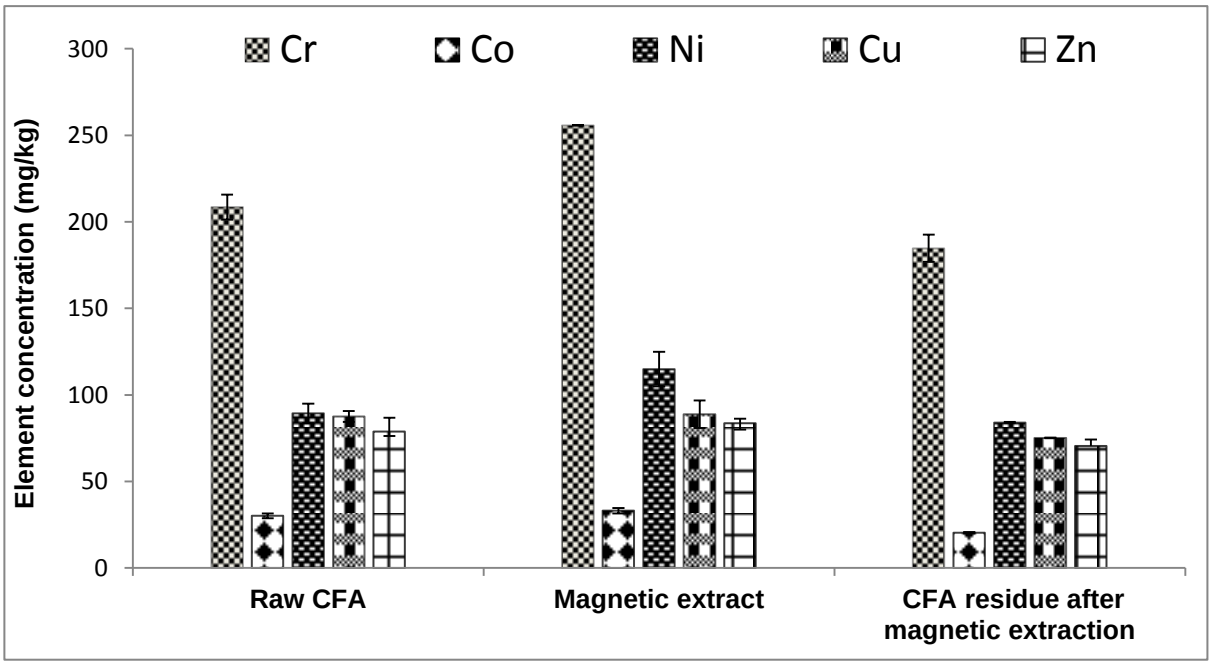

Figure 4.5: Cr, Co, Ni, Cu and Zn levels from magnetic extraction of CFA

As can be seen in Figure 4.5 above, Cr is quite enriched in the magnetic extract followed by Ni and lastly Co, Cu and Zn being slightly enriched. The CFA residue after magnetic extraction still has high levels of Cr, Co, Ni, Cu and Zn but lower than that of the raw CFA.

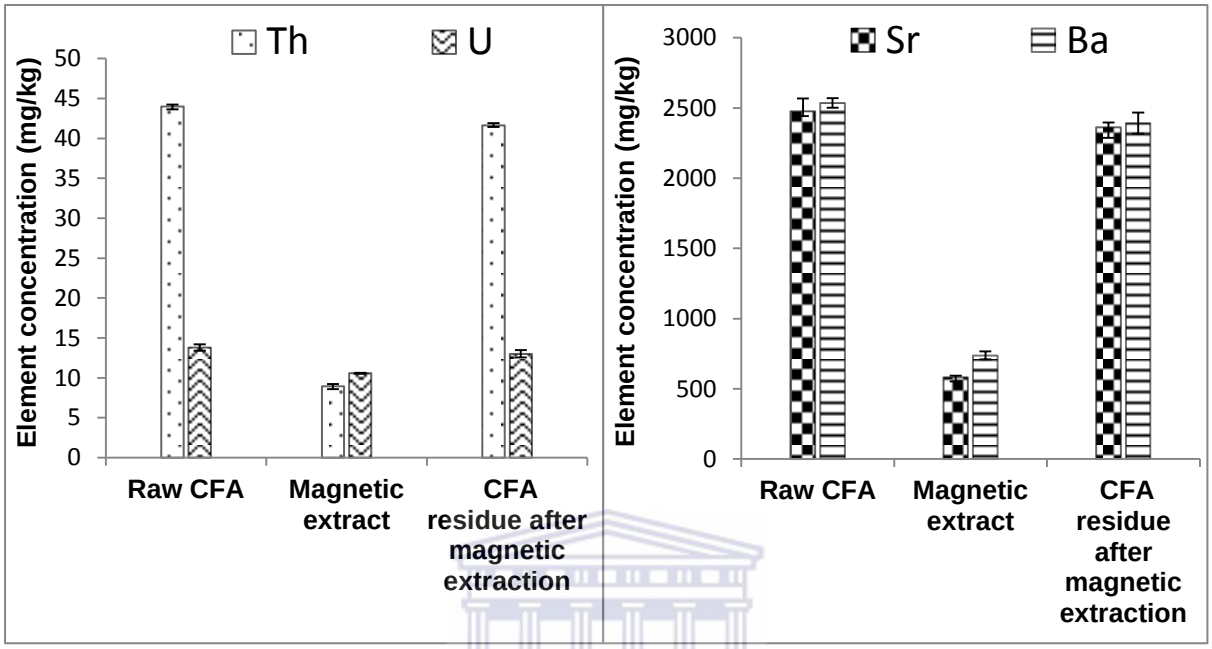

Figure 4.6: Th and U radioactive element levels and Sr and Ba toxic element levels from magnetic extraction of CFA

As can be seen in Figure 4.6 above, Th, U, Ba and Sr are more partitioned to the CFA matrix than to the magnetic extract fraction since their concentrations are relatively similar in both the raw CFA and the CFA residue after magnetic extraction. It is expected that the sum of the element in the magnetic extract and in the coal fly ash residue after magnetic extraction to equal the amount of said element in the raw CFA but it is not the case as seen in Figure 4.5 and Figure 4.6. A reason for this could be that the magnetic extract content is a very small percentage of the raw CFA and its partial removal from the CFA would not affect the relative concentration of elements to a great degree. The CFA residue after magnetic extraction therefore showed similar values to the raw CFA for this reason. Since the magnetic extract is predominantly a Fe based extract and having a total element complement that is lower compared to raw CFA, the subsidiary elements present in the magnetic extract (Figure 4.5)

would show an upconcentration in the magnetic extract. Cr, Co, Ni, Cu and Zn elements also show an affinity for the magnetic extract as explained previously.

The CFA residue after magnetic extraction was analysed for its mineral composition by XRD as described in Section 3.2.4. The data scan was plotted and the mineral phases identified using ICDD: PDF database 1998. The XRD spectrum of the CFA residue after magnetic extraction is presented in Figure 4.7 below.

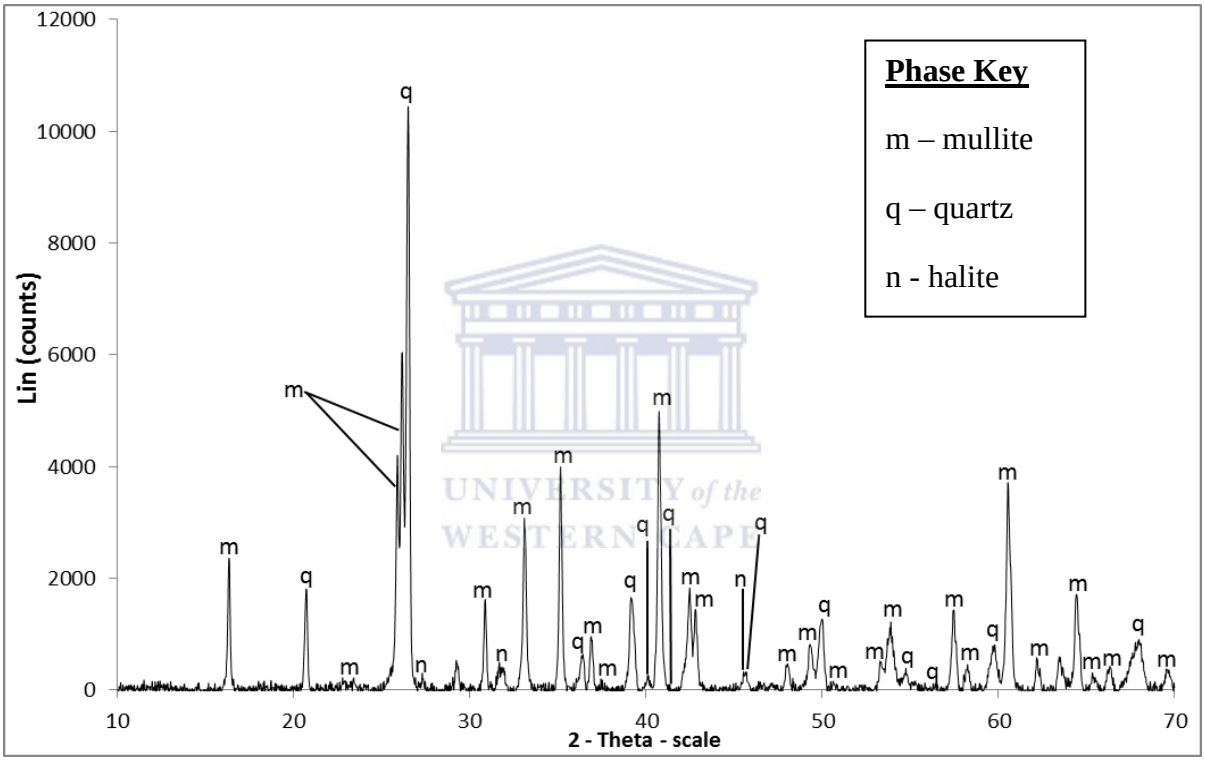

Figure 4.7: XRD spectrum of CFA residue after magnetic extraction

The XRD spectrum of CFA residue after magnetic extraction (Figure 4.7) showed the presence of quartz (SiO_2), mullite (aluminosilicate) and halite (NaCl) mineral phases. The XRD results showed no iron mineral phases. However the XRF results (Table 4.5) showed that Fe_2O_3 was still present at 2.35 % weight percentage on a dry basis. The XRF results showed that the Fe_2O_3 in the CFA residue after magnetic extraction (Table 4.5), decreased by 27.91 % in relation to the raw Matla CFA (Table 4.1). The reason for this discrepancy could be retention of the finer magnetic particles being trapped between the CFA particles when the

bar magnet is applied to the CFA. Fe was therefore not completely removed from the raw CFA by magnetic extraction. Since the particles were also much finer, it was not strongly retained by the bar magnet. Fe could also be included in other mineral phases present in the CFA. The halite mineral phase also diminished and the lime mineral phase was removed when compared to raw CFA (Figure 4.1). A plausible reason for this would be removal by dissolution of soluble salts when the raw CFA was mixed with water for the magnetic extraction step. The halite mineral phase only underwent partial dissolution and this could be the result of an insufficient volume of de-ionised water used for the magnetic extraction to allow the complete dissolution of the halite mineral phase from the CFA.

This CFA residue after magnetic separation was the starting material for all the alkaline and acid leaching tests that were further carried out in this study. The schematic flowchart of the initial treatment of CFA and its subsequent extraction is presented below

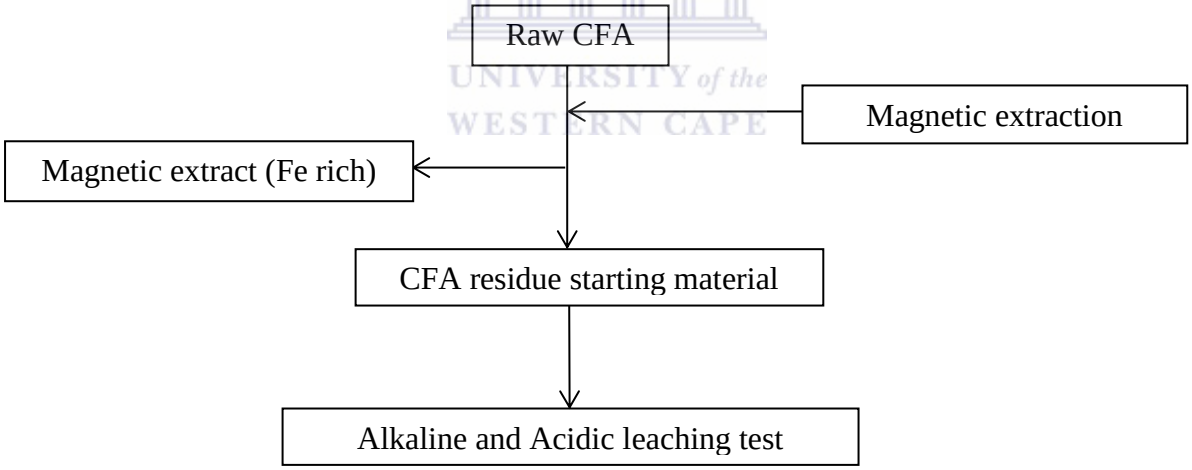

Figure 4.8: Schematic flowchart of initial magnetic extraction treatment of CFA

The following sub-sections will present the outcomes of the alkaline and leaching protocols that were tested on the CFA residue after magnetic extraction.

4.3 Alkaline leaching

As outlined in Chapter 3.3.2, a comparison was made between an indirect and direct alkaline leaching method using the magnetically extracted CFA as the starting material. Both methods used 20 g CFA and 20 g NaOH pellets. For the indirect method the CFA and NaOH were dry mixed to homogeneity and heated at 450 °C for 2 hours. The cooled fused sintered product was then crushed to a fine powder with a pestle and mortar This was to increase the surface area of the fused sintered product which was then stirred in 600 mL of deionised water for 2 hours. In the case of the direct alkaline leaching method, 20 g NaOH was dissolved in 600 mL de-ionised water and 20 g CFA added to this solution. The mixture was then stirred for 2 hours while being maintained at a temperature of 100 °C and thereafter the solids were separated from the liquid by filtration. In both methods the filtrates were analysed using ICP-OES and UV-Vis spectroscopy to compare the level of extraction efficiency. The results are presented below in Figures 4.9 and 4.10 below. The error bar represents 3 experimental replicates.

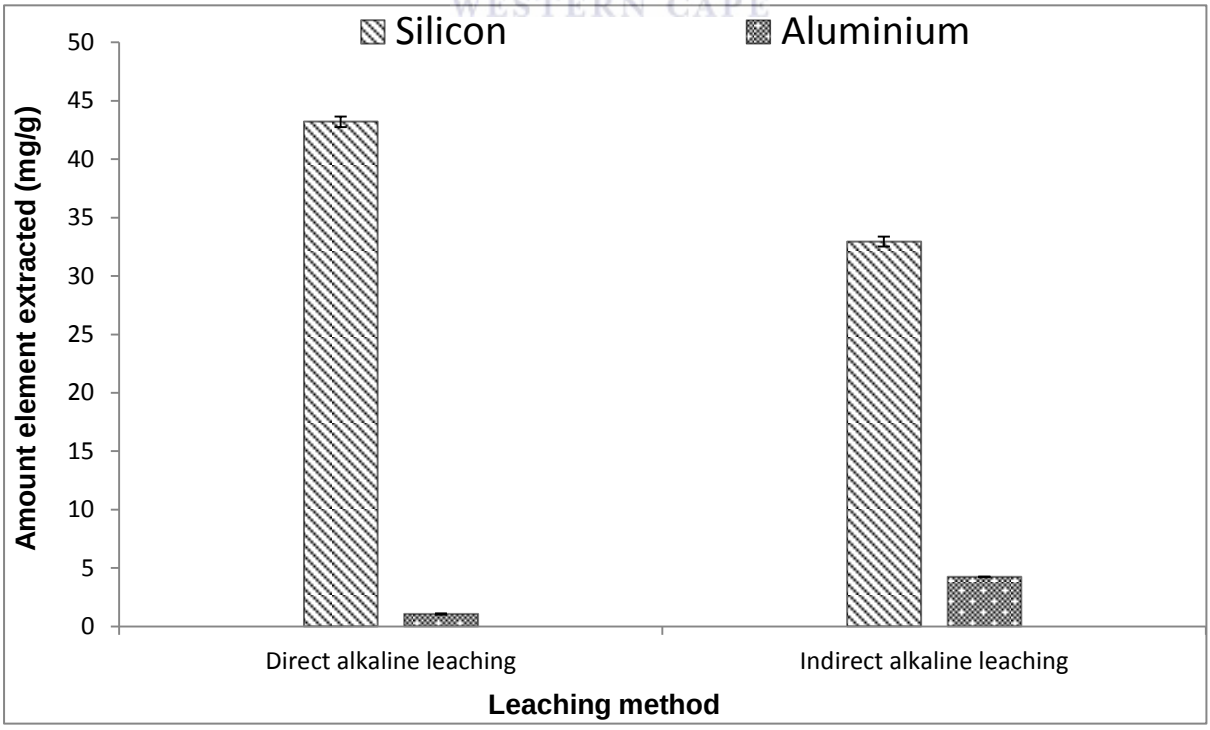

Figure 4.9: Comparison of indirect and direct alkaline leaching (n=3)

Figure 4.9 above reports the amount of elements extracted from 20 g CFA. The percentage element extraction from the residue is presented graphically in Figure 4.10 below,

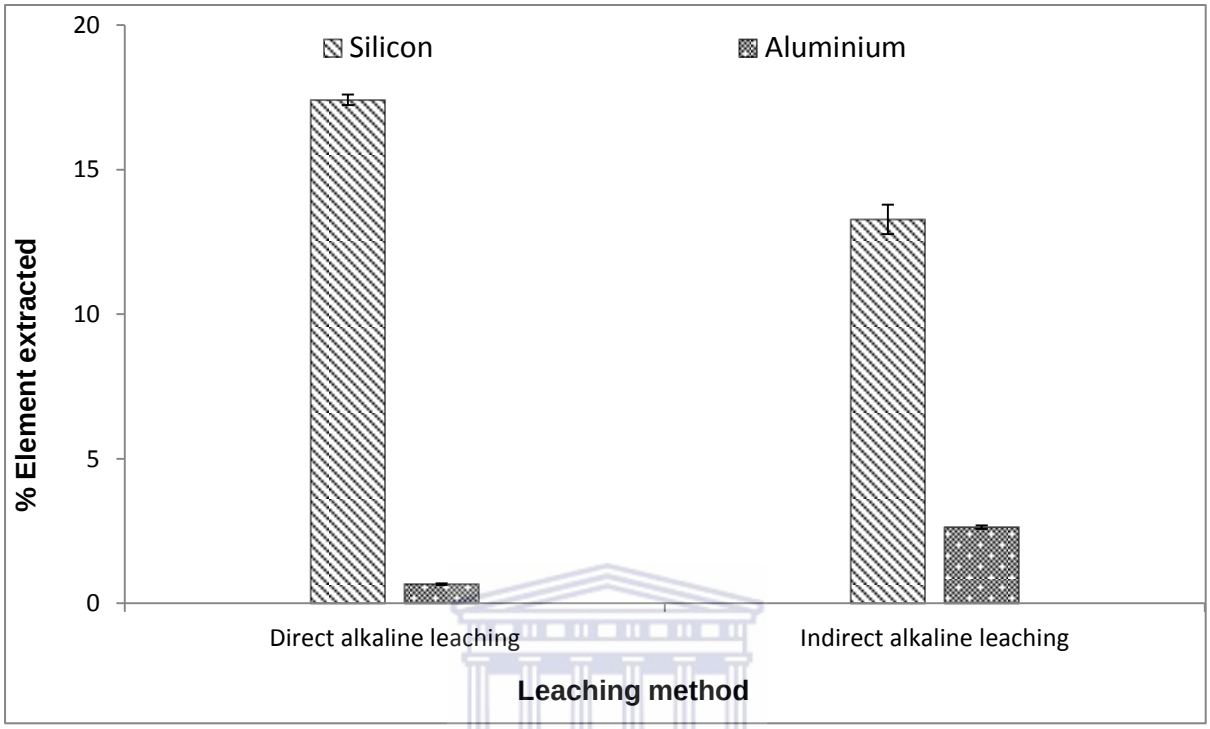

Figure 4.10: Percentage element extracted from CFA via alkaline leaching (n=3)

As can be seen in Figure 4.10 above, the direct leaching method provided a higher Si extraction yield compared to that of indirect alkaline leaching. The indirect alkaline leaching method allowed a higher Al extraction albeit a rather low yield compared to that of the direct alkaline leaching method. Since the extraction yield of Al was less than Si in the direct alkaline leaching method, it justified the choice of the direct alkaline extraction method for Si recovery as it gave a good yield of Si.

Direct alkaline leaching was optimised by firstly setting the concentration of NaOH as the variable in the experimental procedure while the amount of CFA, solution volume and leaching temperature and leaching time remained constant. The NaOH masses used were 20 g, 50 g, 100 g, 150 g, 200 g, 250 g and 300 g dissolved in 600 mL of de-ionised water respectively. The equivalent concentrations therefore varied from 0.83 M to 12.5 M while the

solution volume was set at 600 mL, leaching time 2 hours and leaching temperature 100 °C. The result of varied NaOH concentrations is presented below in Figure 4.11.

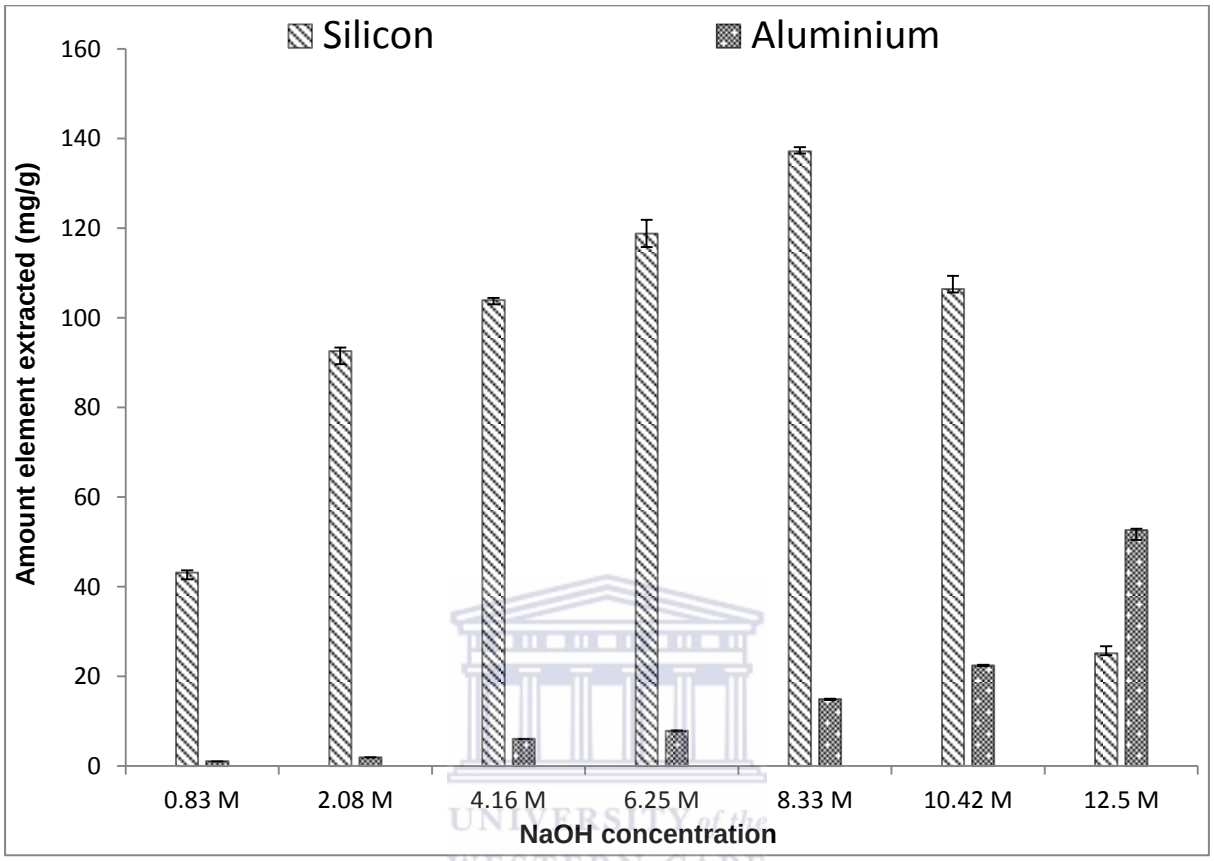

Figure 4.11: Effect of varied NaOH concentration on alkaline leaching (n=3)

20 g CFA was used for all the varied NaOH concentration tests presented in Figure 4.11 above. The leaching time was set at two hours since Bai, (2010), reported a decrease in the extraction of Si after that time. The temperature was also kept at 100 °C. The graphical presentation of Figure 4.11 above therefore presents the amount of Si and Al present in the filtrates after being extracted from the 20 g CFA experimental test samples. The percentage element extraction of the Si and Al is presented in Figure 4.12 below.

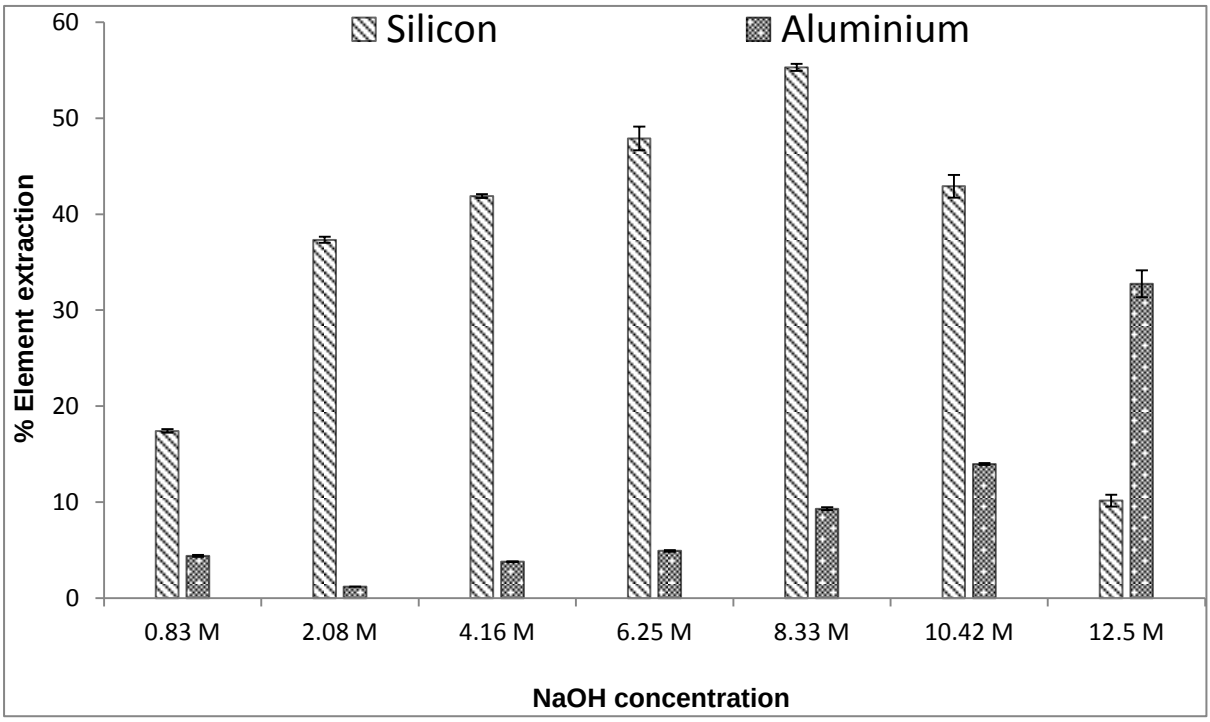

Figure 4.12: Percentage element extracted with varied NaOH concentration alkaline leaching (n=3)

From the percentage extraction graph above (Figure 4.12) the optimal concentration for extraction of Si was chosen to be 6.25 M NaOH. The Si extraction yield is the highest at that NaOH molarity with a minimal amount of co-extraction of Al. The Si extraction difference between 6.25 M and 8.33 M NaOH was approximately 10 % compared to an approximate 47 % difference for the Al extraction. It was also seen that Al extraction increased as the NaOH concentration increased and at the highest 12.5 M NaOH concentration mainly Al was extracted. A possible reason for this increased extraction efficiency could be the amphotericity of Al showing a greater dissolution effect at higher concentrations of NaOH. The increased aluminium dissolution would also hinder the dissolution of Si as described by Jephcott et al., (1950). The highest Si extraction for this study was approximately 55 % using 8.33 M NaOH solution. This is equivalent to a 33 % NaOH solution (200 g NaOH pellets dissolved in 600 mL de-ionised water). Bai et al., (2010) achieved a maximum Si extraction of 62.5 % from a Class F CFA using a 30 % NaOH (equivalent to 7.5 M NaOH) solution for the alkaline leaching. The leaching time used by Bai and co-workers was 1 hour at a

temperature of 100 °C. The main difference between Bai and co-workers and this study was that 2 hours instead of 1 hour leaching time was used for the direct alkaline leaching process.

Since the optimal concentration of NaOH was decided upon to be 6.25 M NaOH, the amount of CFA was varied while the experimental parameters of time and temperature remained unaltered. The second optimisation step therefore used varied CFA ash amounts ranging from 5 g – 40 g while the 6.25 M NaOH concentration, 600 mL solution volume and 2 hour leaching time at 100 °C remained fixed. The results of these tests are presented in Figure 4.13 below.

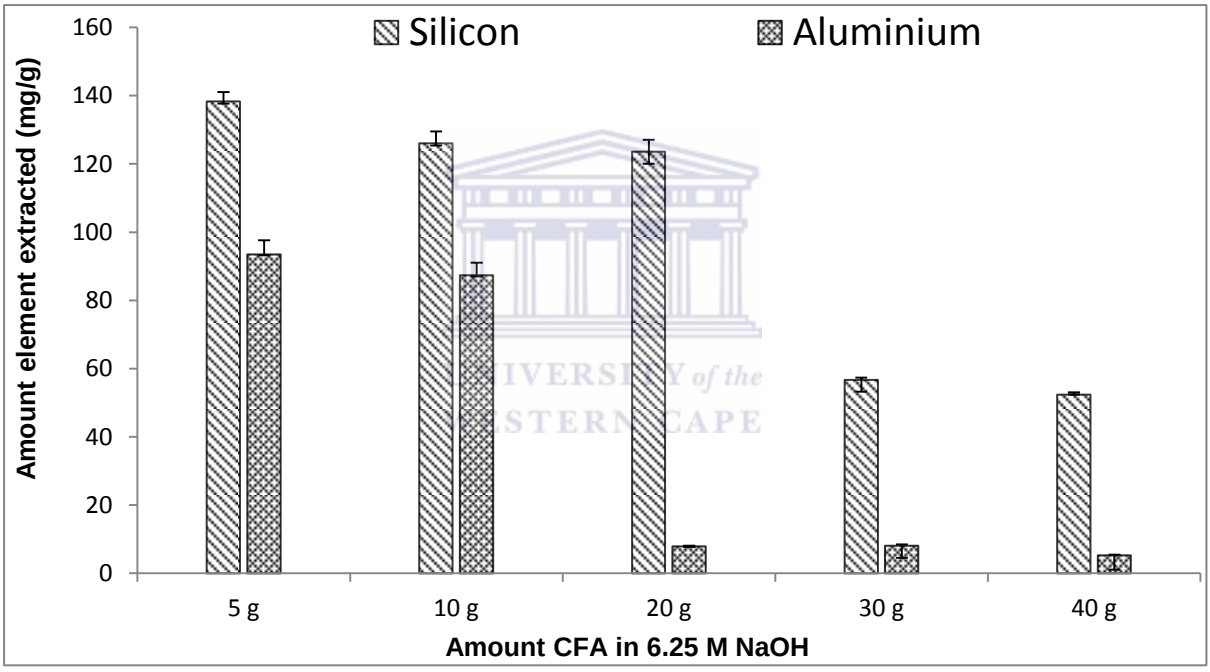

Figure 4.13: Effect of varied CFA masses leached with 6.25 M NaOH (n=3)

The graphical presentation of the percentage element extraction is presented in Figure 4.14 below,

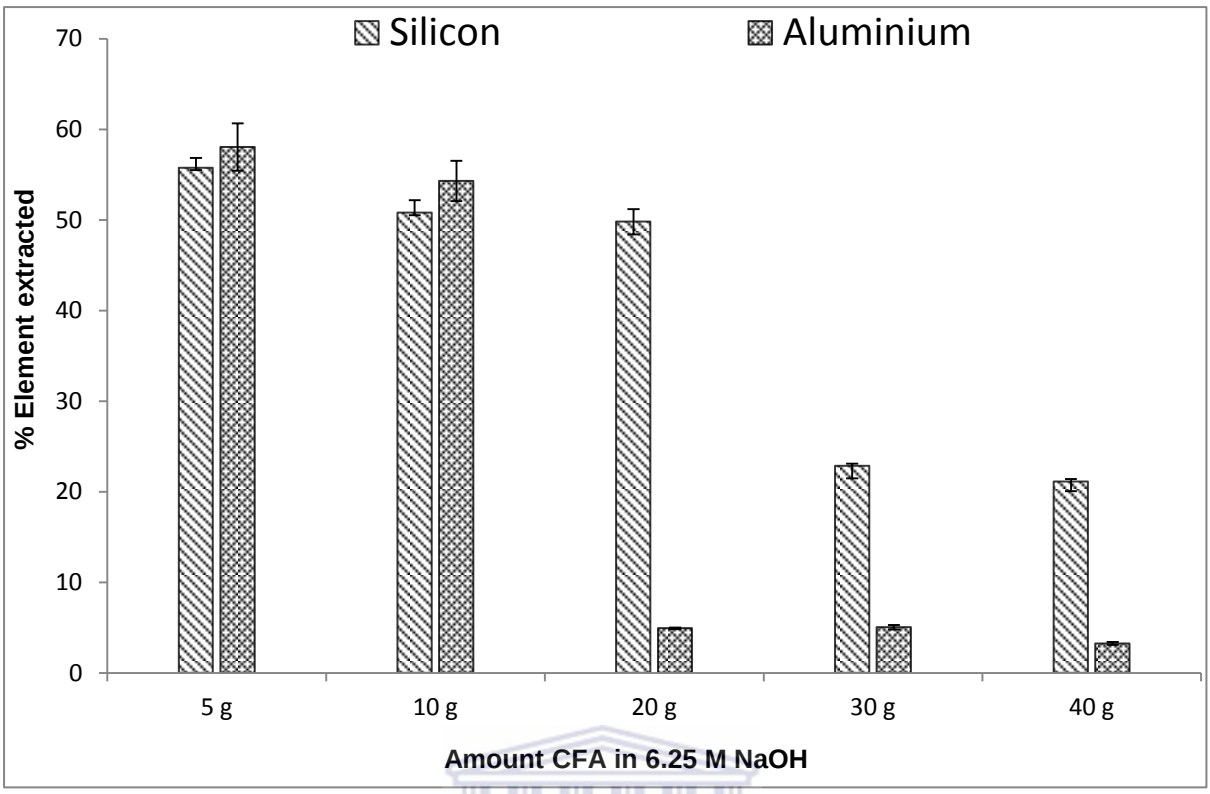

Figure 4.14: Percentage element extracted from varied CFA masses leached with 6.25 M NaOH (n=3)

It can be seen from Figure 4.14 above that the highest extraction of both Si and Al can be achieved when a smaller amount of CFA is leached with NaOH. This could be attributed to increased mass transfer between the CFA particles and the NaOH. Since there are less CFA particles in the leaching system, more of the alkaline leach solution is able to make effective contact between the alkaline leach solution and CFA particles. This effect enhances the reaction to dissolve the target elements. As the mass of the CFA increased, as seen in the 20 g sample, the Si extraction increased to approximately 50 % and Al extraction considerably decreased. However, when 30 g or 40 g CFA samples were added to the 600 mL 6.25 M NaOH solution, a relatively viscous solution was formed and the CFA particles were subjected to resistance whilst being stirred around in solution. It becomes more difficult for all the particles to vortex in the viscous alkaline solution so as to effectively mix with the alkaline solution for leaching to take place. The CFA particles were also hydrated in solution and become heavier to move. Therefore the increased mass of CFA added to the leaching

system makes it difficult for extraction to proceed at a high solid to liquid ratio. An additional reason is that super saturation with respect to Si dissolution is reached and the dissolved Si goes back into solid phase CFA residue. The dissolved Si is therefore lower in the leach filtrates when 30 g or more CFA is leached with 600 mL of the 6.25 M NaOH solution

From the optimisation tests, 20 g CFA was chosen as the optimal mass to be leached with 600 mL of 6.25 M NaOH. It gave a relatively high Si extraction yield with low Al co-dissolution. The 20 g CFA residue after direct alkaline leaching with the chosen optimum concentration of 6.25 M NaOH was analysed via XRD. The XRD spectrum is presented in Figure 4.15 below,

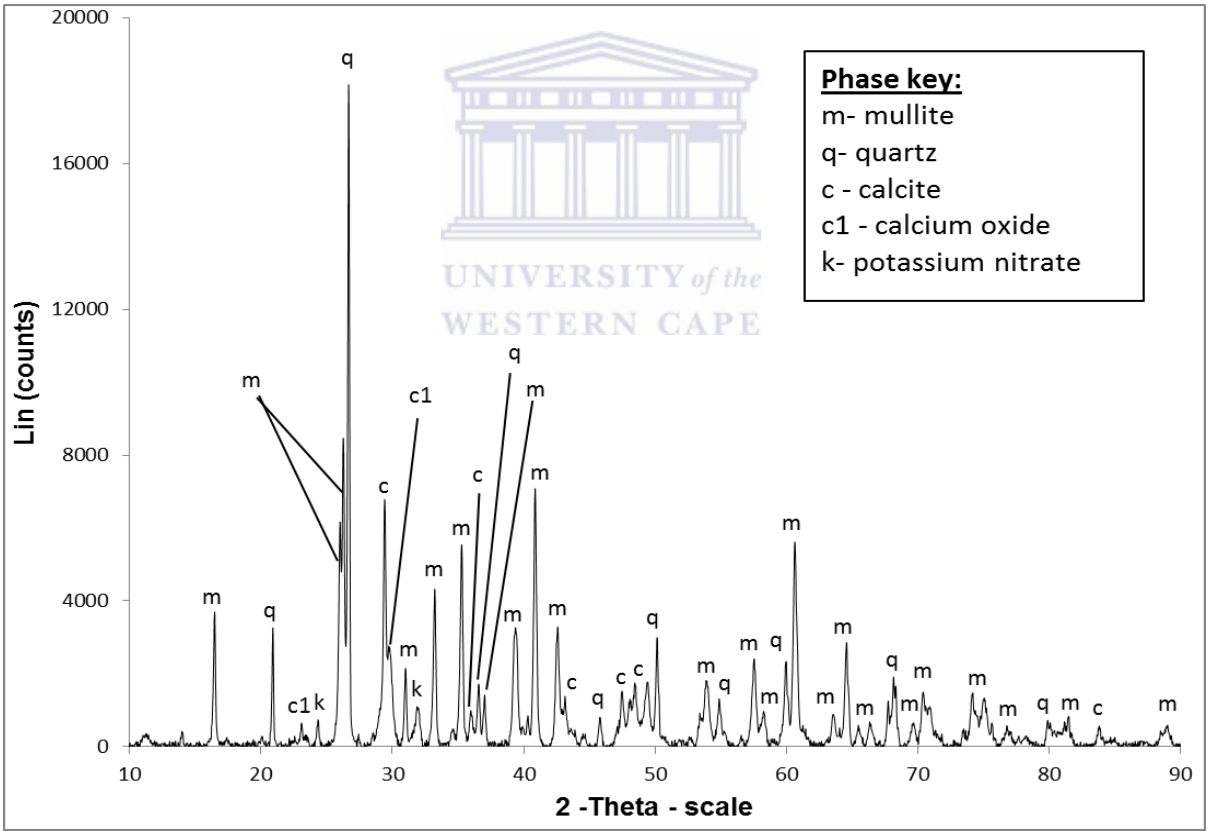

Figure 4.15: XRD spectrum of CFA leached with 6.25 NaOH

The XRD spectrum of the CFA residue remaining after direct alkaline leaching with the optimum chosen concentration of 6.25 M NaOH (Figure 4.15) showed that the mullite and quartz phases remained unaffected in the CFA residue after leaching. Hence the Si that was

extracted originated mainly from the glassy phase of CFA since the quartz and mullite peaks are still very prominent in the XRD scan. The halite (NaCl) mineral phase was removed during the direct alkaline leaching and there was the formation of calcite, calcium oxide and potassium nitrate mineral phases after the 6.25 M NaOH leaching of the CFA. An explanation for the new formed mineral phases in the residues could be that the components of these minerals phases were made available during leaching or during the magnetic extraction step and this allowed these mineral phases to form probably due to supersaturation in solution caused by dissolution of soluble Ca or K containing salts. The additional reaction of atmospheric carbon dioxide with Ca present in the CFA would also contribute to the formation of calcite mineral phases.

4.4 Acidic Leaching

As outlined in Section 3.3.3 three acidic leaching methods were tested. Two of the leaching methods used sulphuric acid and one used hydrochloric acid as the lixiviant.

4.4.1 HCl leaching

As described in Section 3.3.3.1, 20 g of the CFA residue that had previously undergone magnetic extraction was leached with 400 mL of HCl having molarities varying from 0.5 M to 10 M, while stirring rapidly at 100 °C for 2 hours. The results are presented in Figure 4.16 and Figure 4.17 below.

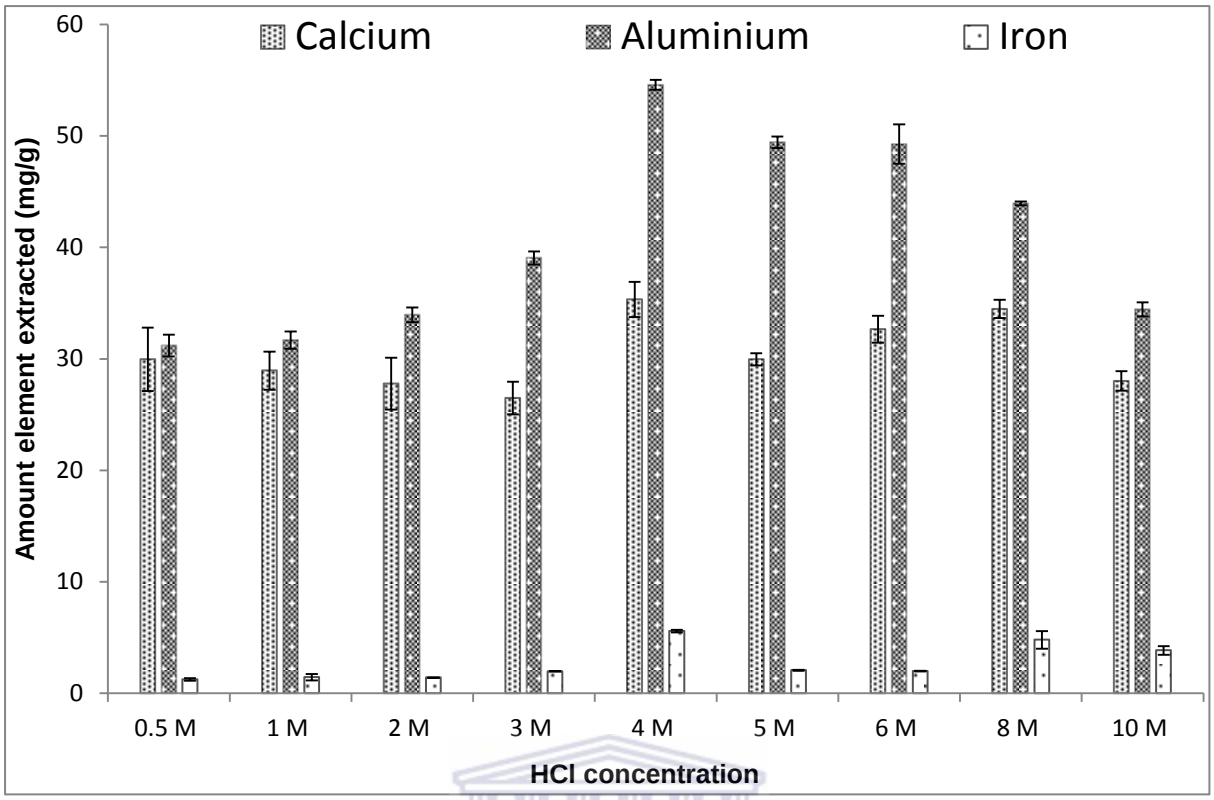

Figure 4.16: HCl leaching of CFA (n=3)

The percentage element extractions are presented in Figure 4.17 below,

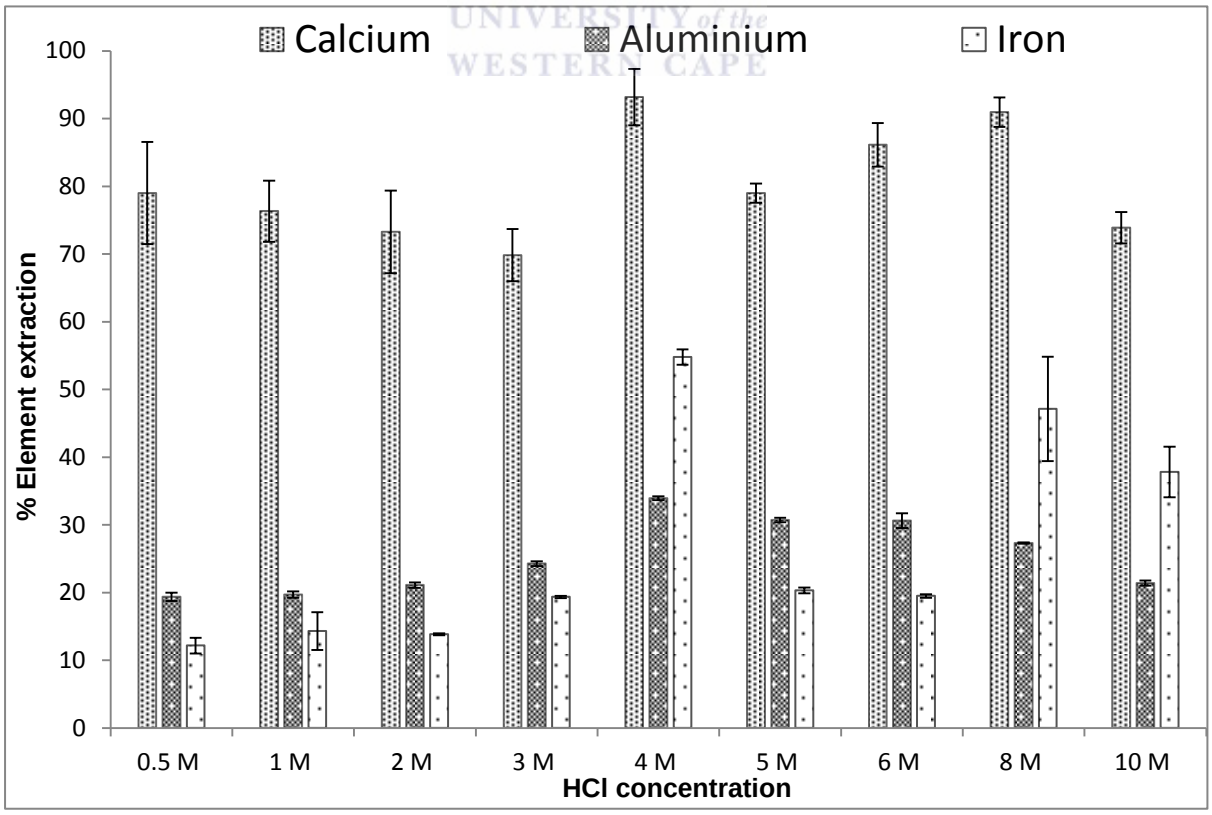

Figure 4.17: Percentage element extractions from HCl leaching (n=3)

The maximum Al extraction yield attained with HCl leaching was approximately 33 % using 4 M HCl (Figure 4.17). The iron content that was still present in the CFA after the magnetic extraction was also extracted with HCl leaching and increased as the concentration of the HCl increased. Since it was seen that the calcium extraction remained relatively constant at 80 % from 0.5 M to 10 M HCl, the extraction tests were then extended to cover 0 M to 0.25 M HCl to see the effect on the Ca extraction efficiency, as shown in Figure 4.18 below,

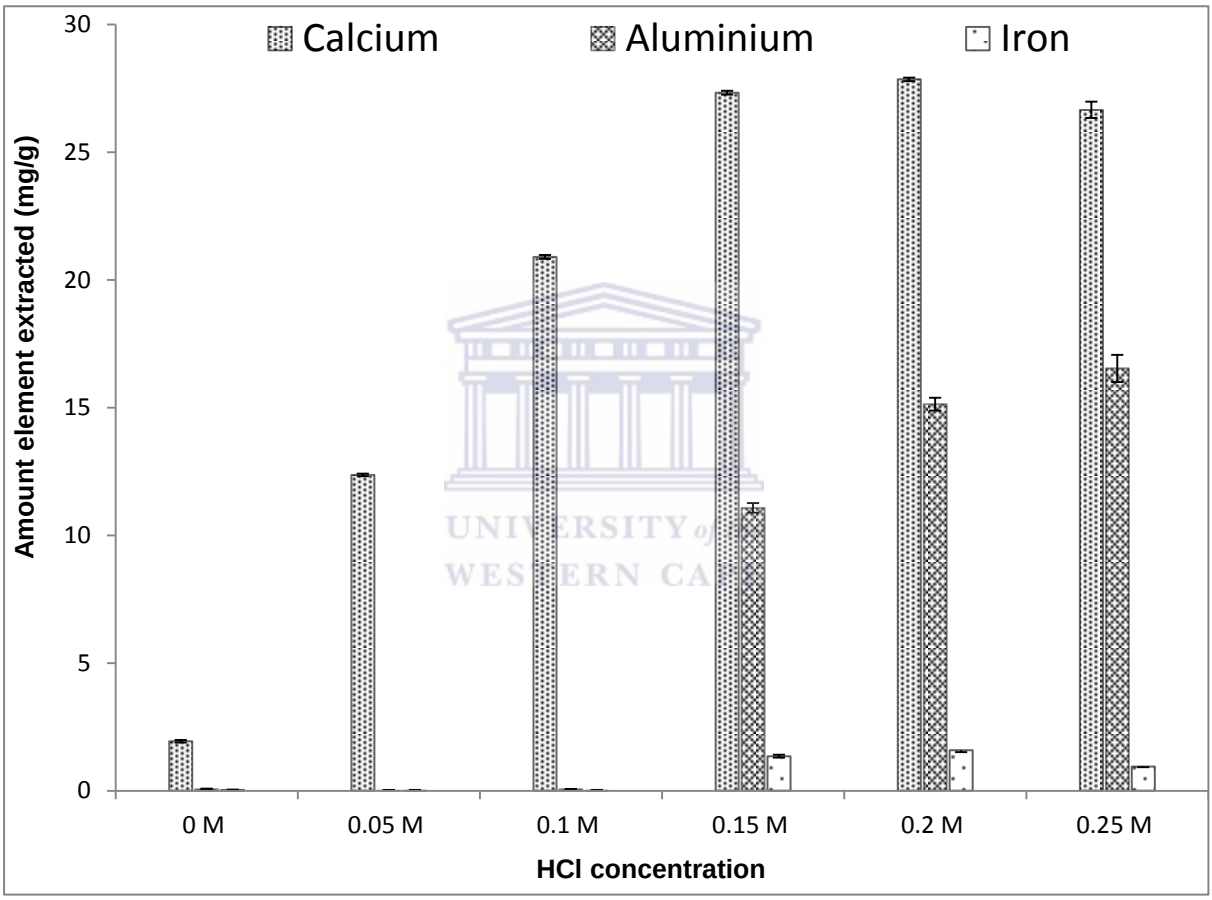

Figure 4.18: Extended HCl leaching of CFA for calcium extraction (n=3)

The percentage element extractions are presented in Figure 4.19 below,

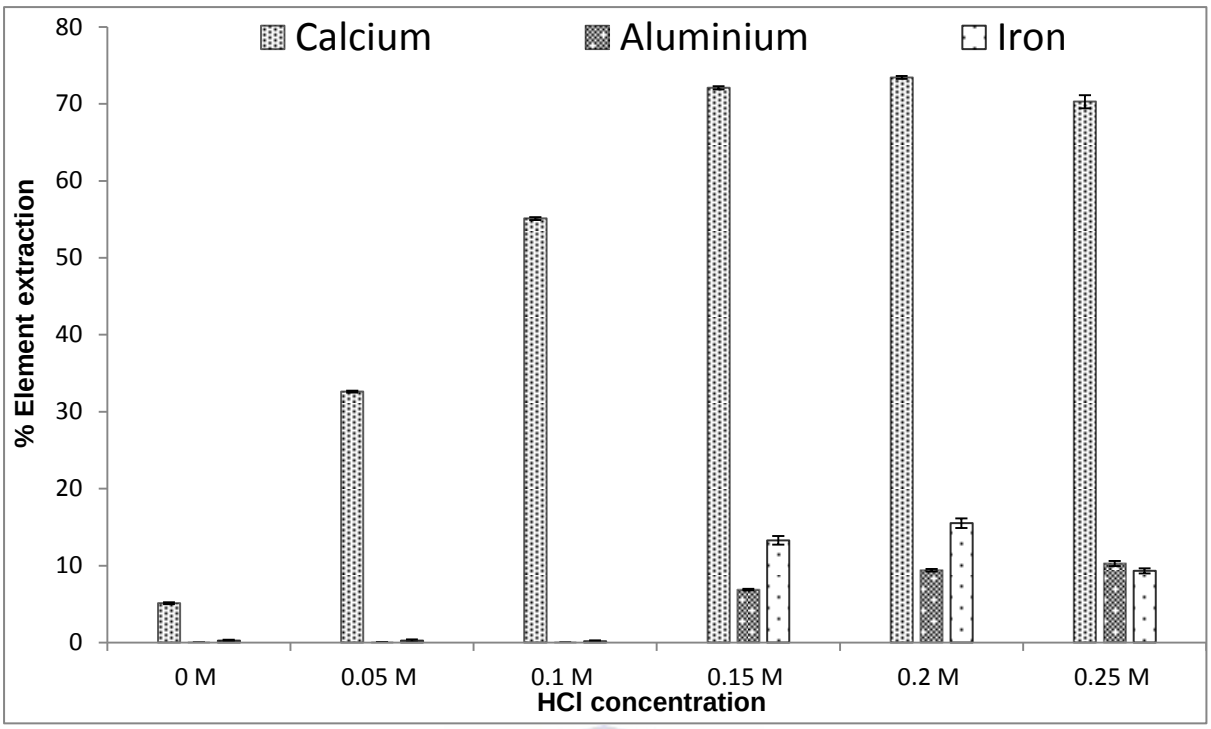

Figure 4.19: Percentage elements extractions for extended HCl leaching of CFA for calcium extraction (n=3)

0.1 M HCl (400 mL solution volume) was seen to be the optimum concentration (Figure 4.19) to extract calcium with minimal concurrent extraction of Al and Fe. The CFA mass used with 0.1 M HCl was then optimised for calcium extraction with minimal co-extraction of Al and Fe. The CFA amounts were varied from 5 g – 40 g and reacted with the optimal determined concentration of 0.1 M HCl. The solution volume of 400 mL, leaching temperature of 100 °C and leaching time of 2 hours were kept constant. Attempting to remove as much Ca as possible without any additional Al and Fe would help to enhance the H_2SO_4 leaching of Al from CFA. The results are shown in Figure 4.20 below,

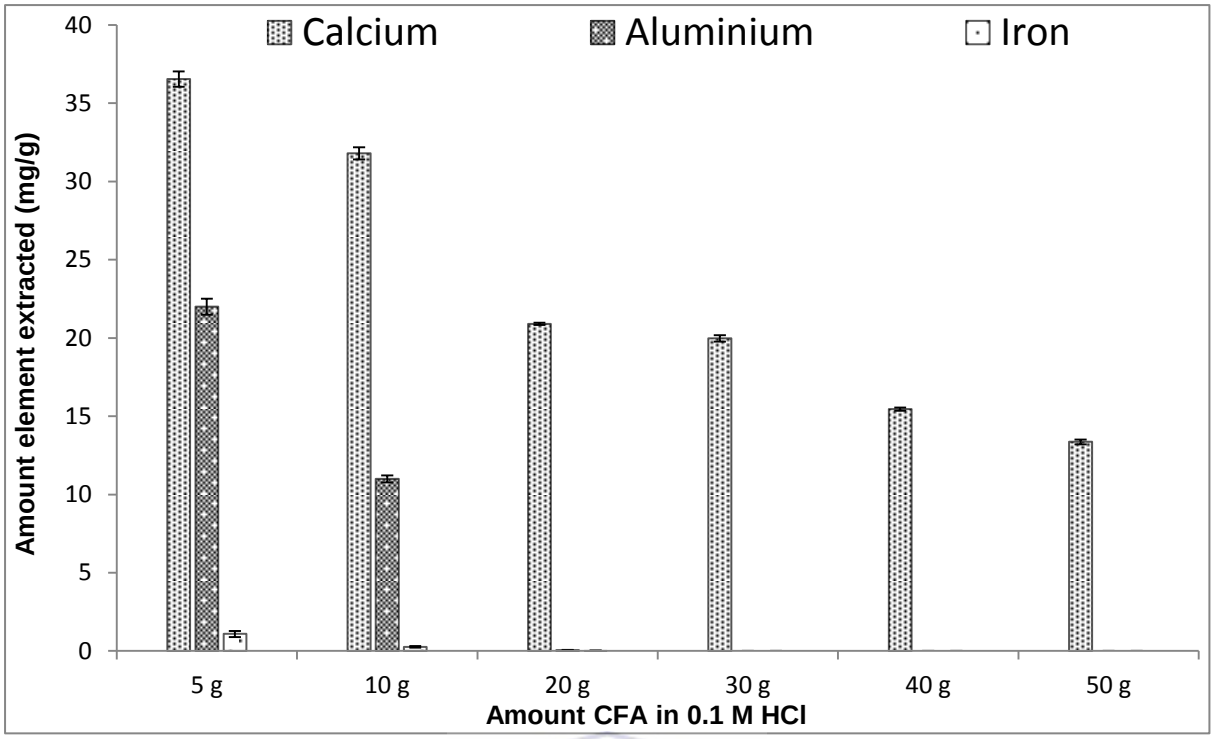

Figure 4.20: Varied CFA masses leached with 0.1 M HCl for calcium extraction (n=3)

The percentage element extractions are presented in Figure 4.21 below to provide a more synoptic view of the optimisation tests.

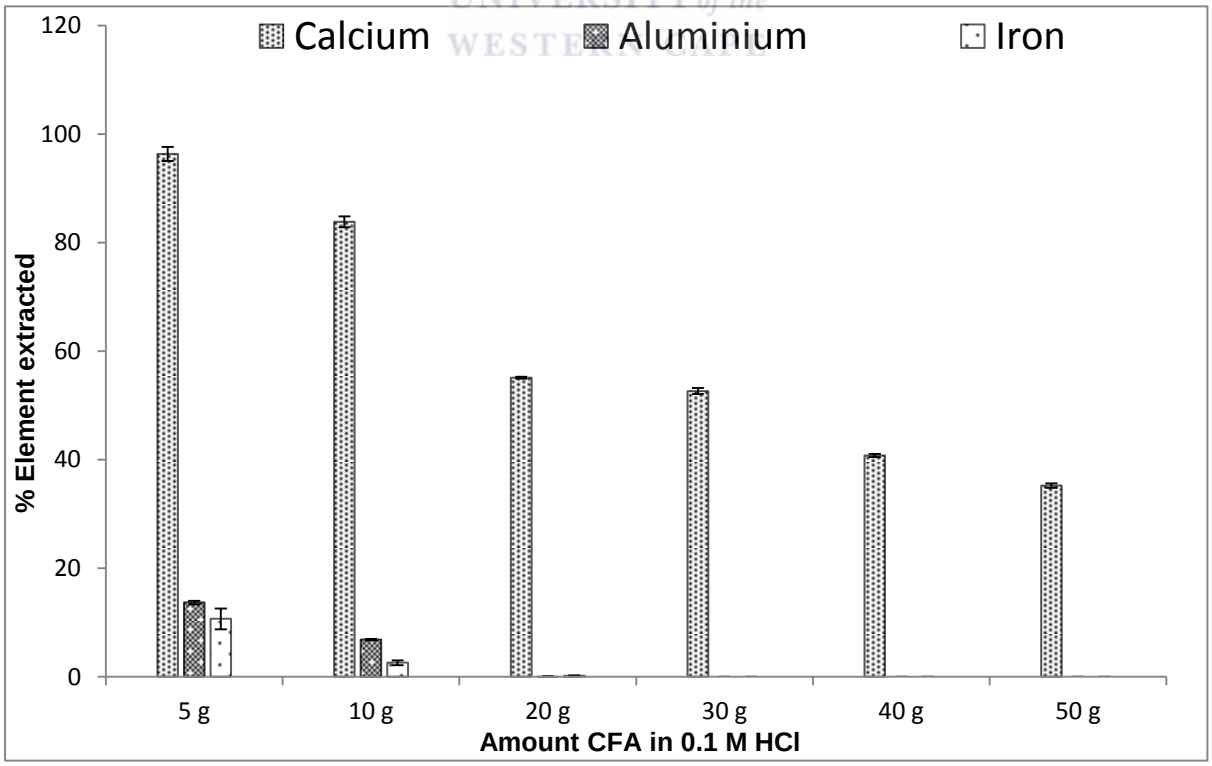

Figure 4.21: Percentage element extractions from varied CFA masses in 400 mL 0.1 M HCl (n=3)

As can be seen in Figure 4.21 above, the calcium extractions are very high (± 100 %) with 400 mL of 0.1 M HCl when lower amounts of CFA are used (5 - 10 g). There is also some co-extraction of Fe and Al. As the mass of CFA increases the calcium extraction starts to taper off. Minimal amounts of Al and Fe are co-extracted when more than 30 g of CFA is leached with 400 mL of 0.1 M HCl. This could be attributed to solution-particle mass transfer and also to the consumption of the H_3O^+ ions of the hydrochloric acid by the calcium in the CFA. The 20 g CFA residue that had been leached with 400 mL of 0.1 M HCl was analysed by XRD and the XRD spectrum is presented in Figure 4.22 below.

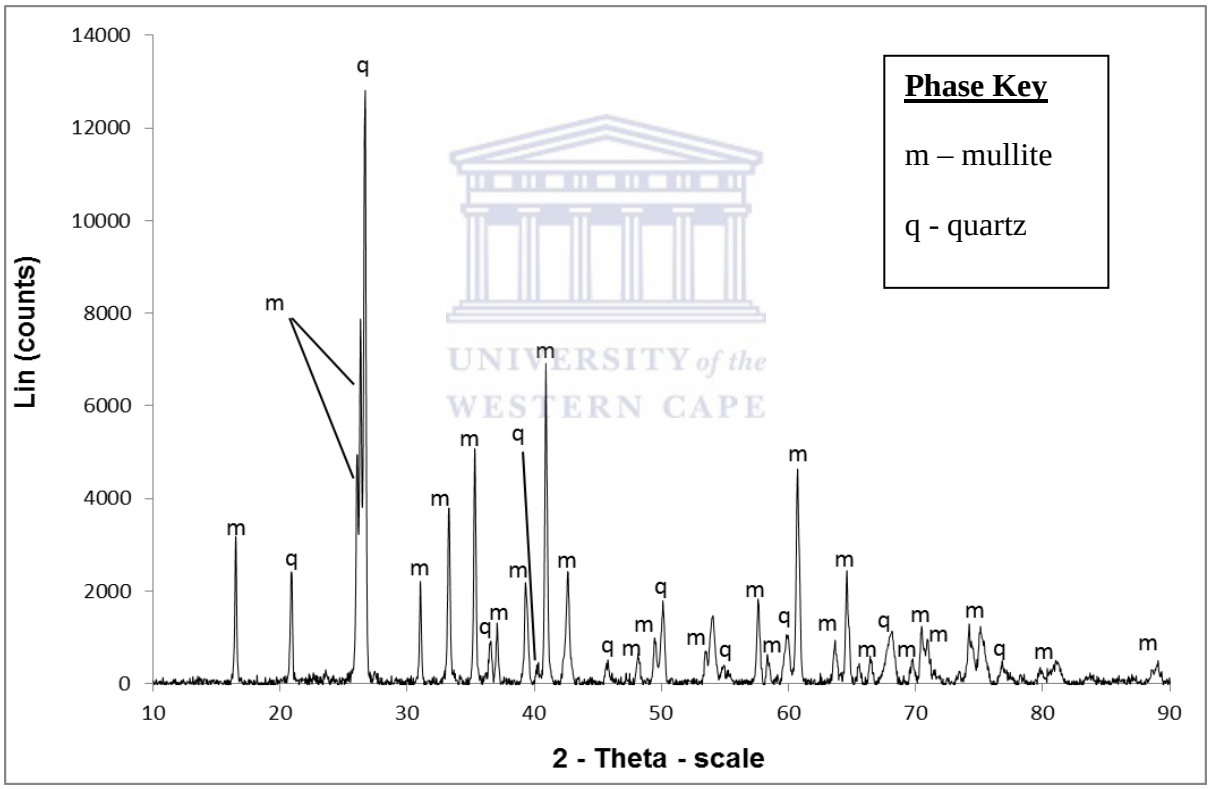

Figure 4.22: XRD spectrum of CFA leached with 0.1 M HCl

The XRD result (Figure 4.22) for the chosen optimal 0.1 M HCl leaching of CFA showed that the mullite and quartz mineral phases of magnetically extracted CFA remained unchanged and the halite (NaCl) mineral phase (as seen in Figure 4.3) was removed. It can be seen from the XRD spectrum in Figure 4.22 that no secondary mineral phases are formed

when 0.1 M HCl is used as the lixiviant and Ca did not form secondary phases as was previously observed (Figure 4.15) when NaOH was used as the lixiviant.

4.4.2 H_2SO_4 leaching

The sulphuric acid leaching processes was investigated via an indirect and direct leaching approach. For the indirect acidic leaching process, as described in Section 3.3.3.2, varying concentrations of H_2SO_4 were mixed with 20 g of magnetically extracted CFA in a liquid: solid ratio of 1:2. Therefore 40 mL of the various H_2SO_4 solutions was mixed with the test 20 g CFA samples. The mixture was then stirred at 450 rpm while heating on a hotplate at 220 °C. The reaction was allowed to proceed until all the liquid evaporated. The reaction vessel then remained on the hotplate at that temperature for a further 30 minutes. This was to allow time for the CFA residue to calcine. Once cooled, de-ionised water was added to the CFA residue in a solid:liquid ratio of 1:6. 120 mL de-ionised water was therefore added to each CFA sample test. This mixture was then stirred rapidly at a temperature range of 85 - 90 °C for 30 minutes to partition the extracted Al into the liquid medium. The result of indirect acidic leaching is presented in Figure 4.23 below.

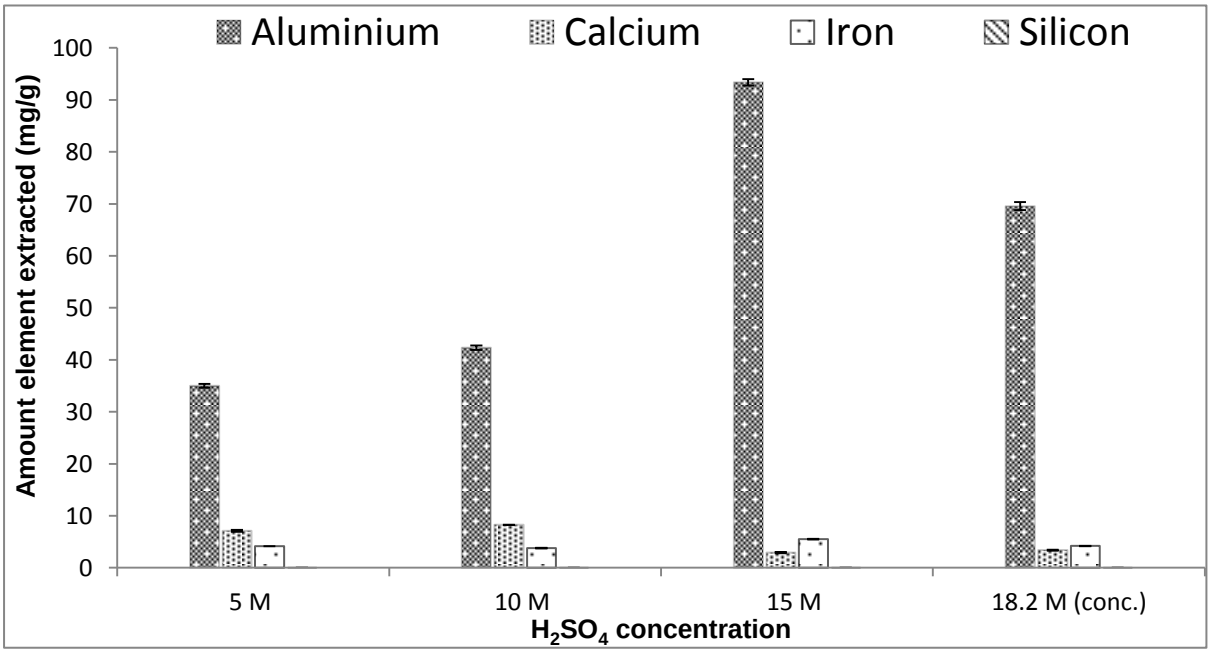

Figure 4.23: Indirect acidic leaching of CFA with varied H_2SO_4 concentrations (n=3)

The percentage element extractions for the indirect acidic leaching are presented in Figure 4.24 below,

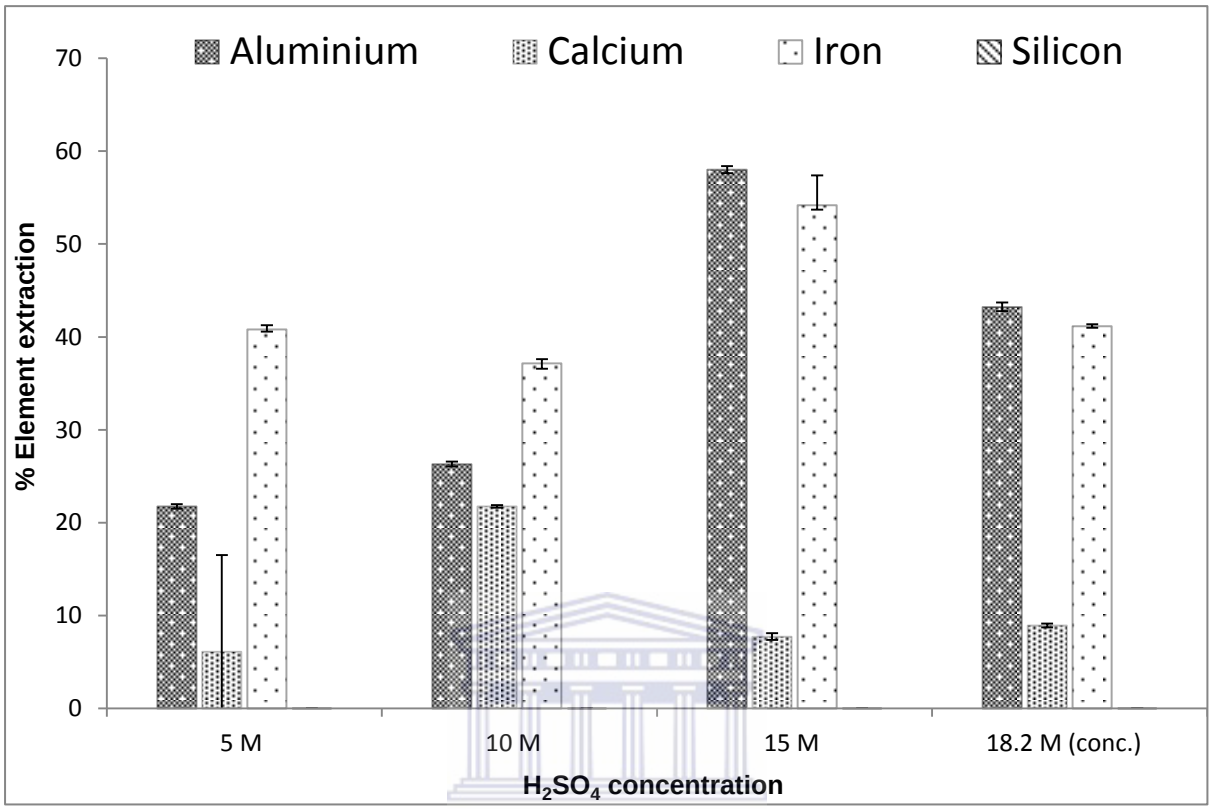

Figure 4.24: Percentage element extractions of CFA using indirect acidic leaching (n=3)

Looking at Figure 4.24, it can be seen that the indirect H_2SO_4 leaching method gave the highest Al extraction yield of 58 % at 15 M H_2SO_4. Fe extraction was also at its highest extraction yield of 54 % using 15 M H_2SO_4. Si extraction was extremely low to negligible when H_2SO_4 was used as the lixiviant. The use of concentrated H_2SO_4 did not give the highest extraction yield and a reason for this could be that concentrated H_2SO_4 solution is too viscous. This higher viscosity hinders the reaction with the CFA by decreasing the stirring speed.

The direct H_2SO_4 leaching process, as described in Section 3.3.3.3, was performed where varying concentrations of H_2SO_4 were directly mixed with magnetically extracted CFA in a liquid: solid ratio of 10 mL:1 g CFA. 200 mL of the varied H_2SO_4 concentrations were therefore added to a 20 g magnetically extracted CFA initial test sample. The mixture was

then refluxed for 2 hours. The reaction vessel was then removed and allowed to cool. De-ionised water was added to the experimental leach tests using H_2SO_4 concentrations higher than 5 molar to dilute the concentration to approximately 5 M H_2SO_4 (makes filtration of the leached solution possible using standard filter paper). The result of the direct acidic leaching is presented in Figure 4.25 below,

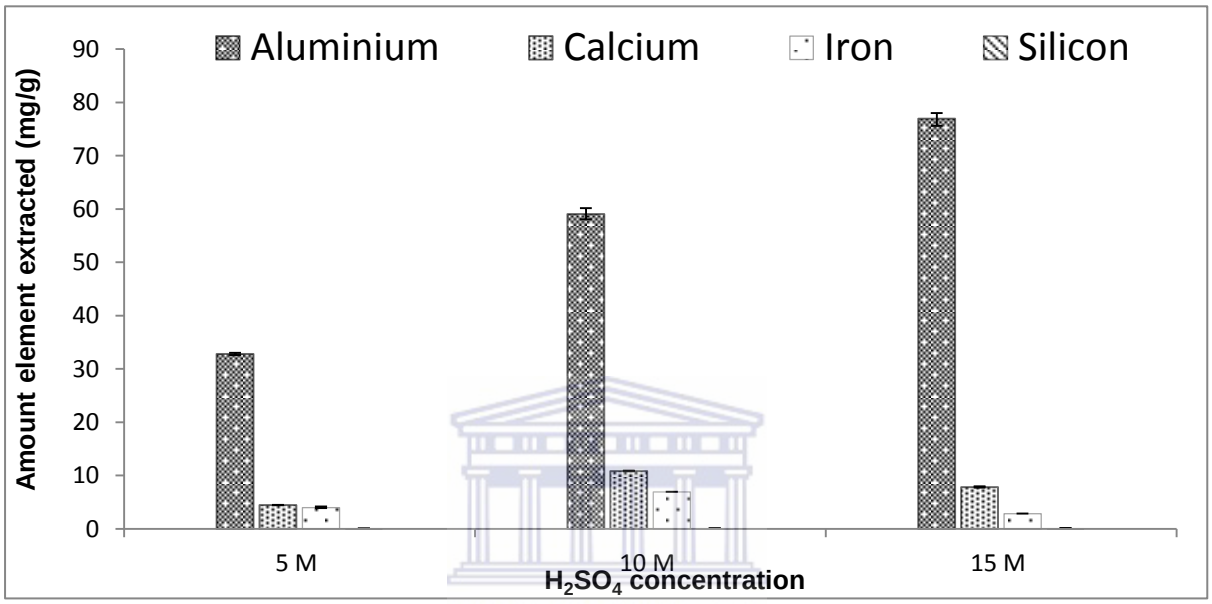

Figure 4.25: Direct acidic leaching of CFA with varied H_2SO_4 concentrations (n=3)

The percentage element extractions for direct acid leaching are presented in Figure 4.26 below,

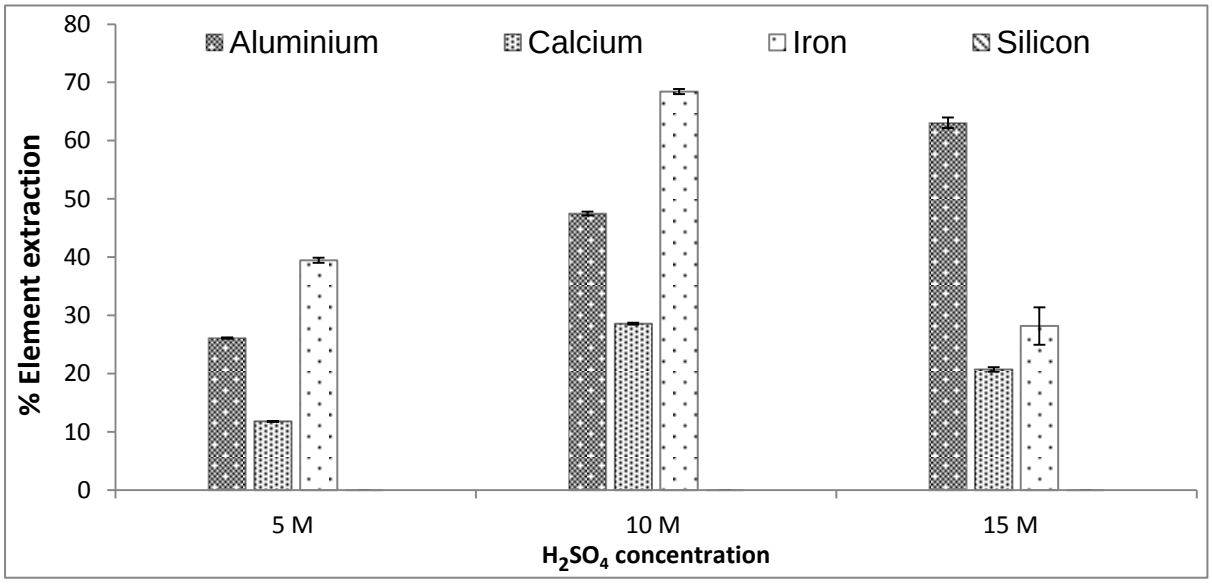

Figure 4.26: Percentage element extractions from CFA using direct acidic leaching (n=3)

The direct acid leaching and indirect acid leaching are plotted alongside each other to provide a comparative view of the results from the 2 acid leaching processes. The comparative plot is presented in Figure 4.27 below.

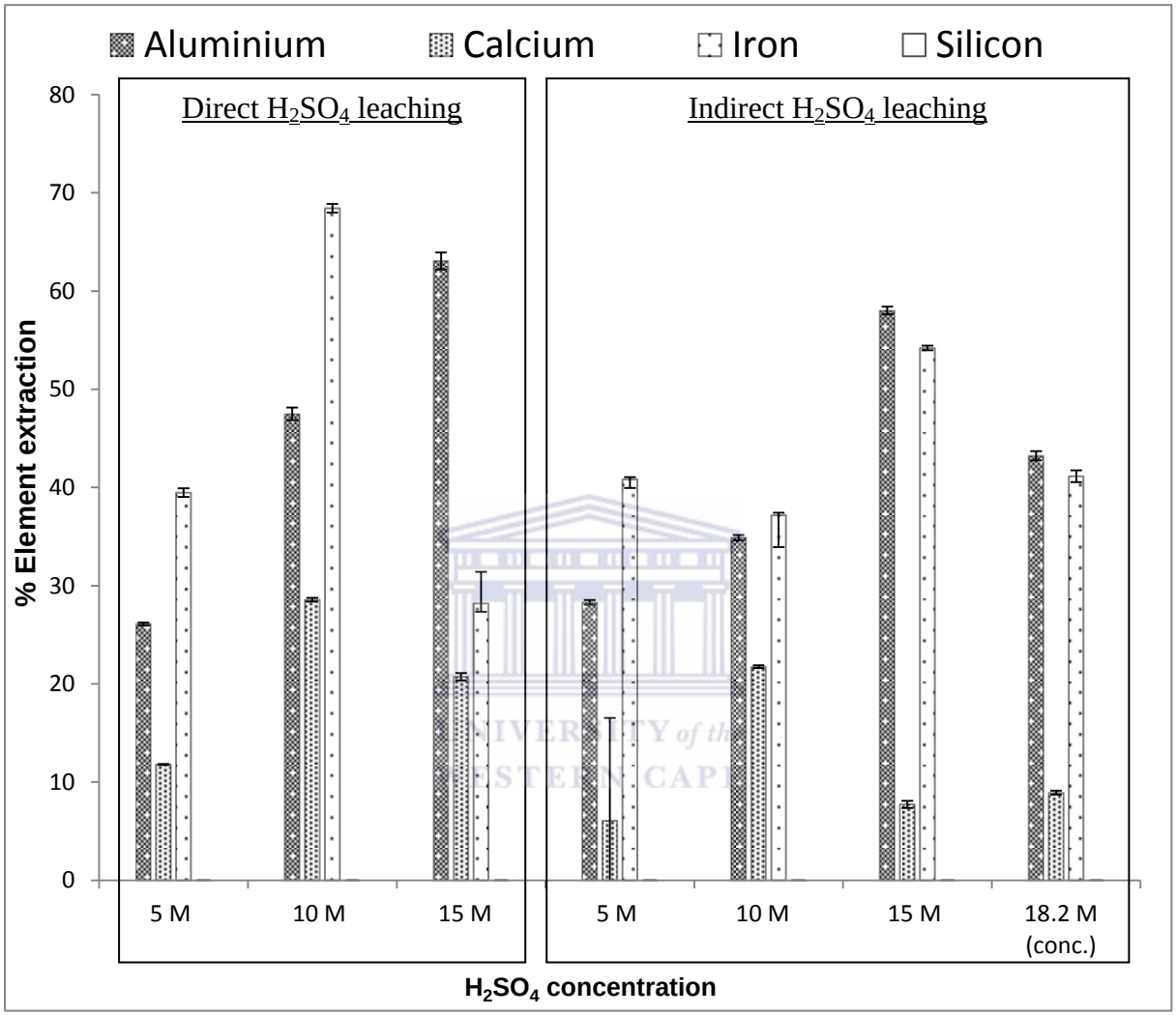

Figure 4.27: Comparative view of Direct vs. Indirect H_2SO_4 leaching (n=3)

Looking at Figure 4.27 above, the direct acid leaching method gave a maximum Al extraction yield of 63 % using 200 mL of 15 M H_2SO_4. The indirect leach method had a similar maximum extraction yield of 58 % at the same 15 M H_2SO_4 concentration. The indirect acid leaching method had an Al extraction yield of 43 % when 18 M (conc.) H_2SO_4 was used. This result is similar to that reported by Nayak et al., (2010) who achieved an Al extraction yield of 41.3 % from a Class F CFA. Nayak and co-workers used a 100 g CFA:100 mL 18 M H_2SO_4 ratio compared to this study's ratio of 20 g CFA:40 mL H_2SO_4. The iron extraction

yield at 15 M H_2SO_4 (refer to Figure 4.27) was higher using indirect leaching when compared to direct acid leaching. The maximum extraction yield of iron was approximately 54 % using indirect 15 M H_2SO_4 leaching compared to 28 % using direct acid leaching at the same acid concentration. Ca extraction was also higher using direct acid leaching compared to indirect acid leaching and it could be attributed to the higher working solution volume being used in the leaching process i.e. the 200 mL solution volume of direct leaching compared to the final 120 mL solution volume of indirect leaching.

The results showed that H_2SO_4 leaching gave a higher Al extraction yield (58 % - 63 %), compared to HCl leaching's extraction efficiency of approximately 30 % across the 4 M to 6 M HCl concentration range (refer to Figure 4.17). Direct H_2SO_4 leaching was thus chosen as the extraction procedure for Al since it gave a higher Al extraction yield and lower Fe co-extraction compared to indirect H_2SO_4 leaching. The higher Ca extraction from direct H_2SO_4 leaching would be minimised by the Ca pre-leaching step that was optimised from the HCl leaching study in Section 4.4.1. Si extraction was extremely low and H_2SO_4 can therefore be said to be a selective lixiviant with regard to separating Al from Si.

The direct H_2SO_4 leaching process was then optimised by extending the H_2SO_4 concentration over a wider test range by varying the molarity of the H_2SO_4 acid from 1 M - 15 M. The volume of acid was kept constant at 200 mL and 20 g CFA test samples were used. The 2 hour leaching time under reflux heating conditions also remained unchanged. The results of these extended tests are presented in Figure 4.28 below,

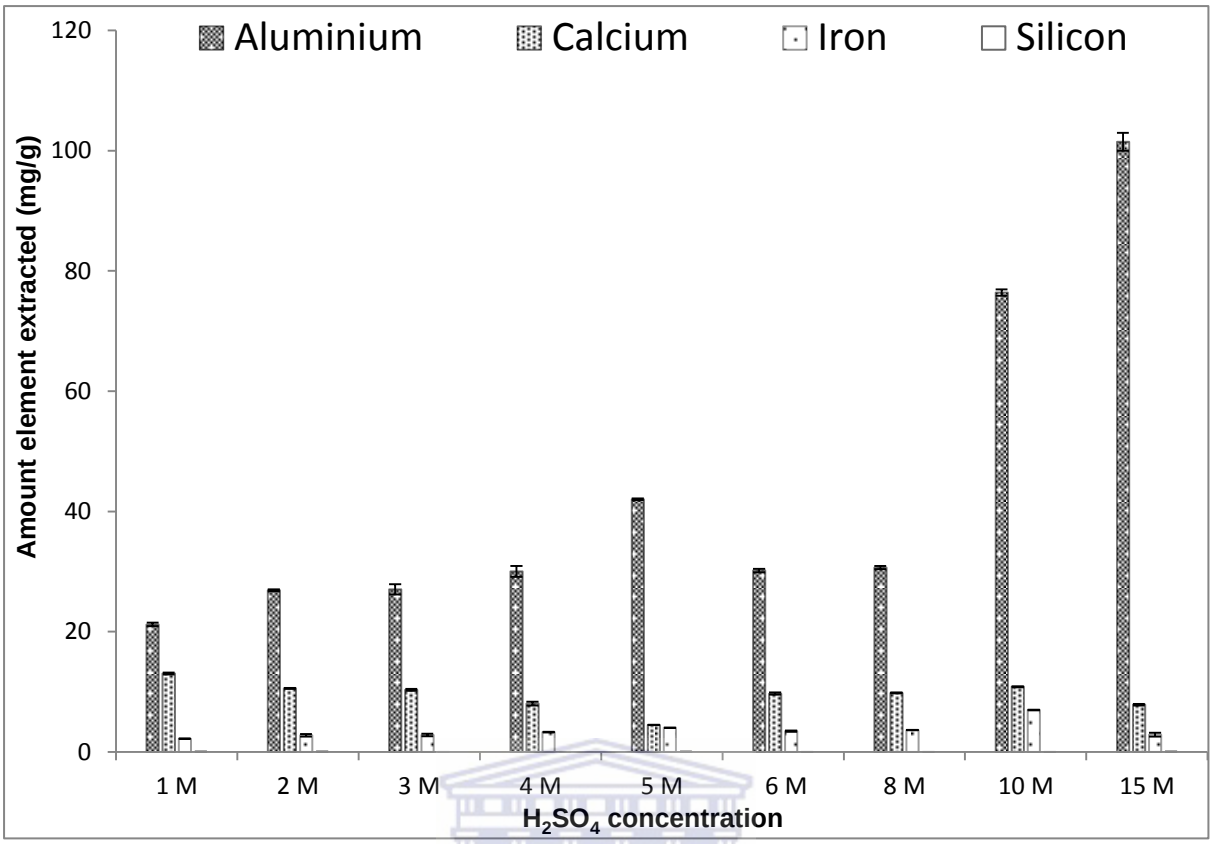

Figure 4.28: Direct H_2SO_4 leaching of CFA with varied H_2SO_4 concentrations [extended] (n=3)

The percentage element extractions are presented in Figure 4.29 below,

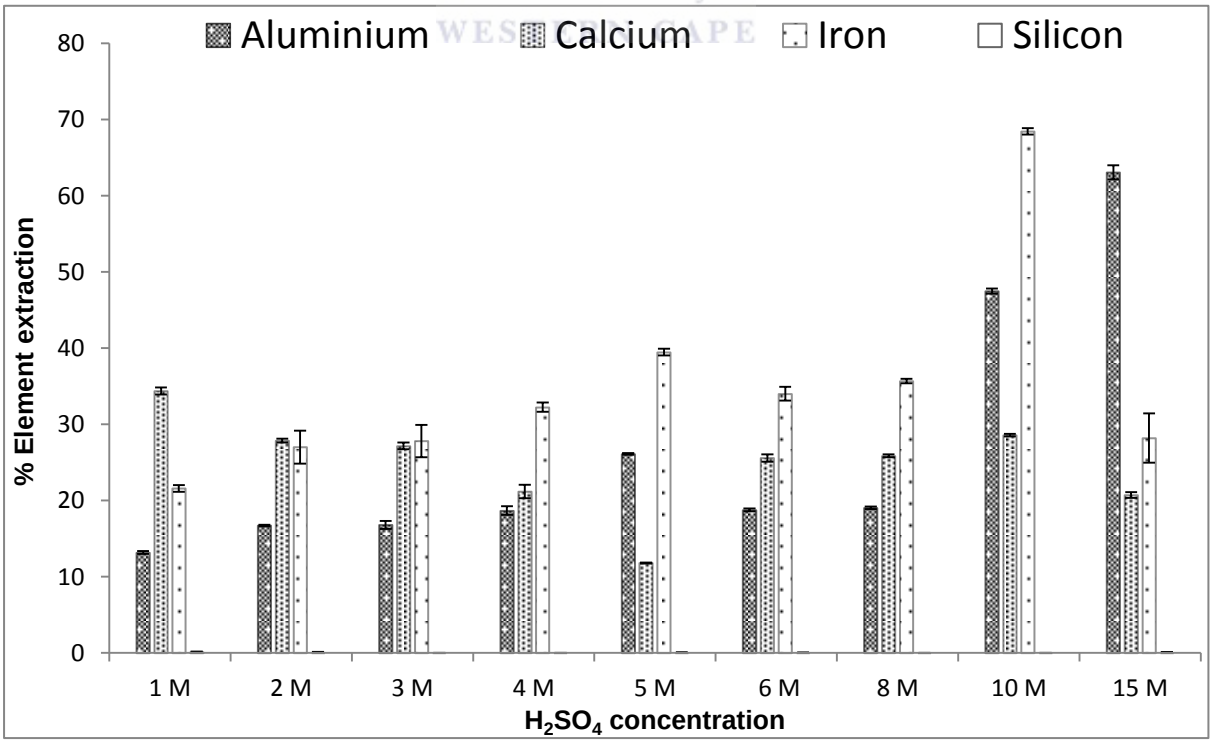

Figure 4.29: Percentage element extractions of CFA using direct acid leaching with varied H_2SO_4 concentrations [extended] (n=3)

As can be seen from Figure 4.29 above there was no significant increase in Al extraction using lower molarities. The highest Al extraction yield was still obtained from 15 M H_2SO_4. Looking at 6 M H_2SO_4, it had a similar Al extraction yield of 18.75 % comparable to Matjie et al., (2005) who achieved an Al extraction yield of 18 %. However, Matjie and co-workers used a 100 g Class F CFA sample leached with a 400 mL solution volume of 6.12 M H_2SO_4 and a leaching time of 4 hours maintained at 80 ° C where this study used 20 g CFA, 200 mL of 6 M H_2SO_4 and a leaching time of 2 hours maintained under reflux. The Fe extraction as seen in Figure 4.29 above was at its highest with 39 % extraction yield at 5 M H_2SO_4 but it was actually relatively similar across the entire acid concentration test range. Ca extraction was also similar across the entire acid concentration test range with the lowest extraction measured at 5 M H_2SO_4. The optimum concentration for direct H_2SO_4 leaching to extract Al as the element of interest was thus decided upon as 15 M H_2SO_4 and the amount of CFA reacting with the 15 M H_2SO_4 was then optimised. The mass of CFA was varied from 5 g – 50 g. while the solution volume of 200 mL 15 M H_2SO_4 and leaching time of 2 hours under reflux remained constant. The results of the CFA mass optimisation is presented in Figure 4.30 below,

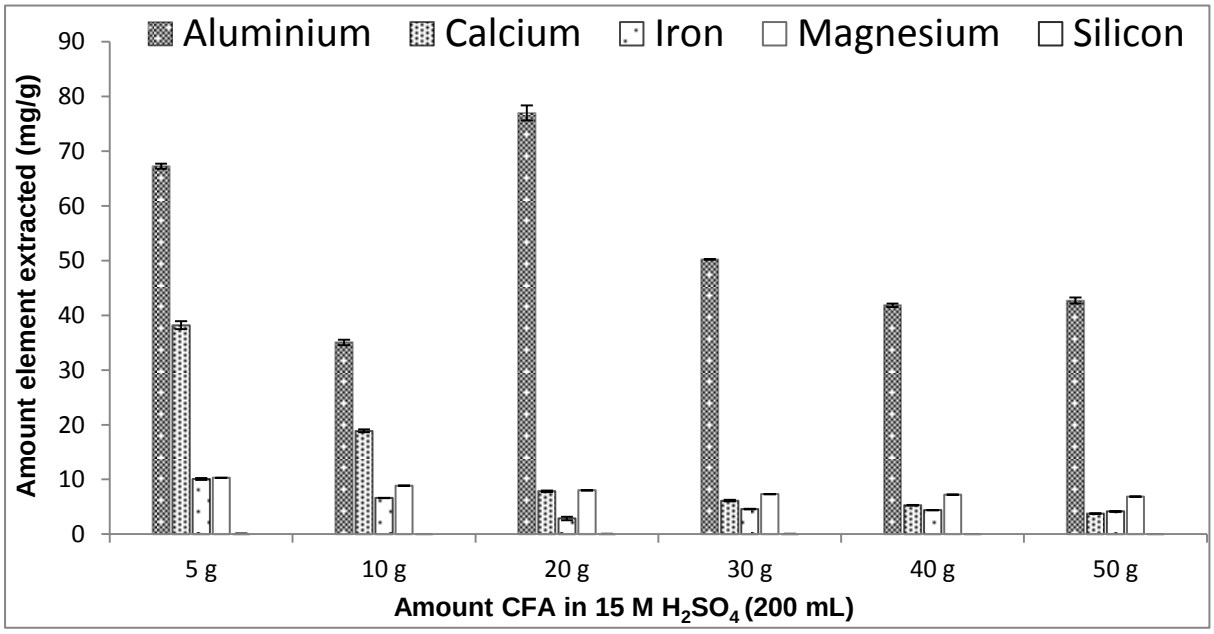

Figure 4.30: Varied CFA masses directly leached with 15 M H_2SO_4 (n=3)

The percentage element extractions are presented in Figure 4.31 below,

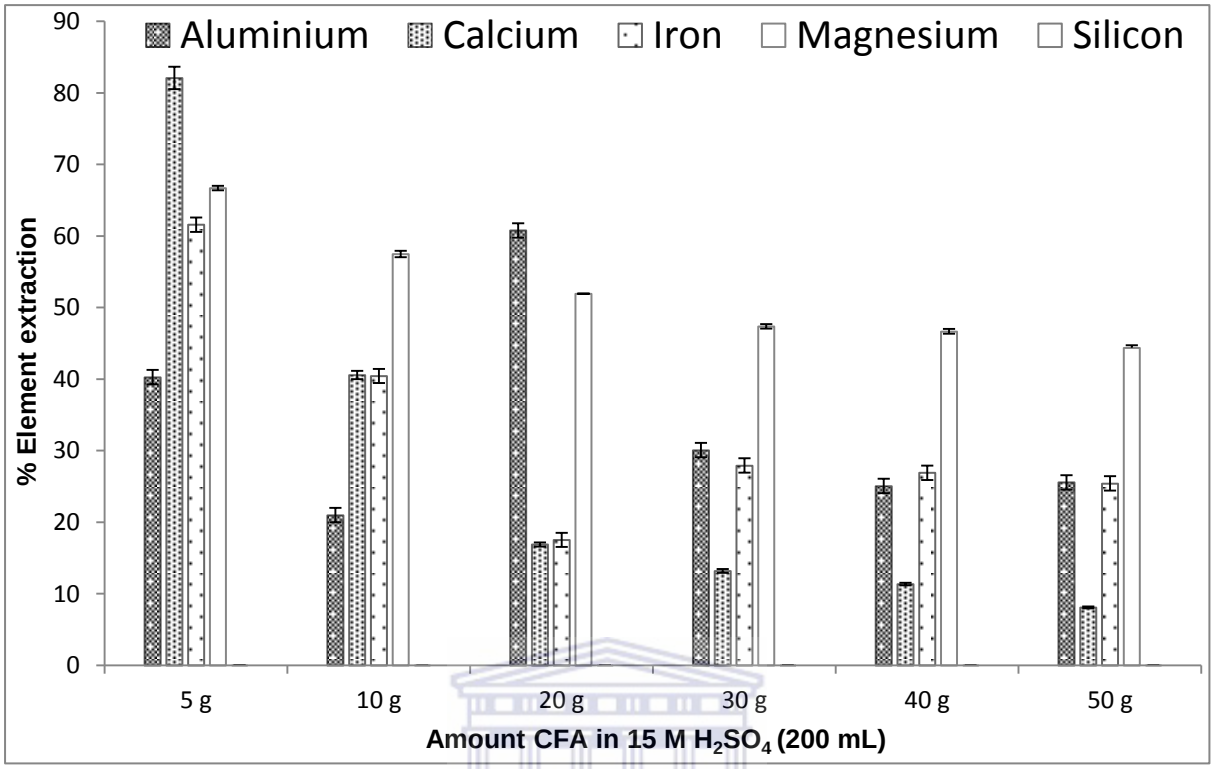

Figure 4.31: Percentage element extractions from varied CFA masses using direct H_2SO_4 leaching (n=3)

Looking at Figure 4.31 above, it can be seen that the smaller CFA mass of 5 g had the highest extraction yield for all the elements of interest except Al which was best extracted from 20 g CFA. This is mostly attributed to the mass transfer principle between the solution and CFA particles. The smaller CFA sample mass allows for greater surface interaction between the acid medium and CFA particles. The smaller CFA mass also offers less resistance to movement while it is being stirred thereby enhancing the leaching process. Ca and Mg are also generally easily soluble cations and their presence in the filtrates is to be expected. The observed effect of the Al extraction tapering off as the CFA mass increased above 20 g could be due to the precipitation of $CaSO_4$ which would also decrease the mass transfer rate between the CFA and acid medium. Since the initial amount of Ca present in CFA will increase as the mass of CFA used increases, so will the probability of increased precipitation of $CaSO_4$ from the interaction with H_2SO_4 occur. This would hinder the dissolution process of

the aluminium present in the CFA by restricting the leach solution contact with the CFA particles (Seidel et al., 1999). The Al extraction was relatively stable but low when 30 g, 40 g and 50 g was used. This could signify a dissolution maximum for the Al was reached when the Ca was converted to $CaSO_4$ or more probably that supersaturation was reached with respect to the formation of gehlenite (Ca_2AlSiO_7) mineral phase (refer to Figure 4.32). The Fe extraction yields also help to substantiate this conclusion since it also has similar yields across the same CFA mass range of 30, 40 and 50 g. The following Section 4.5 will be able to help to test if this claim can be considered feasible. 20 g CFA was thus chosen as the optimum since it had the highest Al yield and the XRD analysis was done on the 20 g CFA residue recovered from the optimally chosen 15 M H_2SO_4 leaching conditions. The XRD spectrum is presented in Figure 4.32 below.

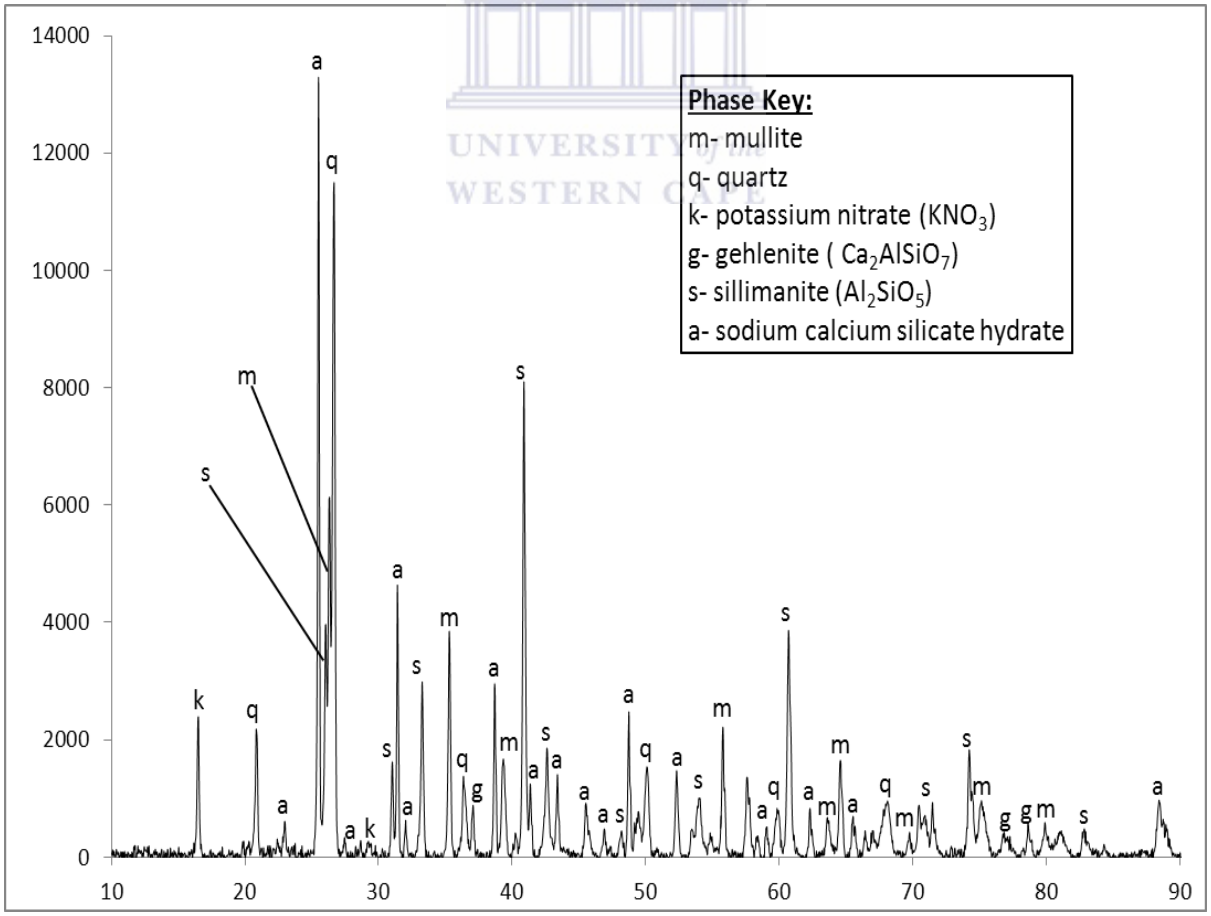

Figure 4.32: XRD spectrum of CFA leached with 15 M H_2SO_4

The XRD result (Figure 4.32) for the 20 g CFA residue recovered from the chosen optimal 15 M H_2SO_4 leaching of CFA showed that the mullite and quartz mineral phases of CFA still remained. Calcium silicate and aluminosilicate mineral phases are present after the sulphuric acid leaching due to dissolution of the Ca and further reaction with dissolved aluminium components of CFA. The XRD spectrum is also showing that dissolved Si is either re-precipitating or recrystallizing into other Si containing mineral phases which would serve to explain why the Si does not leach out under acidic conditions. The gehlenite formation shows a 2 Ca to 1 Al ratio and sillimanite formation shows a 2 Al to 1 Si ratio. These secondary mineral phase formations could provide an explanation for the lowered Ca and Al leaching when larger amounts of CFA are leached with sulphuric acid.

4.5 Sequential Extraction

The sequential extraction experimental plan outlined in Section 3.3.5 used the optimal conditions determined from the tests reported in Section 4.1 through Section 4.4. The final experimental plan was set out as depicted in Figure 4.33,

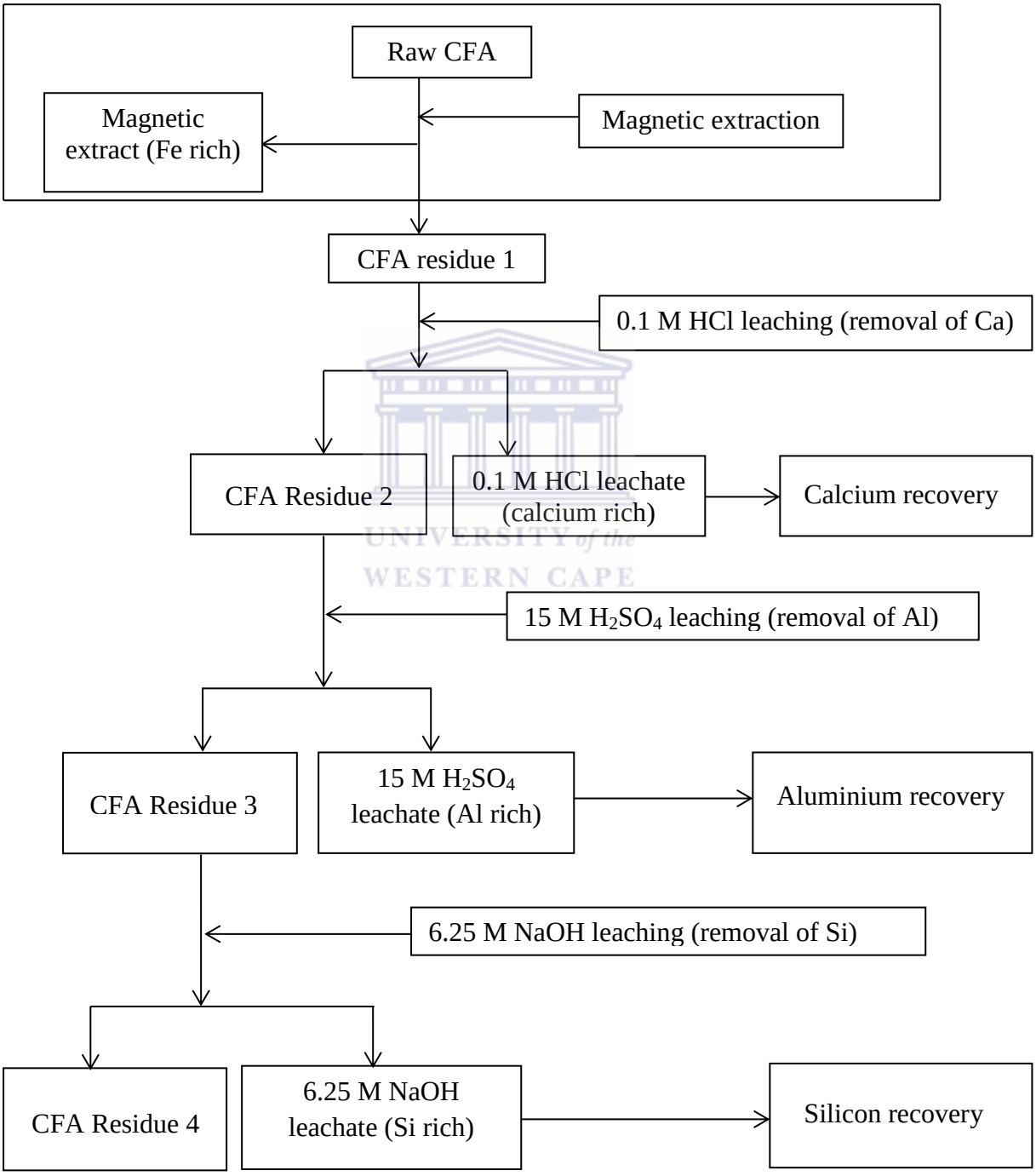

Figure 4.33: Final Sequential extraction experimental plan

Duplicate experiments were done where 20 g CFA sample masses were chosen for the sequential extraction process based on the direct 15 M H_2SO_4 leaching result obtained (refer to Figure 4.31). Firstly, 0.1 M HCl was chosen to selectively remove as much free Ca as possible from the CFA (refer to Figure 4.19) so as to minimise interference with Al extraction. Secondly, 15 M H_2SO_4 was then chosen to remove as much Al as possible from the CFA (refer to Figure 4.31). Lastly for the Si extraction, 6.25 M NaOH was chosen (refer to Figure 4.14). Al, Fe, Ca, Mg were measured via ICP-OES (refer to Section 3.2.2) and Si via the UV-Vis method (refer to Section 3.2.5). The result of the sequential extraction is reported in Figure 4.34 below. The error bar represents 2 experimental replicates.

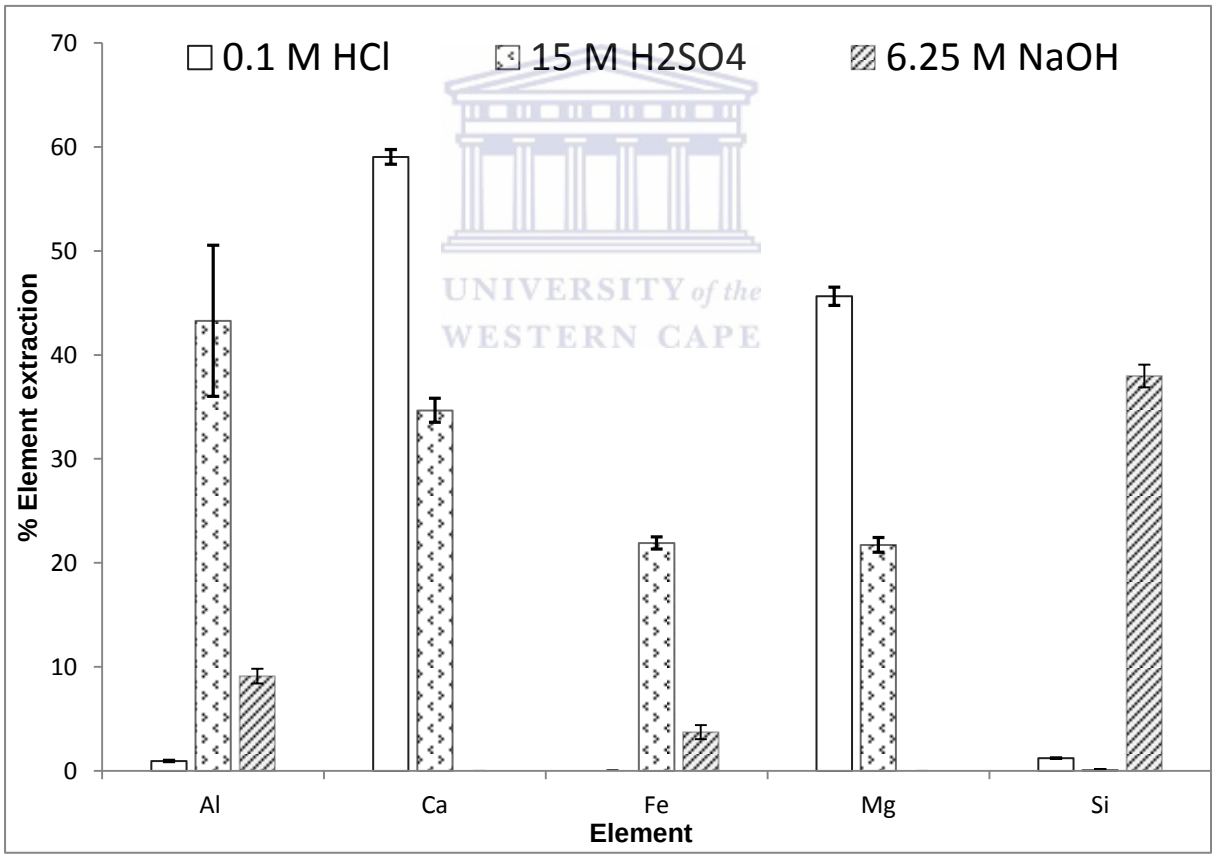

Figure 4.34 Sequential extraction leaching steps of CFA (n=2)

The percentage extraction yield for each step of the sequential extraction process outlined in Figure 4.33 is presented in Figure 4.34 above. As seen in Figure 4.34 above, the first 0.1M HCl leaching step removed approximately 59.1 % Ca and 45.6 % Mg. Al and Si removal for

the 0.1 M HCl leaching step was very low at 0.96 % and 1.22 % respectively. The second, 15 M direct H_2SO_4 leaching step removed 43.3 % Al and also removed an additional 34.7 % Ca from the CFA. The second extraction step also removed 21.9 % Fe and an additional 21.7 % Mg with very low to no silica removal. The third desilication step of the sequential extraction with 6.25 M NaOH treatment removed 37.98 % Si and an additional 9.1 % Al from the CFA. The third desilication step also removed an additional 3.7 % Fe from the CFA as well. The Si removal of 37.98 % from the alkaline leach step was not as high as expected from the preliminary tests (refer to Figure 4.12). The most probable reason for this could be due to the previous acidic leach step carried out on the CFA residue in this sequential procedure. Not all of the acidity from the H_2SO_4 leach step was removed with the additional wash step and a portion of the NaOH used for the alkaline leach step was probably neutralised. The effective NaOH leaching was thus decreased and was lower than when alkaline leaching was used directly on CFA after only the magnetic extraction step. The Si extraction yield for the desilication step via alkaline leaching in the sequential process is similar to Su et al., (2011) who achieved a 40 % Si extraction as their maximum from a Class F CFA using 8 M NaOH as their leach solution and a leaching time of 2 and a half hours. The NaOH concentration for this study was slightly lower at 6.25 M and the leaching time was 2 hours.

The overall extraction yields are presented graphically in Figure 4.35 below by the summation of all the leaching steps carried out in the sequential extraction. The error bar represents 2 experimental replicates.

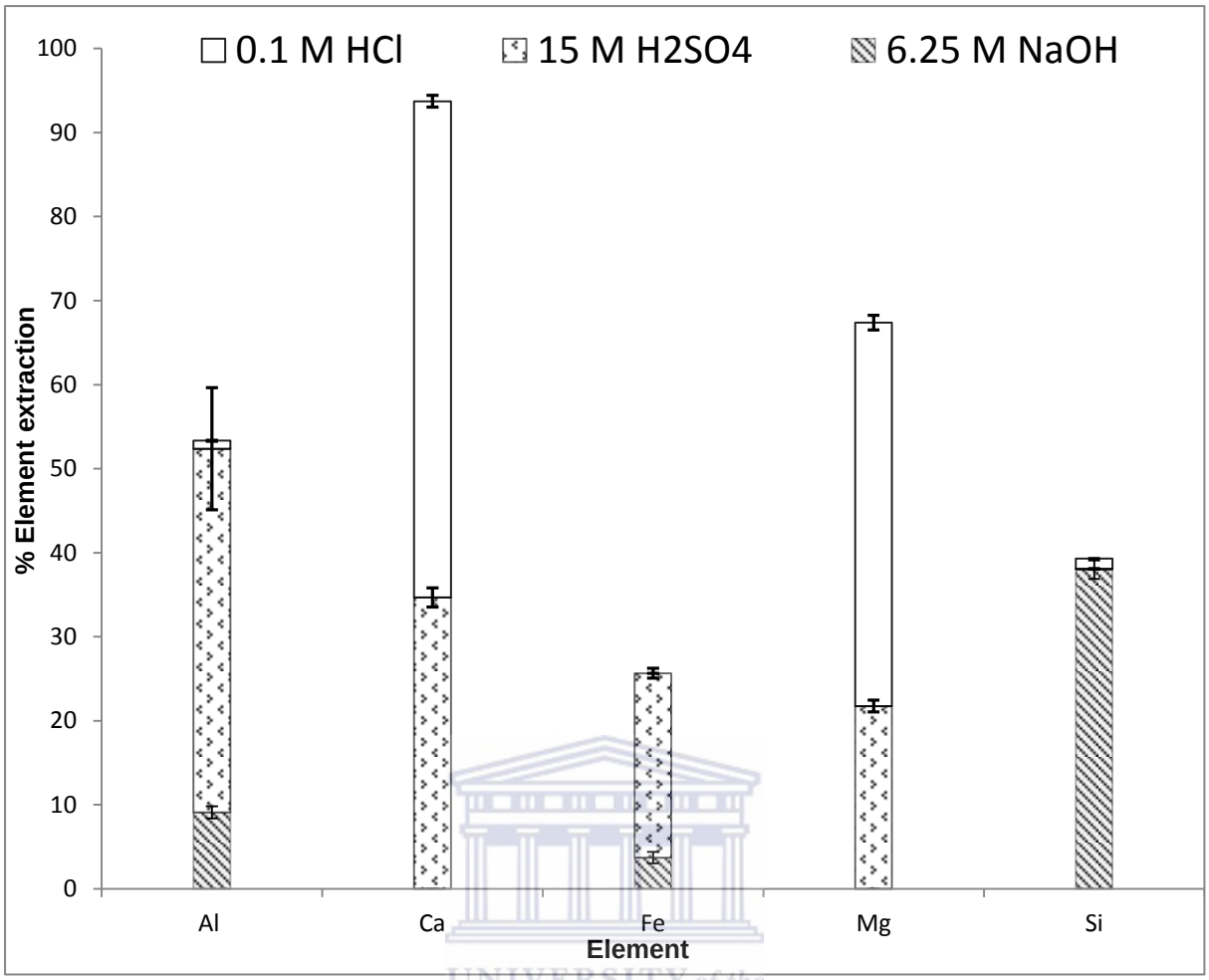

Figure 4.35: Overall percentage element recovery from sequential extraction of CFA (n=2)

The aggregated CFA extraction values attained from the sequential extraction is presented in Figure 4.35 above. The total element extraction for Al, Si, Ca Fe, Mg were 53.36 %, 39.96 %, 93.8 %, 25.6 % and 67.3 % respectively.

The XRD analysis was done on the CFA residue remaining after all the sequential extraction steps were completed. The XRD spectrum is presented in Figure 4.36 below,

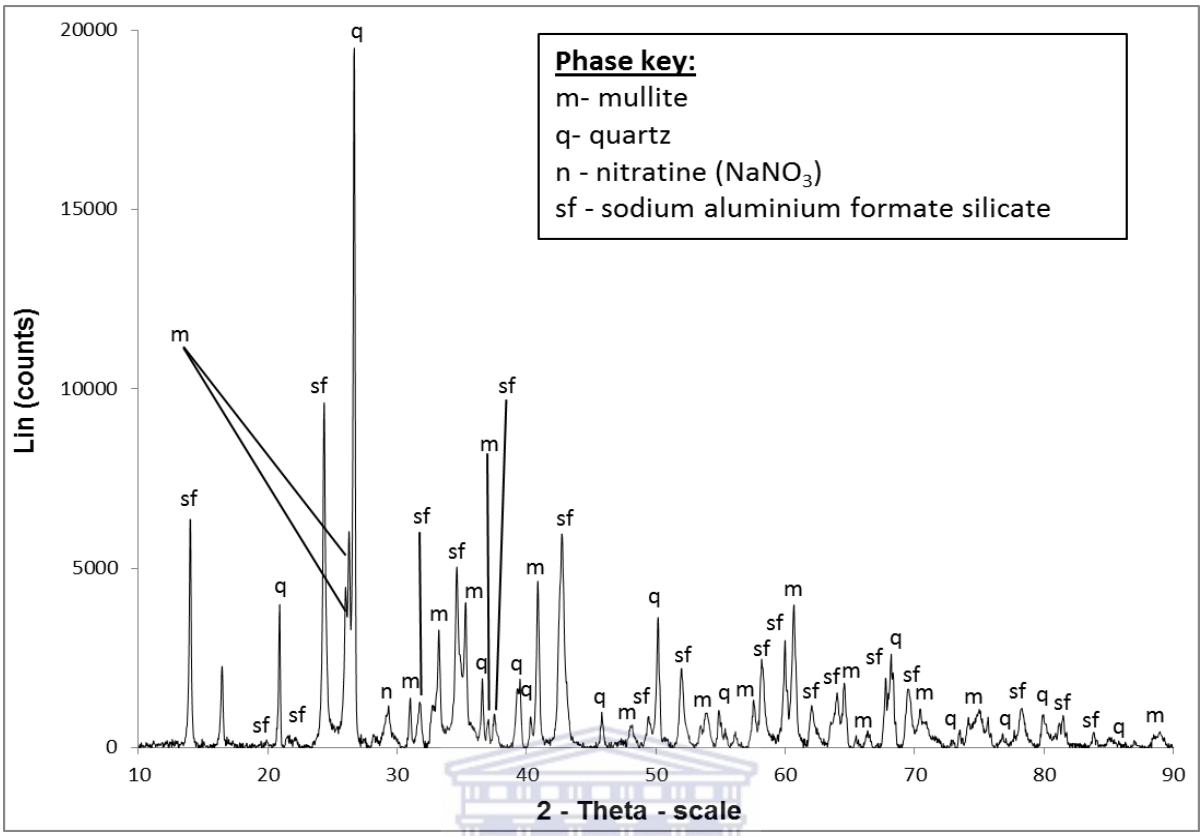

Figure 4.36: XRD spectrum of CFA residue obtained after sequential extraction

Looking at Figure 4.36 above, the XRD spectrum of the final CFA residue after the sequential extraction shows that the quartz and mullite mineral phases of CFA remain generally unaffected by the leaching progressions. A possible explanation for the sodium aluminium silicate mineral phase present in the final CFA residue begins with the acidic leach step. The acidic leach step solubilises the aluminium content and possibly not all the dissolved aluminium was removed during the filtration and washing step. This free Al still present in the CFA residue reacts with the dissolved silicates from the final alkaline leach step to then form the sodium aluminium silicates. The Ca rich phases, as seen in Figure 4.32, when the CFA residue after magnetic extraction was directly leached with 15 M H_2SO_4, did not form since the free Ca was sufficiently removed from the CFA with the HCl pre-leach step.

The CFA residue after the completed sequential extraction was analysed for major and minor elemental content by XRF analysis. Laser ablation-ICP-MS was used for the trace elemental content analysis. The results are presented in Table 4.7 and Table 4.8 below. The results represent the average of 2 experimental replicates.

Table 4.7: Major and Minor Elements in CFA Residue after Completed Sequential Extraction Treatment

CFA residue after completed SET (as is wet basis)		**CFA residue after completed SET (dry basis: corrected and normalised for Loss on Ignition)**			
Elemental Compound	**Weight %**	**Elemental Compound**	**Weight %**	**Major & minor Elements**	**mg/kg**
SiO_2	37.49	SiO_2	32.17	Si	150395
Al_2O_3	26.18	Al_2O_3	22.47	Al	118911
Fe_2O_3	1.06	Fe_2O_3	0.91	Fe	6365
CaO	2.42	CaO	2.08	Ca	14866
MgO	0.99	MgO	0.85	Mg	5127
K_2O	0.02	K_2O	0.02	K	166
P_2O_5	0.01	P_2O_5	0.01	P	44
MnO	0.03	MnO	0.03	Mn	232
Na_2O	13.68	Na_2O	11.74	Na	87094
TiO_2	2.00	TiO_2	1.72	Ti	10311
LOI	13.86	Total	83.88		
Total	97.74				

Table 4.8: Trace elements in CFA residue after completed sequential extraction treatment

Trace element	mg/kg	Trace element	mg/kg	Trace element	mg/kg	Trace element	mg/kg
Sc	34.55	Y	77.95	Nd	94.13	Yb	8.35
V	13.69	Zr	612	Sm	17.14	Lu	1.24
Cr	64.81	Nb	50.27	Eu	3.17	Hf	16.33
Co	9.41	Mo	0.52	Gd	14.48	Ta	5.88
Ni	59.47	Cs	0.93	Tb	2.30	Pb	9.58
Cu	18.80	Ba	3767	Dy	14.33	Th	62.15
Zn	8.13	La	139.54	Ho	2.89	U	4.49
Rb	1.02	Ce	296.64	Er	30.94		
Sr	2459	Pr	26.76	Tm	1.15		

Looking at XRF analysis results (refer to Table 4.7), it can be seen that the sodium content of the CFA after sequential leaching increased compared to raw CFA (refer to Table 4.1) and magnetically extracted CFA (refer to Table 4.5). This is expected since NaOH was the last reagent used in the sequential leaching treatment. The loss on ignition (LOI) was higher at 13.86 % (refer to Table 4.7) compared to 1.64 % LOI of the raw CFA (refer to Table 4.1). This could be attributed to water content since no organic reagents were used in this study. The TiO_2 content in the CFA residue after the completed sequential extraction remained relatively the same when compared to raw CFA (refer to Table 4.1). The CFA residue after sequential extraction treatment showed a decrease in concentration of all trace elements except Ba, Sr, Th and the rare earth elements (REEs) which showed upconcentration when compared to raw CFA.

The following graphical representations depict the trends of particular elements of interest as well as the radioactive and toxic element concentrations between the raw CFA, magnetic extract, CFA residue after magnetic extraction and the CFA residue after sequential extraction treatment (SET).

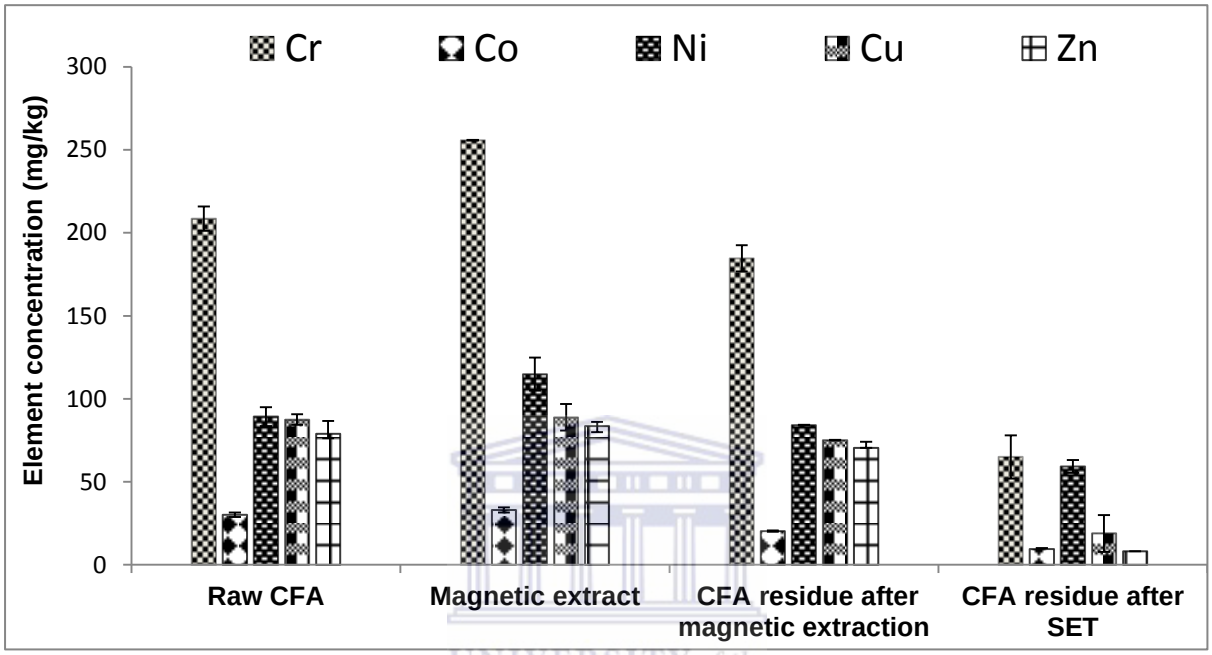

Figure 4.37: Cr, Co, Ni, Cu and Zn element levels after the SET process on CFA

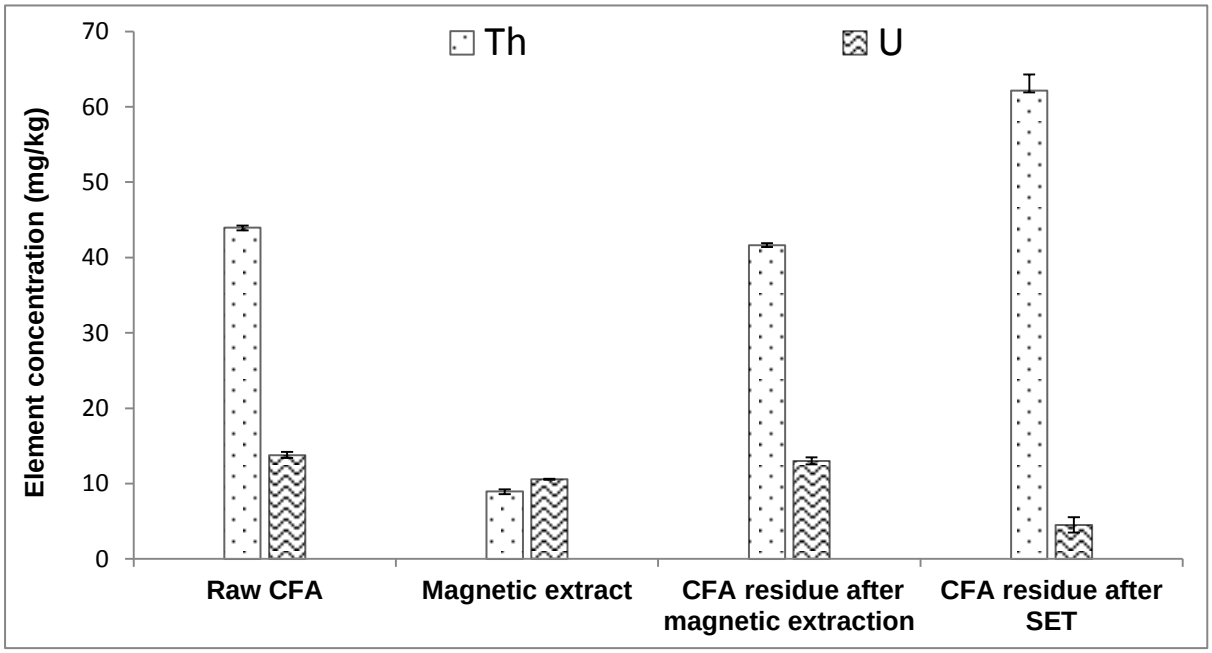

Figure 4.38: Th and U radioactive element levels after SET process on CFA

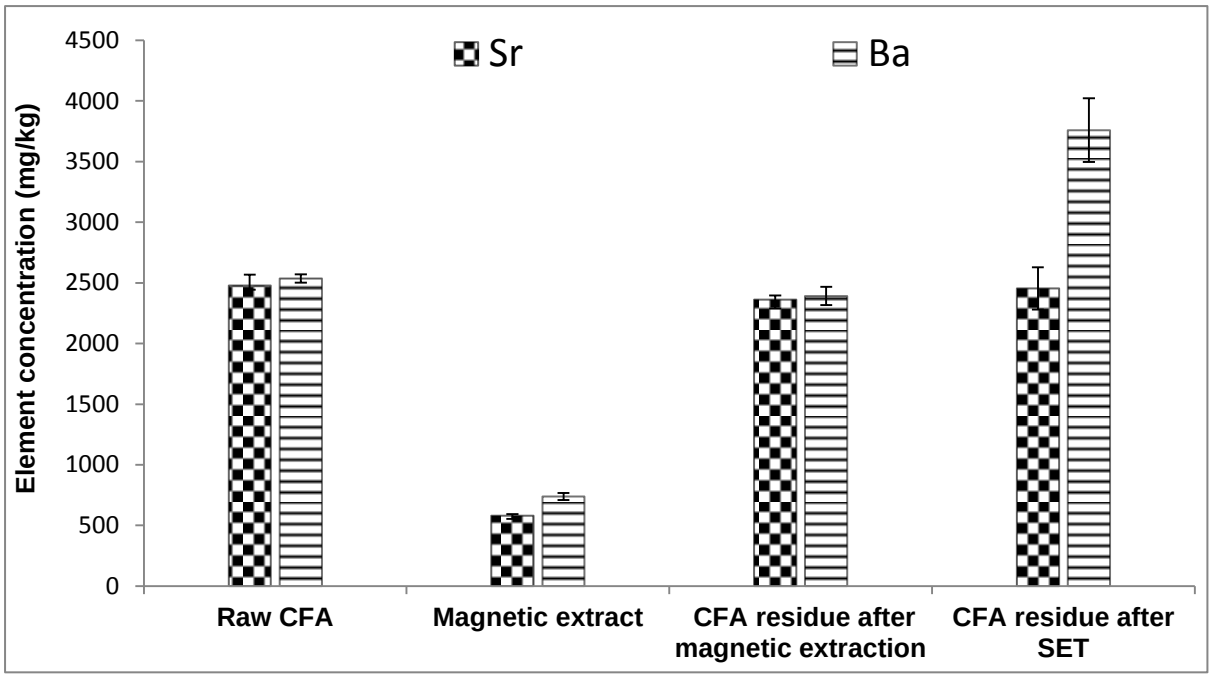

Figure 4.39: Sr and Ba toxic element levels after SET process on CFA

As can be seen from Figure 4.37, Cr, Co, Ni, Cu and Zn levels were decreased in CFA residue after SET when compared to raw CFA. From Figure 4.38, it was seen that radioactive Th content was upconcentrated in the CFA residue after SET while the U content was decreased. Figure 4.39 showed that the Sr content remained relatively similar between the raw CFA, CFA residue after magnetic extraction and the CFA residue after SET while the Ba content was upconcentrated in CFA residue after SET.

Lastly, the leachate solutions from the sequential extraction treatment were analysed for rare earth element content. A comparative view of the rare earth element content in the raw CFA, magnetically extracted CFA residue, sequential extraction leachates and CFA residue after the completed sequential extraction are tabulated in Table 4.9. The standard error included represents 2 experimental replicates.

Table 4.9: Rare earth element levels comparison between CFA and the sequential extraction leachates

Rare Earth Element	Matla Raw CFA (µg/g)	Magnetic extract CFA residue (µg/g)	0.1 M HCl (µg/g)	15 M H_2SO_4 (µg/g)	6.25 M NaOH (µg/g)	CFA residue after SET (µg/g)
La	99.29 ± 0.11	96.070 ± 0.27	0.208 ± 0.004	0.577 ± 0.01	0.005	139.1 ± 3.97
Ce	207.9 ± 1.28	198.5 ± 1.16	0.230 ± 0.002	nd	nd	296.0 ± 9.53
Pr	21.40 ± 0.31	20.36 ± 0.34	nd	nd	0.082 ± 0.01	26.67 ± 0.87
Nd	76.15 ± 0.004	76.14 ± 0.39	nd	0.338 ± 0.01	nd	94.13 ± 2.84
Dy	11.74 ± 0.28	12.06 ± 0.03	0.072 ± 0.002	0.107 ± 0.001	0.007 ± 0.002	14.31 ± 0.590.34
Sm	14.87 ± 0.43	14.46 ± 0.06	0.440 ± 0.02	0.131 ± 0.002	0.555 ± 0.01	17.19 ± 0.780.45
Er	6.985 ± 0.04	6.75 ± 0.10	0.037 ± 0.01	0.081 ± 0.002	nd	30.89 ± 1.48
Eu	2.640 ± 0.06	2.485 ± 0.09	0.013 ± 0.001	0.018	0.004 ± 0.001	3.168 ± 0.09
Gd	12.29 ± 0.10	11.73 ± 0.11	nd	0.330 ± 0.01	0.036 ± 0.003	14.31 ± 0.28
Ho	2.585 ± 0.04	2.460 ± 0.06	0.012 ± 0.002	0.060 ± 0.001	0.017 ± 0.001	2.896 ± 0.08
Lu	1.035 ± 0.04	1.025 ± 0.03	0.009 ± 0.001	nd	0.003 ± 0.0001	1.245 ± 0.04
Tb	2.055 ± 0.10	2.065 ± 0.07	0.026 ± 0.01	0.181 ± 0.01	0.0115 ± 0.005	2.280 ± 0.08
Tm	1.050 ± 0.07	1.065 ± 0.07	0.006 ± 0.001	0.027 ± 0.0003	nd	1.157 ± 0.02
Yb	7.000 ± 0.07	6.605 ± 0.22	0.031 ± 0.001	0.061 ± 0.0003	0.009	8.265 ± 0.09
Y	65.69 ± 1.28	64.16 ± 0.36	0.351 ± 0.001	0.513 ± 0.001	nd	77.73 ± 1.95

SET = sequential extraction treatment nd = not detected

The rare earth elements levels tabulated in Table 4.9 are graphed in Figure 4.40 below to graphically present the partitioning of the rare earth elements through the steps of the sequential extraction treatment.

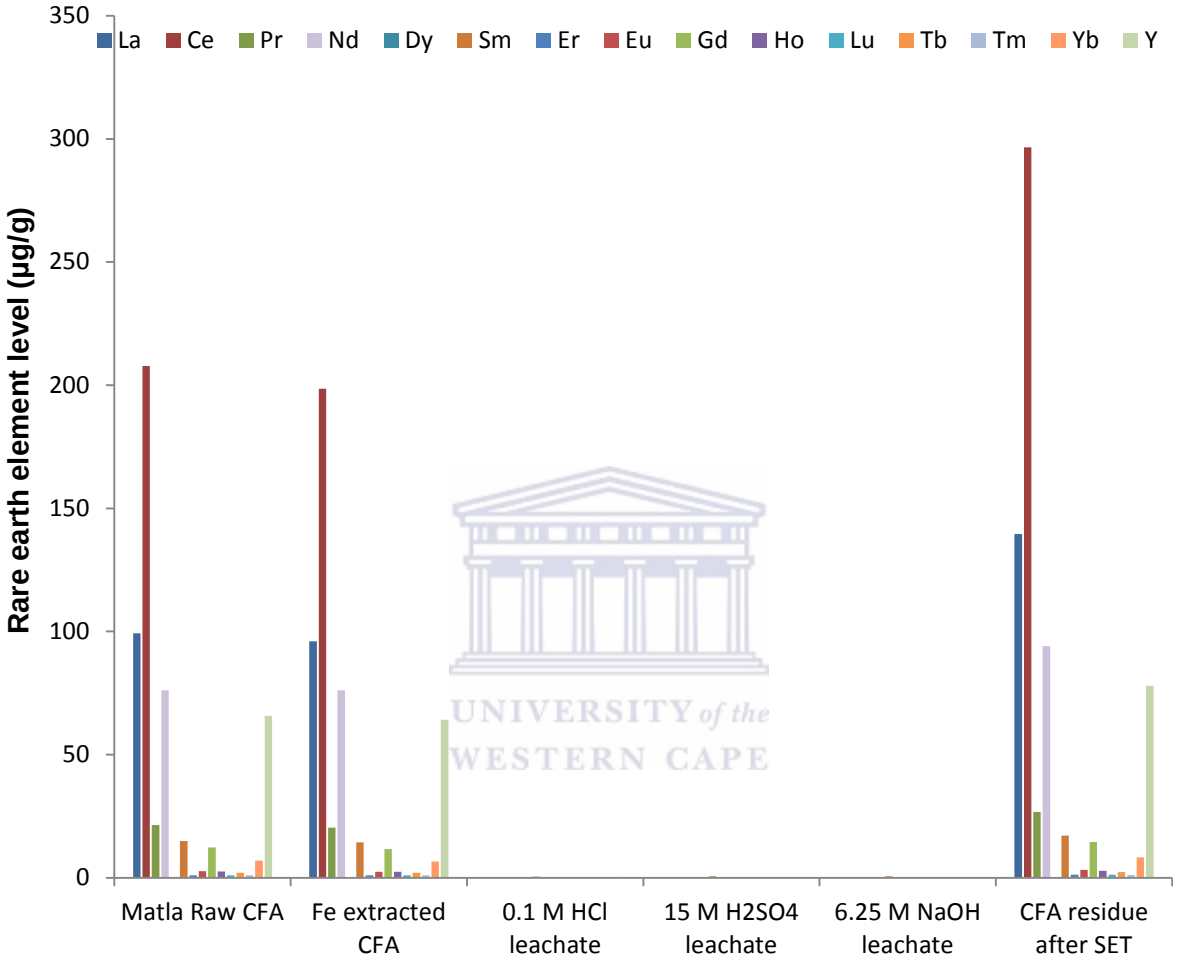

Figure 4.40: Rare earth element concentration level comparison between CFA and the sequential extraction leachates

The leachates (Figure 4.40) showed very low to no detectable amounts of rare earth elements that were leached form the CFA. The graphical presentation of Figure 4.40 shows that the majority of the rare earth elements remain in the CFA residue through the progression of the sequential extraction leaching process and have become enriched due to the partial removal of the major Si and Al major matrix elements. The percentage enrichment of the rare earth elements in the CFA residue after the sequential extraction treatment was calculated against the rare earth element content of the raw CFA. The results are tabulated in Table 4.10 below.

The standard error included represents 2 experimental replicates with the calculated percentage enrichment incorporating the error range.

Table 4.10: Percentage rare earth element enrichment in CFA

Rare Earth Element	Matla Raw CFA (µg/g)	CFA residue after SET (µg/g)	% Rare earth element enrichment (% range)
La	99.29 ± 0.11	139.12 ± 3.97	26.62 – 30.53
Ce	207.9 ± 1.28	296.0 ± 9.53	27.90 – 31.56
Pr	21.40 ± 0.31	26.67 ± 0.87	18.26 – 21.20
Nd	76.15 ± 0.004	94.13 ± 2.84	16.60 – 21.48
Dy	11.74 ± 0.28	14.31 ± 0.34	17.93 – 17.98
Sm	14.87 ± 0.43	17.19 ± 0.45	13.76 – 13.27
Er	6.985 ± 0.04	30.89 ± 1.48	76.38 – 78.31
Eu	2.640 ± 0.06	3.168 ± 0.09	16.13 – 17.15
Gd	12.29 ± 0.098	14.31 ± 0.28	13.09 – 15.08
Ho	2.585 ± 0.04	2.898 ± 0.08	9.70 – 11.82
Lu	1.035 ± 0.04	1.245 ± 0.04	16.60 – 17.19
Tb	2.055 ± 0.102	2.280 ± 0.07	8.35 – 11.49
Tm	1.050 ± 0.07	1.157 ± 0.02	5.37 – 13.27
Yb	7.000 ± 0.07	8.265 ± 0.09	15.30 – 15.32
Y	65.69 ± 1.28	77.73 ± 1.95	15.96 – 15.01

Looking at Table 4.10 above, there was an overall enrichment for all the rare earth elements measured in the CFA after sequential extraction. The percentage enrichment on the lower end

of the standard error variation varied approximately from 5.37 % for Yb to the highest being 76.38 % enrichment for Er.

The Si removal of 37.98 % from the sequential extraction alkaline leach step was not as high as expected from the preliminary tests (Figure 4.14). The most probable reason for this could be due to the previous acidic leach step carried out on the CFA residue. Not all the acidity was removed with the additional wash step and a portion of the NaOH used for the acidic leach step was probably neutralised thereby effectively decreasing the NaOH leaching. A slightly higher Si extraction would probably be achieved if the NaOH concentration were raised to the range of 8 M NaOH; however the Al co-extraction would also be increased. This shouldn't pose a problem if the objective would be rare earth element enrichment. The acidic leaching step of 15 M H_2SO_4 did not effectively remove all possible free Al present in the CFA leaching system since the alkaline leach step managed to extract a further 9 % from the CFA. A probable explanation for this could be due to the alkaline conditions managing to free some of the Al attached to the siliceous material that the acidic leaching was not able to attack and allow dissolution to take place. The Si extraction yield attained for the desilication step via alkaline leaching was similar to Su et al., (2011) who achieved 40 % Si extraction as their maximum using 8 M NaOH as their leach solution and a leaching time of 2 and a half hours. The NaOH concentration for this study was slightly lower at 6.25 M and the leaching time was 2 hours.

In the following chapter 5 the research questions asked in chapter 1 will be answered and the conclusions will be drawn from this study.

Chapter Five

5. Conclusions and Recommendations

This chapter answers the research questions asked in Chapter 1 and provides the conclusions and possible applications of the findings in this study.

5.1 Conclusion

5.1.1 Magnetic extraction

The magnetic extraction of CFA achieved a magnetic extract where the iron oxide content made up 74.84 % of the total magnetic extract composition. This equates to 52.33 % elemental iron. All the trace elements (including rare earth elements) concentrations, when compared to the raw CFA, decreased in the magnetic extract except for Co, Ni and Zn which showed enrichment in the magnetic extract. The bulk of the trace elements and rare earth elements thus remained in the CFA residue after magnetic extraction and are thus not associated with the Fe fraction. The identified mineral phases of hematite, magnetite and maghemite detected by XRD analysis confirmed that the magnetic extract comprised predominantly of iron oxide. There were trace amounts of Si and Al that were also present in the magnetic extract mainly due to the fine CFA particulate matter that was trapped between the particles of the magnetic extract itself. Therefore further purification of the magnetic fraction may be desirable.

5.1.2 Alkaline leaching

Direct alkaline leaching was determined to be the best choice for extracting Si from CFA since it provided higher Si recovery compared to indirect alkaline leaching. The optimal NaOH concentration for direct alkaline leaching for Si extraction was determined to be 600 mL of 6.25 M NaOH for the optimal leaching mass of 20 g CFA. This NaOH concentration

provided the highest Si yield of 49.8 % with minimal Al (4.92 % yield) being co-extracted when 20 g magnetically extracted CFA was leached. The mullite and quartz mineral phases in the CFA were unaffected by direct alkaline leaching and remained in the CFA residue as confirmed by XRD analysis. It could therefore be concluded that the Si was extracted mainly from the amorphous glassy phase of the CFA. To fully recover Si form CFA, the quartz and mullite phases would need to be digested.

5.1.3 Acidic leaching

Of the three acidic leaching methods tested, HCl leaching was best suited for the extraction of Ca and direct H_2SO_4 leaching for extracting Al from CFA compared to indirect H_2SO_4 leaching.

HCl leaching only achieved a maximum Al yield of 30 % across the 4 M to 6 M HCl concentration range but it was seen that HCl leaching managed to extract high amounts of Ca from the CFA even when lower concentrations of HCl were used. The optimum concentration of HCl for Ca leaching from 20 g of CFA was determined to be 400 mL of 0.1 M HCl. When various amounts of CFA were leached it was seen that Ca extraction was higher when low amounts of CFA (5 g – 10 g) were leached but there was also co-extraction of Fe and Al. The Ca yields as well as Al and Fe co-extraction decreased when more than 30 g CFA was leached with 400 mL of 0.1 M HCl. The best selective Ca extraction yield was 55 % with Al and Fe co-extraction of 0.03 % and 0.16 % respectively from 20 g CFA.

H_2SO_4 leaching was seen to be more effective at extracting Al when compared to HCl leaching. Direct H_2SO_4 leaching gave a higher Al extraction yield of 63 % from 20 g CFA when 200 mL of 15 M H_2SO_4 was used. The indirect H_2SO_4 leaching method gave a slightly lower Al extraction yield of 58 % from 20 g CFA. A higher Fe extraction yield of 54 % was obtained using indirect H_2SO_4 leaching compared to 28 % from direct H_2SO_4 leaching. Both

direct and indirect H_2SO_4 leaching were best performed using 20 g CFA. The direct H_2SO_4 leaching gave a higher Ca extraction of 20.7 % compared to 7.73 % when indirect H_2SO_4 leaching was used. Direct H_2SO_4 leaching was thus chosen as the extraction procedure for Al since it gave a higher Al extraction yield and lower Fe co-extraction compared to indirect H_2SO_4 leaching. The higher Ca extraction from direct H_2SO_4 leaching would be minimised by the use of a Ca pre- leaching step in the optimised HCl leaching procedure. In both direct and indirect H_2SO_4 leaching Si was not extracted and H_2SO_4 can therefore be regarded as a selective lixiviant for Al.

5.1.4 Sequential extraction treatment

The sequential extraction treatment (SET) sequence was formulated to firstly perform magnetic extraction on the CFA to remove the magnetic fraction from CFA residue and then use the magnetically extracted CFA as starting material for the rest of the sequential treatment. 20 g of the CFA residue after magnetic extraction was used as the optimum mass for subsequent extraction. The next step in the SET was removal of Ca from the 20 g magnetically extracted CFA by leaching with 400 mL of 0.1 M HCl for 2 hours at 100 °C. Ca removal was done first so as to minimise Ca interference with Al when acidic leaching is carried out on the CFA. The Ca extraction yield from HCl leaching was 59.1 % and 45.6 % Mg. The Ca extraction from the SET HCl leach step was higher than the optimum preliminary HCl leaching that gave a 55 % Ca yield. The next sequential leach step was to remove Al by direct acidic leaching of all the Ca depleted HCl leached CFA residue using 200 mL of 15 M H_2SO_4 under reflux for 2 hours. The acidic leaching step was carried out before the alkaline leach step with the notion that the removal of Al would provide less interference of Al co-extraction when alkaline leaching is performed to recover Si. The direct H_2SO_4 leaching gave an Al yield of 43.3 % as well an additional yield of 34.7 % Ca. This Al yield from the SET leach step was low at 43.3 % compared to a 63 % Al extraction

yield obtained from the preliminary optimum direct H_2SO_4 leach test. The final SET step was to remove Si by direct alkaline leaching of the H_2SO_4 leached CFA residue using 600 mL of 6.25 M NaOH at 100 °C for 2 hours. The Si yield from the direct alkaline leaching step of the SET removed 37.98 % Si, an additional 9.1 % Al and a further 3.7 % Fe from the CFA residue. The Si extraction yield from the SET alkaline leach test was also low at 37.98 % compared to 49.8 % obtained from the preliminary optimal direct NaOH leaching test.

The total aggregate extractions of Si, Al, Ca, Fe and Mg from CFA for this study were therefore 53.36 %, 39.96 %, 93.8 %, 25.6 % and 67.3 % respectively. Overall the extractions for Si and Al are comparable to the individual optimised alkaline (6.25 M NaOH) and acidic (15 M H_2SO_4) optimised leach tests.

5.1.5 Rare Earth Element Enrichment

The leachates from the SET, i.e., 0.1 M HCl leachate, 15 M H_2SO_4 leachate and 6.25 M NaOH leachate showed very low to no detectable amounts of rare earth elements that were leached from the CFA. The majority of the rare earth elements remained in the CFA residues throughout the entire progression of the SET leaching process. The rare earth elements are in effect enriched in the CFA residue as a result of the partial removal of the major Si and Al CFA matrix elements. The enrichment achieved ranged from the lowest at 5.37 % for Tm to the highest of 76.38 % for Er.

5.1.6 Conclusions to the research questions

Referring to Chapter 1 the following research questions were asked,

- What percentage of the major constituents of CFA will be recovered by dissolving the amorphous glassy phase of the CFA?

The total element extraction for Al, Si, Ca Fe, Mg were 53.36 %, 39.96 %, 93.8 %, 25.6 % and 67.3 % for each element respectively.

- Will removing the amorphous glass phase of CFA make it easier to recover the trace elements, particularly rare earth elements, present?

  Yes and the removal of this glassy phase as seen by the reclaimed Si and Al, results in the enrichment of the rare earth elements present in the residues of CFA which indicates that rare earth elements are associated with quartz and mullite.

- Will breaking the alumina-silicate mineral compounds increase the yield of aluminium and silicon recovery while not affecting the trace element partitioning from the CFA?

  Neither the alumina- silicate mineral compounds (mullite) nor the quartz mineral phases in the CFA were able to be broken down into its simpler constituents or removed during the SET leaching process. This was confirmed by the XRD analysis of the CFA residue after the SET leaching process and therefore it can be concluded that the SET leaching conditions were not sufficient to increase the extraction efficiency of the elements of interest. Although it would theoretically cause an increase in the Si and Al extraction yields, if mullite and quartz mineral phases could be removed from the CFA matrix, it could not be assessed by this study if the trace element partitioning would be affected.

- Do the trace elements remain in the solid residues after extracting Si and Al to be removed at a later stage?

  The trace elements Sc, V, Co, Ni, Cu, Zn, Rb, Mo, Cs, Pb and U were decreased in the CFA residue after SET leaching process while Ba, Sr and Th levels were enriched. All the rare earth elements viz, La, Ce, Pr, Nd, Dy, Sm, Er, Eu, Gd, Ho, Lu, Tb, Tm,

Yb and Y were enriched in the CFA residue after the SET leaching process. This means that the SET process managed to upconcentrate the REEs for future use.

Overall in conclusion it can be said that this study showed that the removal (albeit partial) of Si, Al, Fe, Ca etc. from CFA makes it possible to enrich the rare earth element content in the CFA residue matrix. It is also shown that the REEs are not extracted from CFA by the HCl, H_2SO_4 and NaOH lixivants used in the SET process of this study. Since very few studies consider the tracing of the REEs during extraction studies for Si and Al from CFA, this body of work is useful with regard to providing information with respect to REEs behaviour during alkaline leaching with NaOH and acidic leaching with HCl and H_2SO_4. This study also found that secondary mineral phases are formed in the CFA residues after the alkaline and acidic leaching of the CFA, which could impact on the recoveries achieved.

5.2 Recommendations for future work:

As mentioned in Chapter 4, Si and Al removed from the CFA originate predominantly from the amorphous phase of the CFA since the quartz and mullite mineral phases still remain after the SET. It is hypothesised that the extraction yields could be slightly increased with adjustment of the SET conditions. The NaOH concentration should be set slightly higher to alleviate the neutralisation action of the acidic residue after the direct acid leaching step. However, depending upon whether the goal is to remove the Si and Al as separate entities, it would be advised to not increase the concentration of the NaOH too much so as to prevent greater co-extraction of the Al with the Si. An energy consumption determination would need to be conducted to decide if the yield return is economically suited for the conditions the extracted Al would be used for.

References

Adamson, J; Irha, N.; Adamson, K.; Steinnes, E. and Kirso, U. (2010), 'Effect of oil shale ash application on leaching behaviour of arable soils: An experimental study', *Oil Shale*, 27 (3), 250 – 257.

Adriano, D.C., Page, A.L., Elseewi, A.A., Chang, A.C. and Straughan, I. (1980), 'Utilization and disposal of fly ash and other coal residues in terrestrial ecosystems: A review', *Journal of Environmental Quality*, 9, 333 – 344.

Adriano, D.C.; Weber, J.; Bolan, N.S.; Paramasivam, S.; Koo, Bon Jun and Sajwan, K.S. (2002), 'Effects of high rates of coal fly ash on soil, turfgrass and groundwater quality', *Water, Air, and Soil Pollution*, 139, 365 – 385.

Ahmaruzzaman, M. (2010), 'A review on the utilization of fly ash', *Progress in Energy and Combustion Science*, 36, 327 – 363.

Akinyemi, S.A.; Akinlua, A.; Gitari, W.M.; Akinyeye, R.O.; Petrik, L.F. (2011), 'The leachability of major elements at different stages of weathering in dry disposed coal fly ash', *Coal Combustion and Gasification Products*, 3, 28-40.

Akinyemi, S.A.; Gitari, W.M.; Akinlua, A. and Petrik, L.F. (2012), 'Mineralogy and geochemistry of sub-bituminous coal and its combustion products from Mpumalanga Province, South Africa', *Analytical Chemistry*, Dr. Ira S. Krull (Ed.), InTech, DOI: 10.5772/50692. Available from: http://www.intechopen.com/books/analytical-chemistry/mineralogy-and-geochemistry-of-sub-bituminous-coal-and-its-combustion-products-from-mpumalanga-province

Amonette, James E.; Kim, Jungbae; Russell, Colleen K.; Palumbo, Anthony V. and Daniels, W. Lee (2003), 'Enhancement of soil carbon sequestration by amendment with fly ash', *International Ash Utilisation Symposium*, Centre for Applied Energy Research, University of Kentucky, Paper No.47.

Asencios, Yvan J.O. and Sun-Kou, María R. (2012), 'Synthesis of high-surface-area γ-Al_2O_3 from aluminum scrap and its use for the adsorption of metals: Pb(II), Cd(II) and Zn(II)', *Applied Surface Science*, 258, 10002 – 10011.

ASTM Standard C618-08, American Society for Testing and Materials (2008), 'Standard specification for coal fly ash and raw or calcined natural pozzolan for use in concrete', ASTM International, West Conshohocken, PA, USA.

Authier-Martin, M.; Forte, G.; Ostap, S. and See, J. (2001), 'The mineralogy of bauxite for producing smelter-grade alumina', *Journal of the Minerals, Metals and Materials Society*, 53, 36 – 40. (2001)

Babajide, Omotola; Musyoka, Nicholas; Petrik, Leslie and Ameer, Farouk (2012), 'Novel zeolite Na-X synthesized from fly ash as a heterogeneous catalyst in biodiesel production', *Catalysis Today*, 190, 54 – 60.

Bai, G.H.; Qiao, Y.H.; Shen, B.; Chen, S.L. (2011), 'Thermal decomposition of coal fly ash by concentrated sulfuric acid and alumina extraction process based on it', *Fuel Process Technology*, 92, 1213 – 1219.

Bai, Guanghui; Wei Teng, Wei; Wang, Xianggang; Hui Zhang, Hui and Xu, Peng (2010), 'Processing and kinetics studies on the alumina enrichment of coal fly ash by fractionating silicon dioxide as nano particles', *Fuel Processing Technology*, 91, 175 – 184.

Basu, P. (1983), 'Reactions of iron minerals in sodium aluminate solutions', *Light Metals*, New York. pp. 83 – 98.

Belyaeva, O.N.; Haynes, R.J. and Sturm, E.C. (2012), 'Chemical, physical and microbial properties and microbial diversity in manufactured soils produced from co-composting green waste and biosolids', *Waste Management*. 32, 2248 – 2257.

Bliem, Roland Pavelec, Jiri; Gamba, Oscar; McDermott, Eamon; Wang, Zhiming; Gerhold, Stefan; Wagner, Margareta; Osiecki, Jacek; Schulte, Karina; Schmid, Michael; Blaha, Peter; Diebold, Ulrike and Gareth S. Parkinson (2015), 'Adsorption and incorporation of transition metals at the magnetite Fe_3O_4(001) surface', *Physical Review B*. 92, 075440.

Blissett, R.S. and Rowson, N.A. (2012), 'A review of the multi-component utilisation of coal fly ash', *Fuel*, 97, 1 – 23.

Böke, Nuran; Birch, Grant D.; Nyale, Sammy M. and Petrik, Leslie F. (2015), 'New synthesis method for the production of coal fly ash-based foamed geopolymers', *Construction and Building Materials*, 75, 189 – 199.

Borisov, Oleg V.; Mao, Xianglei and Russo, Richard E. (2000), 'Effects of crater development on fractionation and signal intensity during laser ablation inductively coupled plasma mass spectrometry', *Spectrochimica Acta Part B*, 55, 1693 – 1704.

Brinker, C.J. and Scherer, G.W. (1990), Chapter 14: Applications. In: *Sol - Gel Science, The Physics and Chemistry of Sol - Gel Processing*. Academic Press, San Diego, CA, pp.839 – 880.

Brouwer, Peter (2010), *Theory of XRF*, Pananalytical B.V. 3rd edition, PanAnalytical B.V. Almelo, Netherlands.

Burnet G, Murtha MJ, Wijatno H. (1977), In: *3rd Kentucky Coal Refuse Disposal and Utilization Seminar*, Lexington, Kentucky, 83, 11 – 12.

Carter, W.K. (1943), U.S. Pat 2,329,589 (National Aluminate Corp).

Cho, H.; Oh, D. and Kim, K. (2005), 'A study on removal characteristics of heavy metals from aqueous solution by fly ash', *Journal of Hazardous Materials B*, 127, 187 – 195.

Coradin, Thibaud; Eglin, David and Livage, Jacques (2004), 'The silicomolybdic acid spectrophotometric method and its application to silicate/biopolymer interaction studies. *Spectroscopy*. 18, 567 – 576.

Corte, Della; Francesco Giuseppe, Francesco and Rao, Sandro (May 2013), 'Use of amorphous silicon for active photonic devices', *IEEE Transactions on Electron Devices*, 60 (5), 1495 – 1505.

Cussler, E. L. (1984), *Diffusion*. Cambridge University Press. New York.

Decarlo, V.A.; Seeley, F.G.; Canon, R.M.; Mcdowell, W.J. and Brown, K.B. (1978), 'Evaluation of potential Processes for the recovery of resource', Oak Ridge National Laboratory, ORNL/TM-6126. Available from: http://web.ornl.gov/info/reports/1978/3445603550761.pdf (Last accessed 10 May 2016)

Demir, Ilham' Hughes, Randall E. and DeMaris, Philip J. (2001), 'Formation and use of coal combustion residues from three types of power plants burning Illinois coals', *Fuel* 80 (11), 1659 – 1673.

Dilmore, R.M. and Neufeld, R.D. (2001), 'Autoclaved aerated concrete produced with low-NOx burner/selective catalytic reduction fly ash', *Journal of Energy Engineering*, 127, 37 – 50.

Dmitrevski, G.E.; Martynova, L.G.; Antoshenko, E.I and Lukomskaya, Z.T. (1969), Zhurnal Prikladnoi Khimii. Moscow, 44, 2451.

Eckenfelder, W.W. (2000), *Industrial Water Pollution Control*. McGraw-Hill. Boston.

Elseewi,A.A.; Page, A.L. and Grimm, S.R. (1980), 'Chemical characterization of fly ash aqueous system', *Journal of Environmental Quality*, 9, 424 – 428.

Eriksson, J. and Björkman, B. (2004), 'MgO modification of slag from stainless steelmaking', In: *VII International Conference on Molten Slags Fluxes and Salts*, The South African Institute of Mining and Metallurgy, 455 – 460.

Eskom, (2016a), 'Matla power station', http://www.eskom.co.za/Whatweredoing/ElectricityGeneration/PowerStations/Pages/Matla_Power_Station.aspx. (Last accessed 23 May 2016)

Eskom, (2016b), 'Coal in South Africa', www.eskom.co.za/AboutElectricity/FactsFigures/Documents/CO0007CoalSARev14.pdf. (Last accessed 10 May 2016)

Eskom, (2016c), 'Ash management in Eskom', www.eskom.co.za/AboutElectricity/FactsFigures/Documents/CO0004AshManagementRev12.pdf. (Last accessed 10 May 2016)

Eze, Chuks P.; Fatoba, Olanrewaju; Madzivire, Godfrey; Ostrovnaya, Tatyna M.; Petrik, Leslie F.; Frontasyeva, Marina V. and Nechaev, Alexander (2013a), 'Elemental composition of fly ash: A comparative study using nuclear and related analytical techniques', *Chemistry-Didactics-Ecology-Metrology*, 18(1 – 2), 19 – 29.

Eze, Chuks P.; Nyale, Sammy M.; Akinyeye, Richard O.; Gitari, Wilson M.; Akinyemi, Segun A.; Fatoba, Olanrewaju O. and Leslie F. Petrik (2013b), 'Chemical, mineralogical and morphological changes in weathered coal fly ash: A case study of a brine impacted wet ash dump', *Journal of Environmental Management*, 129, 479 – 492.

Fatoba, O.O. (2007), 'Chemical compositions and leaching behaviour of some South African fly ashes', MSc thesis submitted in Department of Chemistry, University of Western Cape.

Feist, M.; Molchanov, V.N.; Kazanskii, L.P.; Torchenkova, E.A. and Spitsyn, V.I. (1980), Zhurnal Neorganicheskoi Khimii. 25, 733 In: Coradin, Thibaud; Eglin, David and Livage, Jacques. (2004), 'The silicomolybdic acid spectrophotometric method and its application to silicate/biopolymer interaction studies', *Spectroscopy*, 18, 567 – 576.

Felker, K.; Seeley, F.; Egan, Z. and Kelmers, D. (1982), 'Aluminum from fly ash', *International journal of Chemtech Research*, 2, 123 – 126.

Font, O.; Querol, X.; Lopez-Soler, A.; Chimenos, J.M.; Fernandez, A.I.; Burgos, S. and Pena, F.G. (2005), 'Ge extraction from gasification fly ash', *Fuel*, 84, 1384 – 1392.

Frondel, C. (1962), *The system of mineralogy of DANA, 7th ed Vol. 3 Silica minerals*, Wiley, New York, p. 154.

Quercia, G.; Spiesz, P.; Hüsken, G and Brouwers, H.J.H. (2014), 'SCC modification by use of amorphous nano – silica', *Cement & Concrete Composites*, 45, 69 – 81.

Gaoxiang, Du and Hao, Zheng Shuilin Ding (2009), 'Process optimisation of reaction of acid leaching residue of asbestos tailing & NaOH aqueous solution', *Science China Technological Sciences*. 52 (1), 204 – 209.

Gilbert, Crisanda (2013), 'Synthesis and characterisation of iron nanoparticles by extraction from iron rich waste material for the remediation of acid mine drainage', MSc Thesis submitted in the Department of Chemistry, University of Western Cape.

González, A.; Navia, R. and Moreno, N. (2009), 'Fly ashes from coal and petroleum coke combustion: current and innovative potential applications', *Waste Management and Research*, 27, 976 – 987.

Goodboy, K.P. (1976), 'Investigation of a Sinter Process for Extraction of Al_2O_3 from Coal Wastes'. *Metallurgical and Material Transactions B*. 7, 716 – 718.

Goto, K.; Okura, T and Kagama, I. (1953), Kagaku Tokyo. 23, p. 26 In: Iler, Ralph K. (1979), *The Chemistry of Silica: Solubility, Polymerisation, Colloid and Surface Properties and Biochemistry*, John Wiley and Sons Inc, USA.

Grashchenkov, D.V.; Balinova, Yu. A. and Tinyakova, E.V. (2012), 'Aluminium oxide ceramic fibres and materials based on them', *Glass and Ceramics*, 69, (3 – 4): (Russian Original, Nos. 3 – 4, March – April, 2012)

Grasshoff, K.; Kremling, K. and Ehrhardt, M. (1999), *Methods of seawater analysis*, Wiley-VCH Verlag GmbH, D-69469, Weinheim, Federal Republic of Germany.

Grzymek, J. (1976), 'Prof. Grzymek's Self-Disintegration Method for the Complex Manufacture of Aluminium Oxide and Portland cement', In: *Proceedings of Sessions 105th AIME annual meeting*, Las Vegas, Nevada, 29 – 39.

Guzzon, M; Mapelli, C; Memoli, F and Marcozzi, M. (2007), 'Recycling of ladle slag in the EAF: Improvement of the foaming behaviour and decrease of the environmental impact', *Revue de Métallurgie*, 104, 171 – 178.

Hamouda, Aly A. and Hossien, A. Akhlaghi Amiri (2014), **'**Factors affecting alkaline sodium silicate gelation for in-depth reservoir profile modification', *Energies*, 7, 568 – 590.

Haynes, R.J. (2009), 'Reclamation and revegetation of fly ash disposal sites – Challenges and research needs', *Journal of Environmental Management*, 90, 43 – 53.

Hosterman, J.W.; Patterson, S.H. and Good, E.E. (1990), 'World non-bauxite aluminium resources excluding alunite', Washington: US Government Printing Office, p. 51.

Hou, Xiandeng and Jones, Bradley T. (2000), 'Inductively coupled plasma/optical emission spectrometry', In: *Encyclopaedia of Analytical Chemistry*, R.A. Meyers (Ed.), John Wiley & Sons Ltd., Chichester. pp. 9468 – 9485.

http://www.construction.murrob.com/projects/MatlaPowerStation.htm (Last accessed 23 May 2016)

Hudson, L.K.; Misra, C.; Perrotta, A.J.; Wefers, K. and Williams, F.S. (2000), 'Aluminium Oxide', *Ullmann's Encyclopaedia of Industrial Chemistry*, Wiley Interscience.

Ilavský, Ján; Barloková, Danka and Munka, Karol (2015), 'The use of iron-based sorption materials and magnetic fields for the removal of antimony from water', *Pollution Journal of Environmental Studies*. 24 (5), 1983 – 1992

Iler, R.K. (1973), 'Effect of adsorbed alumina on the solubility of amorphous silica in water', *Journal of Colloid Interface Science*, 43, 399 – 408.

Iler, Ralph K. (1979), *The Chemistry of Silica: Solubility, Polymerisation, Colloid and Surface Properties and Biochemistry*. John Wiley and Sons Inc. USA.

Isaacs, L. (1924), 'Presence of silicon in tissues: A micro method for the determination of silicon', *Bulletin de la Société de Chimie Biologique*, 6, 157 – 168.

Iyer, Ramasubramania (2002), 'The surface chemistry of leaching of CFA', *Journal of Hazardous Materials B*, 93, 321 – 329.

Izquierdo, M. and Querol, X. (2012), 'Leaching behaviour of elements from coal combustion fly ash: an overview', *International Journal of Coal Geology*, 94, 54 – 66.

Jephcott, C.M. and Johnston, J.H. (1950), Archives of Industrial Hygiene and Occupational Medicine. 1, 323 – 340. In: Kennedy, George C. (1950), 'A portion of the system silica-water', *Economic Geology*, 45(7), 629 – 653.

Ji, H.M.; Lu, H.X.; Hao, X.G. and Wu, P. (2007), 'High purity aluminia powders extracted from fly ash by the calcining-leaching process', *Journal of the Chinese Ceramic Society*, 35, 1657 –1660.

Jordens, Adam; Cheng, Ying Ping and Waters, Kristian E. (2013), 'A review of the beneficiation of rare earth element bearing minerals', *Minerals Engineering*, 41, 97 – 114.

Kamath, S.R. and Proctor, A. (1998), 'Silica gel from rice hull ash:preparation and characterization', *Cereal Chemistry*, 75, 484 – 487.

Kelmers, A. D.; Egan, B. Z.; Seeley, F. G. and Campbell, G. D. (1981), 'Direct acid dissolution of aluminium and other metals from fly ash', *The Metallurgical Society of AIME*, TMS Paper A 81–24,

Kelmers, A.D.; Canon, R.M.; Egan, B.Z.; Felker, L.K.; Gilliam, T.M. and Jones, G. (1982), 'Chemistry of the direct acid leach, calsinter, and pressure digestion-acid leach methods for recovery of aluminum from fly ash', *Resources and Conservation*, 9, 271 – 279.

Laxamana, N.B. (1982), 'Binders from rice hull ash low - cost housing materials', *Forbride-Dig. College: Forest Products Research and Industries Development Commission*. 11, 27 – 30.

Lecuyer, I.; Bicocchi,S.; Ausset, P. and Lefevre, R. (February 1996), 'Physico-chemical characterisation and leaching of desulphurisation coal fly ash', *Waste Management & Research*, 14 (1), 15 – 28.

Lender, P.W. and Ruiter, R., 'Novel inorganic materials and heterogeneous catalysis: preparation and properties of high surface area silicon carbide and silicon oxynitrides' In: Sheats, J.E.; Carraher, C.E.; Pittman, C.U.; Eldin, M. and Currell, B. (Eds.). (1990), *Inorganic and Metal-Containing Polymeric Materials*, PlenumPress, New York, 187 – 195.

Lin, Kuang-Hui. (1984), *Perry's Chemical Engineers Handbook*, 50th ed. Perry and Green, pp. 4 – 9.

Lior, N. (2010), 'Sustainable energy development: the present (2009) situation and possible paths to the future', *Energy*, 35, 3976 – 3994.

Liu, Kang; Xue, Jilai and Zhu, Jun (2012), 'Extracting alumina from coal fly ash using acid sintering-leaching-process', *Light Metals*, Edited by: Carlos E. Suarez TMS (The Minerals, Metals & Materials Society), pp.201 – 206

Liu, Yufei; Guy, Owen James; Patel, Jash; Ashraf, Huma and Knight, Nick (2013), 'Refractive index graded anti-reflection coating for solar cells based on low cost reclaimed silicon'. *Microelectronic Engineering*. 110, 418 – 421.

Lyon, R.J.P. (1962), 'Infrared confirmation of 6-fold coordination of silicon in stishovite', *Nature*, 196, 266.

Madzivire, G.; Gitari, W.M.; Vadapalli, V.R.K. and Petrik, L.F. (2015), 'Jet loop reactor application for mine water treatment using fly ash, lime and aluminium hydroxide', *International Journal of Environmental Science and Technology*, 12, 173 – 182.

Malainey, Mary E. (2011), *A Consumer's Guide to Archaeological Science Analytical Techniques*, Springer Science and Business Media, LLC.

Manz, OE. (1999), 'Coal fly ash: a retrospective and future look', *Fuel*, 78 (2), 133 – 136.

Maroto-Valer, M.; Taulbee, D. and Hower, J. (2001), 'Characterization of differing forms of unburned carbon present in fly ash separated by density gradient centrifugation', *Fuel*, 80, 795 – 800.

Matjie, R.H.; Bunt, J.R. and Van Heerden, J.H.P. (2005), 'Extraction of alumina from coal fly ash generated from a selected low rank bituminous South African coal', *Mineral Engineering*, 18 (3), 299 – 310.

Mattigod, S. V.; Rai, D.; Eary, L. E. and Ainsworth, C. C. (1990), 'Geochemical factors controlling the mobilization of inorganic constituents from fossil fuel combustion residues: 1. Review of the major elements', *Journal of Environmental Quality*, 19, 188 – 201.

Mazzocchitti, G; Giannopoulou, I and Panias, D. (2009),'Silicon and aluminium removal from ilmenite concentrates by alkaline leaching. *Hydrometallurgy*, 96, 327 – 332.

McDowell, W.J. and Seeley, F.G. (1981), 'Salt-soda sinter process for recovering aluminium from fly ash', US patent 4254088.

Mehta, P.K. (1987), 'Natural pozzolans: Supplementary cementing materials in concrete', *CANMET* **(**Canada Centre for Mineral and Energy Technology) *Special Publication*, 86, 1 – 33.

Mitsyuk, B.M.; Dorosh, A.K.; Skryshevskii, A.F. and Vysotskii Z.Z. (1966), *Ukrainskii Khimicheskii Zhurnal*, 32, 833 In: Iler, Ralph K. (1979), *The Chemistry of Silica: Solubility, Polymerisation, Colloid and Surface Properties and Biochemistry*, John Wiley and Sons Inc. USA.

Mittal, Davinder (1997), 'Silica from ash: A valuable product from waste material', *Resonance*, 2 (7), 64 – 66.

Mullin, J.B. and Riley, J.P. (1955), 'The colorimetric determination of silicate with reference to sea and natural waters', *Analytica Chimica Acta*, 12, 162.

Muriithi, Grace N.; Petrik, Leslie F.; Fatoba, Olanrewaju; Gitari, Wilson M.; Doucet, Frédéric J.; Nel, Jaco; Nyale, Sammy M.; Chuks, Paul E. (September 2013)a, 'Comparison of CO_2 capture by ex-situ accelerated carbonation and in in-situ naturally weathered coal fly ash', *Journal of Environmental Management*, 127, 212 – 220.

Muriithi, Grace Nyambura (2013b), 'Reuse of South African fly ash for CO_2 capture and Brine Remediation', PhD Thesis submitted to the Department of Chemistry, University of Western Cape.

Muriithi, Grace Nyambura; Gitari, Wilson Mugera; Petrik, Leslie Felicia and Ndungu, Patrick Gathura (2011), 'Carbonation of brine impacted fractionated coal fly ash: implications for CO_2 sequestration', *Journal of Environmental Management*, 92, 655 – 664.

Musyoka, N.M.; Petrik, L. and Hums, E. (2012), 'Synthesis of zeolite A, X and P from a South African Coal fly ash', *Advanced Materials Research*, Vols. 512 – 515. pp. 1757 – 1762.

Nath, P. and Sarker, P. (2011), 'Effect of fly ash on the durability properties of high strength concrete', *Procedia Engineeing*, 14, 1149 – 1156.

Nayak, N. and Panda, Chitta R. (2009), 'Aluminium extraction and leaching characteristics of Talcher Thermal Power Station fly ash with sulphuric acid', *Fuel*, 89 (1), 53 – 58.

Nehari, S.; Gorin, C.; Lin, I.J. and Berkovich, A. (1996), 'Process for recovery of alumina and silica', US patent 5993758.

Nonavinakere, S. and Reed, B.E. (1995), 'Fly ash enhanced metal removal process', In: Sengupta, A.K. (Ed.), *Hazardous and Industrial Wastes: Proceedings of the Twenty-seventh Mid-Atlantic Industrial Waste Conference*, Technomart Publishing.

Nyale, Sammy (2011), 'Chemical, physical and morphological changes in weathered brine slurried coal fly ash', MSc thesis submitted in the Department of Chemistry, University of Western Cape.

Nyale, Sammy M.; Babajide, Omotola O.; Birch, Grant D.; Böke, Nuran and Petrik, Leslie (2013), 'Synthesis and characterization of coal fly ash-based foamed geopolymer', *Procedia Environmental Sciences*, 18, 722 – 730.

Nyale, Sammy M.; Eze, Chuks P.; Akinyeye, Richard O.; Gitari, Wilson M.; Akinyemi, Segun A.; Fatoba, Olanrewaju O. and Petrik, Leslie F. (2014), 'The leaching behaviour and geochemical fractionation of trace elements in hydraulically disposed weathered coal fly ash', *Journal of Environmental Science and Health, Part A*, 49, (2), 233 – 242.

Padilla, R and Sohn, H.Y. (1985), 'Sodium aluminate leaching and desilication in lime soda sinter process for alumina from coal wastes', *Metallurgical and Materials Transactions B*, 16B (4), 707 – 713.

Palumbo, A.V.; McCarthy, J.F.; Amonette, E.; Fisher, L.S.; Wullschleger, S.D. and Daniels, W. Lee (2004), 'Prospects for enhancing carbon sequestration and reclamation of degraded lands with fossil-fuel combustion by-products', *Advances in Environmental Research*, 8, 425 – 438.

Palumbo, Anthony V.; Tarver, Jana R.; Fagan, Lisa A.; McNeilly, Meghan S.; Ruther, Rose; Fisher, Suzanne L. and Amonette, James E. (2007), 'Comparing metal leaching and toxicity from high pH, low pH, and high ammonia fly ash', *Fuel*, 86, 1623 – 1630.

Panagiotopoulou, Ch.; Kontori, E.; Perraki,Th. and Kakali, G. (2007), 'Dissolution of aluminosilicate minerals and by-Products in alkaline media', *Journal of Materials Sciences*, 42, 2967 – 2973.

Pandey, V.C. and Singh, N. (2010), 'Impact of fly ash incorporation in soil systems', *Agriculture, Ecosystems and Environment*, 136, 16 – 27.

Pedersen H. (1927), 'Process of manufacturing aluminum hydroxide',US Patent 1,618,105.

Pedersen, H. (1924), 'Improved process for the production of iron from ores', British Patent 232,930.

Padilla, R and Sohn, H.Y. (1985a), 'Sintering kinetics and alumina yield in lime soda sinter process for alumina from coal wastes', *Metallurgical and Materials Transactions B*, 16B, (2), 385 – 395.

Padilla, R and Sohn, H.Y. (1985b), 'Sodium aluminate leaching and desilication in lime Soda sinter process for alumina from coal wastes', *Metallurgical and Materials Transactions B*, 16B (4), 707 – 713.

Ram, L.C.; Srivastava, N.K.; Jha, S.K.; Sinha, A.K.; Masto, R.E. and Selvi, V.A. (2007), 'Management of lignite fly ash for improving soil fertility and crop productivity', *Environmental Management*, 40, 438 – 452.

Ram, L.C.; Srivastava, N.K.; Tripathi, R.C.; Jha, S.K.; Sinha, A.K.; Singh, G. and Manoharan, V. (2006), 'Management of mine spoil for crop productivity with lignite fly ash and biological amendments'. *Journal of Environmental Management*, 79, 173 – 187.

Reynolds, R., Kruger R. and Rethman N. (1999), 'The manufacture and evaluation of soil (SLASH) prepared from fly ash and sewage sludge', *International Ash Utilisation Symposium. Centre for Applied Energy Research*,. University of Kentucky, Paper 1.

Rule, J.M. (1951), U.S. Pat 2,577,484. Du Pont.

Sarker, P.K. and McKenzie, L. (2009), 'Strength and hydration heat of concrete using fly ash as a partial replacement', *Proceedings of 24th Biennial Conference of the Concrete Institute of Australia*, Sydney, Australia

Sarker, P.K. (2011), 'Bond strength of reinforcing steel embedded in geopolymer concrete', *Materials and Structures*, 44, 1021–1030.

Sarker, P.K.; Haque, R. and Ramgolam, V. (2012), 'Fracture behaviour of heat cured fly ash based geopolymer concrete', *Materials and Design*, 44, 580–586.

Seidel, A and Zimmels, Y. (1998), 'Mechanism and kinetics of aluminum and iron leaching from coal fly ash by sulphuric acid', *Chemical Engineering Science*, 53, 3835–3852.

Seidel, A; Sluszny, A; Shelef, G and Zimmels, Y. (1999), 'Self-inhibition of aluminum leaching from coal fly ash by sulphuric acid', *Chemical Engineering Journal*, 72, 195 – 207.

Sharma, Sudhir K. and Kaira, Naveen (2006), 'Effect of flyash incorporation and productivity of crops: A Review', *Journal of Scientific & Industrial Research*, 65, 383 – 390.

Shcherban, S.; Raizman, V. and Pevzner, I. (1995), 'Technology of coal fly ash processing into metallurgical and silicate chemical products'. Kazakh Politechnical University, Alma-Ata., Available from: https://web.anl.gov/PCS/acsfuel/preprint%20archive/Files/40_4_ CHICAGO_08-95_0863.pdf (Last Accessed 23 May 2016)

Shemi, A; Mpana, R.N.; Ndlovu, S.; van Dyk, L.D.; Sibanda,V. and Seepe, L. (2012), 'Alternative techniques for extracting alumina from coal fly ash', *Minerals Engineering*, 34, 30 – 37.

Shemi, A., Ndlovu, S.; Sibanda, V and van Dyk, L.D. (2014), 'Extraction of aluminium from coal fly ash: Identification and optimization of influential factors using statistical design of experiments', *International Journal of Mineral Processing*, 127, 10 – 15.

Shoumkova, A.S. (2006), Physio-chemical characterisation and magnetic separation of coal fly ashes from Varna, Bobov Dol and Maritza-Istok I power plants, Bulgaria: I- Physico chemical characteristics', *Journal of the University of Chemical Technology and Metallurgy*, 41, (2), 175 – 180.

Shumkov, S and Shoumkova, A. (2002), 'Magnetic separation of coal fly ash', *Journal of the University of Chemical Technology and Metallurgy*, 35, 565 – 570.

Shumkov, SH and Shoumkova, A.S. (2004), 'Magnetochemical treatment of coal fly ash', *Bulgarian Chemistry and Industry*, 75, 37 – 40.

Simcoe, Charles R. (2014), 'Aluminum: The light metal - Part II', *Advanced Materials & Processes*, 172 (10), 32 – 33.

Soroczak, M. M.; Eaton, H. C. and Tittlebaum, M. E. (1987), 'An ESCA and SEM study of changes in the surface composition and morphology of low calcium coal fly ash as a function of aqueous leaching', *Materials Research Society Symposia Proceedings*, Material Research Society, 86, 37 – 47.

Speight, James G. (2005), *Handbook of coal analysis*. John Wiley and sons Inc. U.S.A.

Stöber,W. (1963), 'Physico-chemical properties of coesite and stishovite in comparison with quartz'; Grundfragen Silikoseforsch, 6, 35 – 48.

Su, Shuang Qing; Yang, Jing; Ma, Hong Wen; Jiang, Fan; Liu, Yu Qin and Li, Ge (2011), 'Preparation of ultrafine aluminum hydroxide from coal fly ash by alkali dissolution process', *Integrated Ferroelectrics*, 128, 155 – 162.

Sumner, Malcolm E. (2000), *Handbook of Soil Sciences*, CRC Press, United States of America.

Taylor, H.F.W. (1997), *Cement Chemistry*. 2nd ed. Thomas Telford, London.

Temuujin, J.; van Riessen, A. and MacKenzie, K.J.D. (2010), 'Preparation and characterisation of fly ash based geopolymer mortars', *Construction and Building Materials*, 24, 1906 – 1910.

Thomas, Robert. (2004), *Practical guide to ICP-MS*. Marcel Dekker, Inc.

Tong, Z.F.; Zou, Y.F. and Li, Y.J. (2008), 'Roasting activation mechanism of coal fly ash with KF assistant', *Chinese Journal of Nonferrous Metals*, 18, 403 – 406.

Trinh, Thuat T., Jansen, Antonius P. J. and van Santen, Rutger A. (2006), 'Mechanism of oligomerization reactions of silica', *Journal of Physical Chemistry B*, 110 (46), 23099 – 23106.

Truesdale, V.W. and Smith, P.J. (1975), 'The formation of molybdosilicic acids from mixed solutions of molybdate and silicate', *Analyst*, 100, 203 – 212.

Unob, Fuangfa; Wongsiri, Benjawan; Phaeon, Nuchnicha; Puanngam, Mahitti; Shiowatana, Juwadee (2007), 'Reuse of waste silica as adsorbent for metal removal by iron oxide modification', *Journal of Hazardous Materials*, 142, 455 – 462.

van Holde, K. E.; Johnson, W. C. and Ho, P.S. (1998), 'X-Ray Diffraction', *Principles of Physical Biochemistry*, Chapter 6, 242-311, Prentice-Hall, Inc.

Vázquez-Almazán, María C.; Ventura, Eusebio; Enrique, Rico; Rodríguez-García, y Mario E. (2012), 'Use of calcium sulphate dihydrate as an alternative to the conventional use of aluminium sulphate in the primary treatment of wastewater', *Water SA*. 38 (5).

Ward, Colin R. and French, David (2005), 'Relation between coal and fly ash mineralogy based on quantitative X-Ray diffraction methods', *World of Coal Ash (WOCA)*, Lexington, Kentucky, USA.

Wibberley, Louis J. and Wall, Terry F. (1982), 'Alkali-ash reactions and deposit formation in pulverized-coal-fired boilers: experimental aspects of sodium silicate formation and the formation of deposits', *Fuel*, 61 (1), 93 – 99.

Willey, J.D. (1974), 'The effect of pressure on the solubility of amorphous silica in seawater at 0°C', *Marine Chemistry*, 2 (4), 239 – 250.

Wu, C.Y.; Yu H.F.; Zhang, H.F. (2012), 'Extraction of aluminium by pressure acid-leaching method from coal fly ash', *Transactions of* Nonferrous *Metals* Society *of* China, 22, 2282 – 2288.

Yao, Z.T. (2013), 'Generation, characterization and extracting of silicon and aluminium from coal fly ash' In: Sarker, P.K. (Ed.) (2013), *Fly Ash: Sources, Applications and Potential Environmental Impacts. Nova Science Publishers*, New York, pp. 3–58.

Yao, Z.T.; Ji, X.S.; Sarker, P.K.; Tang, J.H.; Ge, L.Q.; Xia, M.S. and Xi, Y.Q. A. (2015), 'Comprehensive review on the applications of coal fly ash', *Earth-Science Reviews*, 141, 105–121.

Yao, Z.T.; Xia, M.S.; Sarker, P.K. and Chen, T. (2014), 'A review of the alumina recovery from coal fly ash with a focus in China', *Fuel*, 120, 74–85.

Zeng, L. (2003), 'A method for preparing silica-containing iron(III) oxide adsorbents for arsenic removal', *Water Research*, 37, 4351 – 4358.